Electronic Supporting Information

Room-temperature luminescence from Pd(II) and Pt(II) complexes: From mechanochromic crystals to flexible polymer matrices

Matias E. Gutierrez Suburu,[a,b] Iván Maisuls,[a,b] Jutta Kösters,[a] Cristian A. Strassert*[a,b]

[a]Institut für Anorganische und Analytische Chemie, Westfälische Wilhelms-Universität Münster, Corrensstraße 28/30, D-48149 Münster, Germany.

[b]CeNTech, SoN, CiMIC, Westfälische Wilhelms-Universität Münster, Heisenbergstraße 11, D-48149 Munster, Germany

* ca.s@wwu.de

1) Synthesis and characterization

All the synthetic precursors and solvents (analytical grade) were used as purchased without further purification.

NMR spectra were recorded at the Organisch-Chemisches Institut in Münster (WWU) on an Avance 400 from Burker Analytische Messtechnik or an DD2 500 from Agilent. The ^{1}H-NMR and ^{13}C-NMR chemical shifts (δ) of the signals are given in parts per million and are referenced to the residual proton signal in the deuterated solvent DCM-d_2 (^{1}H: 5.32 ppm / ^{13}C: 54.0 ppm). The signal multiplicities are abbreviated as follows: s, singlet; d, doublet; t, triplet; q, quartet; m, multiplet.

Exact mass (EM) determination by mass spectrometry (MS) was carried out at the Organisch-Chemisches Institut in Münster (WWU) using a LTQ Orbitap LTQ XL (Thermo-Fisher Scientific, Bremen) with electron spray injection (ESI).

N,N-bis(2-bromopyrid-6-yl)-4-methoxyaniline (1).

2,6-Dibromopyridine (4.930 g, 20.8 mmol), $Pd_2(dba)_3$ (0.154 g, 0.168 mmol), 4-methoxyaniline (1.064 g, 8.62 mmol), NaO^tBu (2.323 g, 23.20 mmol) and 1,1'-bis(diphenylphosphino)ferrocene (0.196 g, 0.354 mmol) were combined in toluene (100 mL) under argon atmosphere. The reaction mixture was degassed during the heating process and reacted at 110°C for 12–14 h to yield a dark brown solution. Once at room temperature, the solution was filtered and poured into water (100 mL), the residue was washed with ethyl acetate. The aqueous phase was extracted with ethyl acetate (3 x 50 mL). The combined organic phases were washed with water (25 mL) and brine (25 mL), dried with Na_2SO_4, filtered, concentrated and the crude compound was adsorbed onto silica gel. This was loaded onto a column packed with silica gel to perform a column chromatography separation with cyclohexane/ethyl acetate as the eluent (9: 1) to yield a yellow solid (1.269 g, 34%).

^{1}H NMR (500 MHz, CD_2Cl_2): δ = 7.41 (t, J = 7.9 Hz, 2H), 7.15 – 7.11 (m, 2H), 7.10 (dd, J = 7.7, 0.7 Hz, 2H), 7.00 – 6.96 (m, 2H), 6.94 (dd, J = 8.2, 0.7 Hz, 2H), 3.84 (s, 3H).

^{13}C NMR (126 MHz, CD_2Cl_2): δ = 158.9, 157.7, 139.9, 139.8, 136.4, 129.9, 122.1, 115.5, 115.0, 55.9.

EM (ESI+, MeOH, m/z): calcd. for $[M + K]^+$, 473.90373; found, 473.90340.

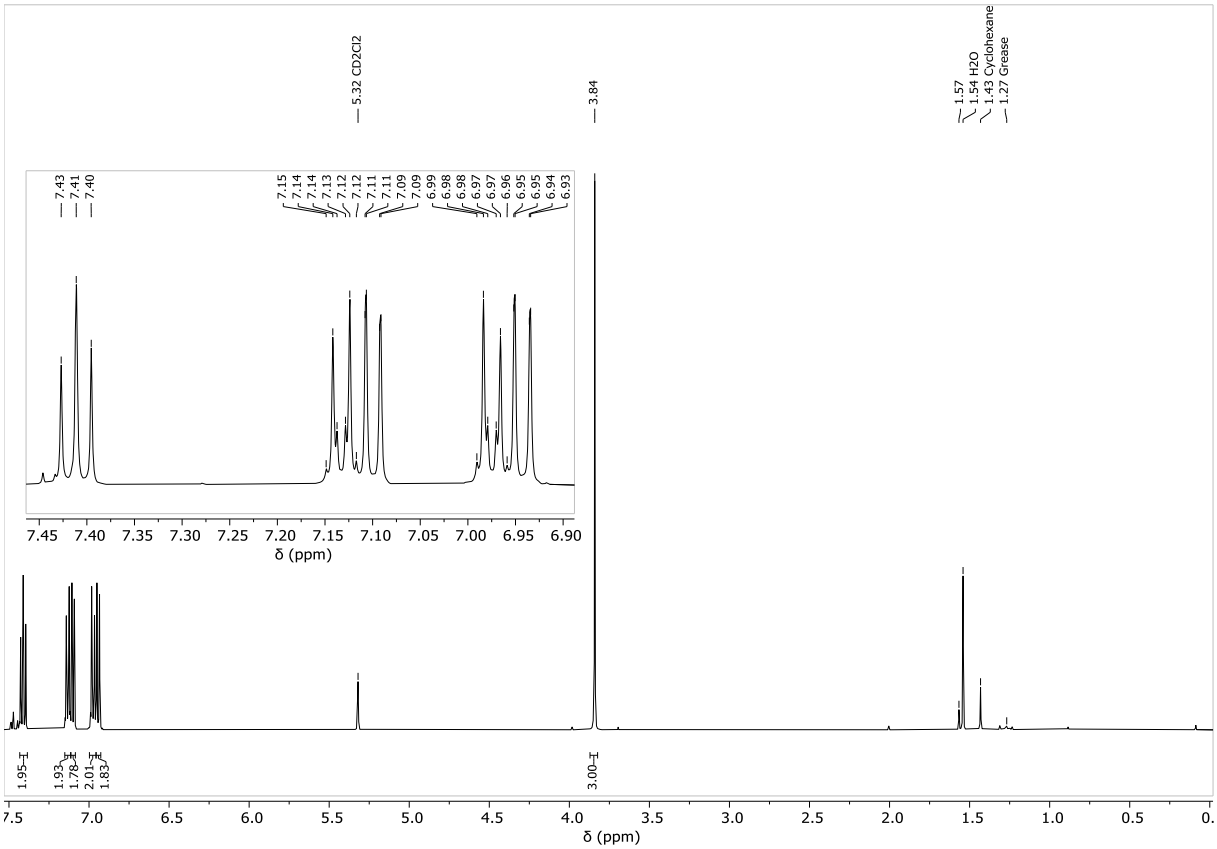

Figure S1. ^{1}H-NMR spectrum (400 MHz, CD_2Cl_2) of **1**.

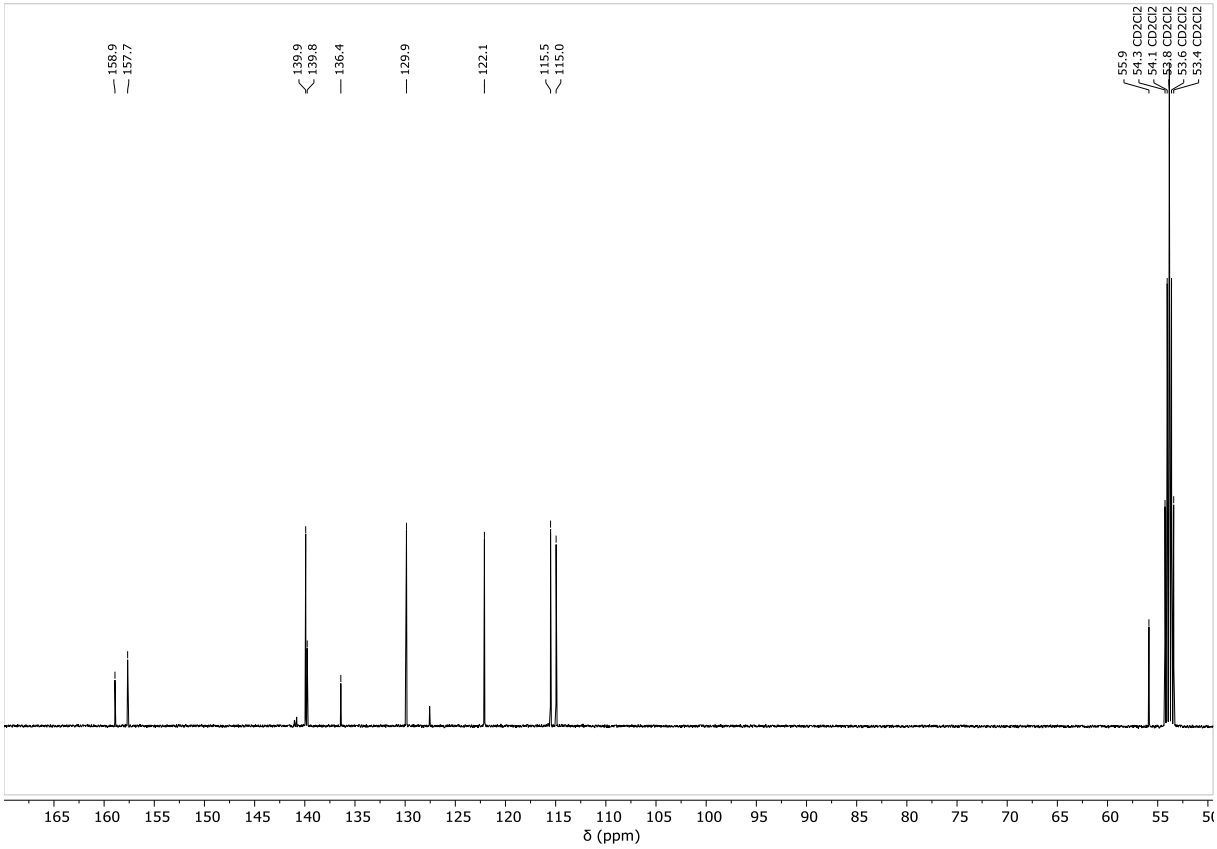

Figure S2. ^{13}C-{^{1}H}-NMR spectrum (126 MHz, CD_2Cl_2) of **1**.

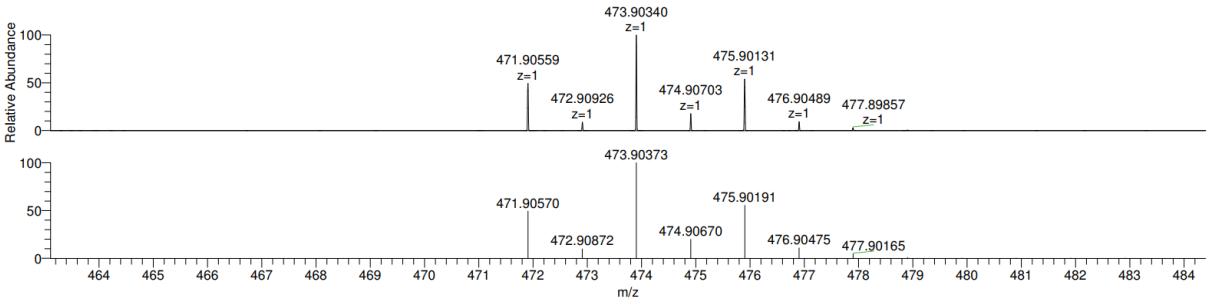

Figure S3. ESI-MS (MeOH) of **1**.

N,N-bis(2-(4-methoxyphenyl)pyrid-6-yl)-4-methoxyaniline (L_{OMe}).

N,N-bis(2-bromopyrid-6-yl)-4-methoxyaniline (0.517 g, 1.19 mmol), $Pd(PPh_3)_4$ (0.172 g, 0.15 mmol) and 4-methoxyphenylboronic acid (0. 422 g, 2.78 mmol) were combined in THF (70 mL) and degassed by bubbling with Ar. The solution was heated up to reflux and aqueous K_2CO_3 (2 M, 5 mL) was added under Ar flux. The reaction mixture was refluxed for 12 h to yield a yellow solution. Afterwards, THF was removed under reduced pressure, the occurring precipitate was dissolved in EtOAc (30 mL), and the solution washed with water (25 mL) and brine (25 mL). The organic phase was dried with Na_2SO_4, filtered, concentrated and the crude compound was adsorbed onto silica gel. This was loaded onto a column packed with silica gel to perform a column chromatography separation with cyclohexane/ethyl acetate as the eluent (100:1 to 50:1) and crystallized from a mixture of CH_2Cl_2 and *n*-heptane to yield white crystals (0.317 g, 54 %).

^{1}H NMR (400 MHz, CD_2Cl_2): δ = 7.84 – 7.80 (m, 4H), 7.60 (dd, J = 8.2, 7.6 Hz, 2H), 7.33 (dd, J = 7.6, 0.7 Hz, 2H), 7.27 – 7.23 (m, 2H), 7.00 – 6.95 (m, 4H), 6.92 – 6.88 (m, 4H), 3.85 (s, 3H), 3.81 (s, 6H).

^{13}C NMR (126 MHz, CD_2Cl_2): δ = 160.9, 158.3, 158.2, 155.4, 138.3, 132.4, 130.2, 128.4, 115.2, 114.4, 114.4, 113.4, 56.0, 55.8.

EM (ESI+, MeOH, m/z): calcd. for $[M + H]^+$, 490.21252; found, 409.21362.

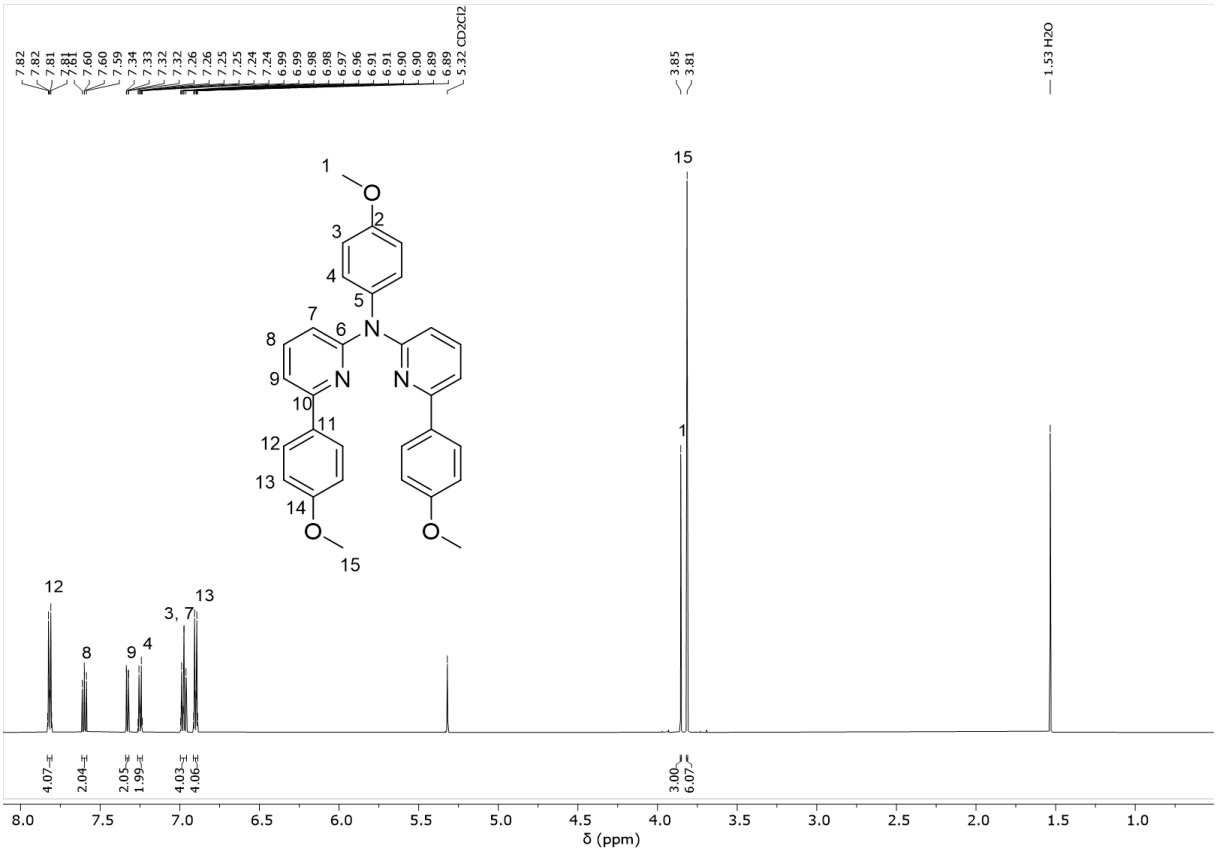

Figure S4. ^{1}H-NMR spectrum (400 MHz, CD_2Cl_2) of $\mathbf{L_{OMe}}$.

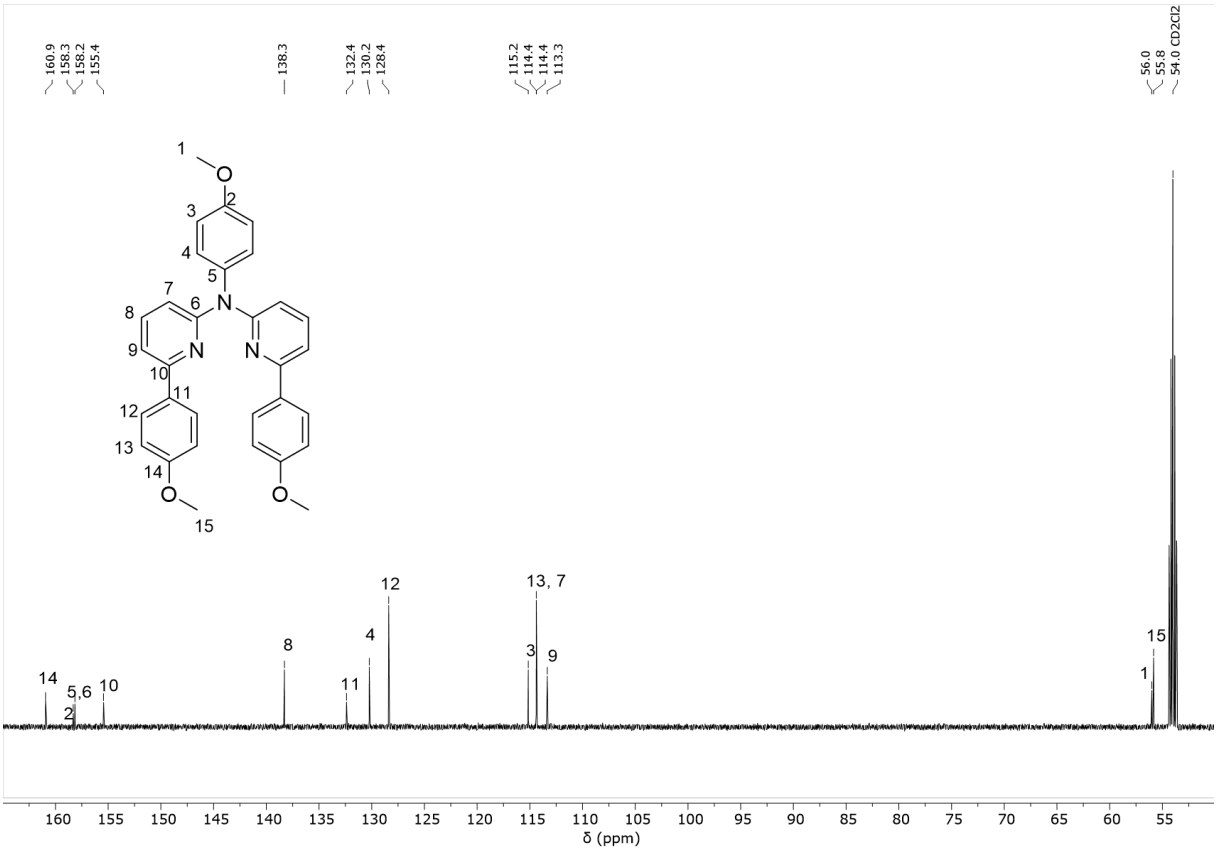

Figure S5. ^{13}C-{^{1}H}-NMR spectrum (126 MHz, CD_2Cl_2) of $\mathbf{L_{OMe}}$.

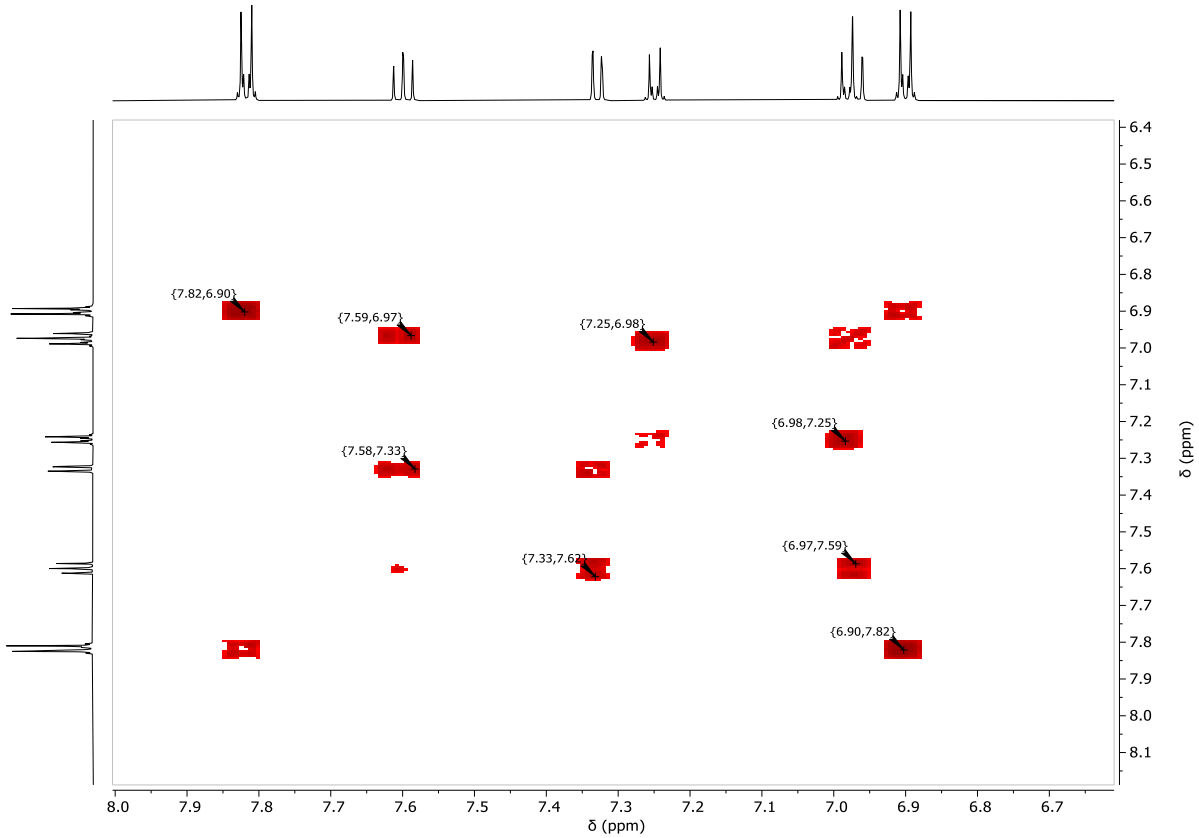

Figure S6. $^{1}H/^{1}H$-COSY-NMR spectrum (400 MHz/400 MHz, CD_2Cl_2) of $\mathbf{L_{OMe}}$.

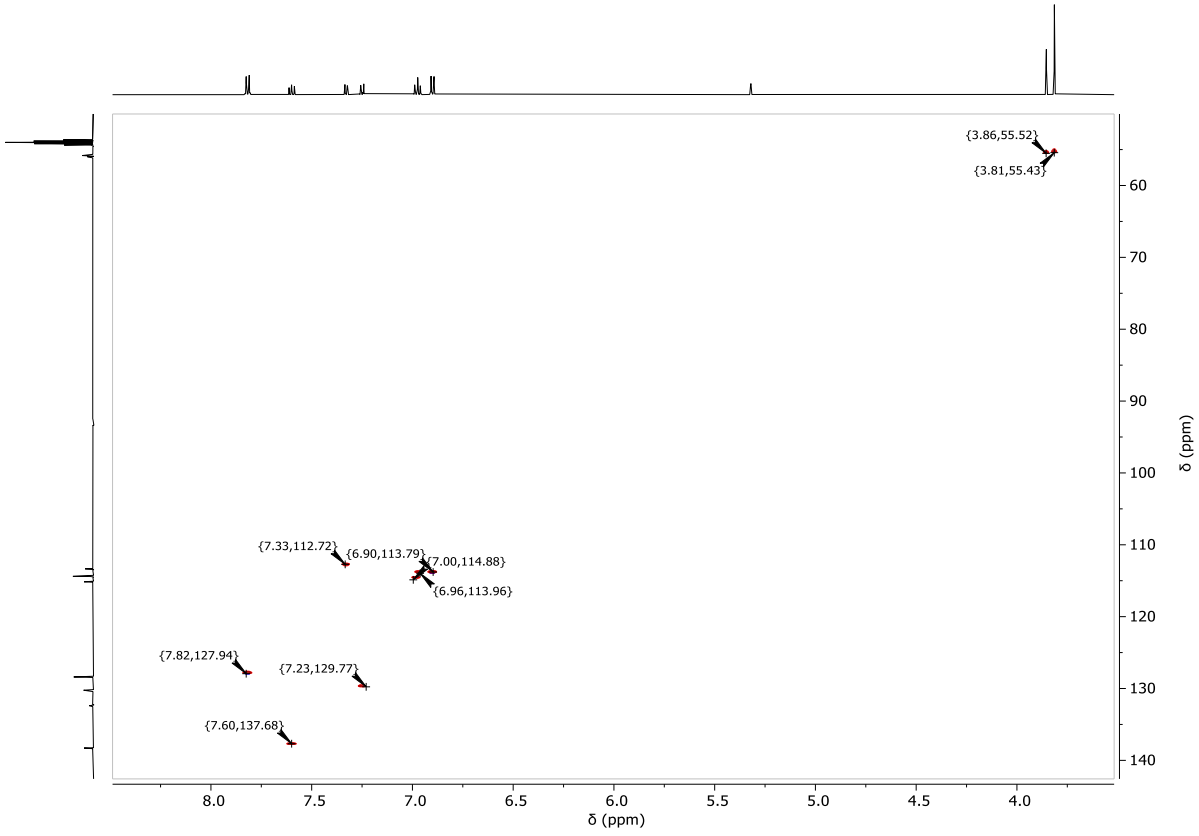

Figure S7. $^{1}H/^{13}C$-gHSQC-NMR spectrum (400 MHz/126 MHZ, CD_2Cl_2) of $\mathbf{L_{OMe}}$.

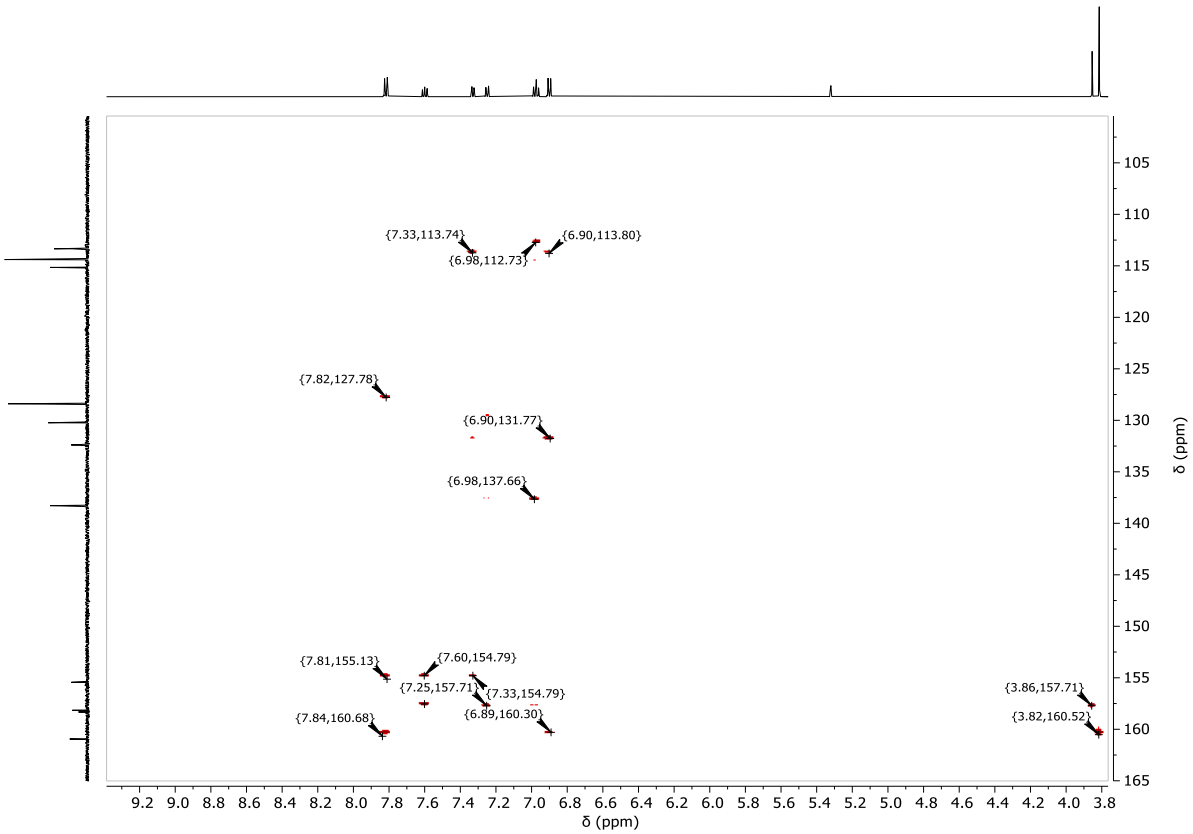

Figure S8. $^{1}H/^{13}C$-gHMBC-NMR spectrum (400 MHz/126 MHz, CD_2Cl_2) of $\mathbf{L_{OMe}}$.

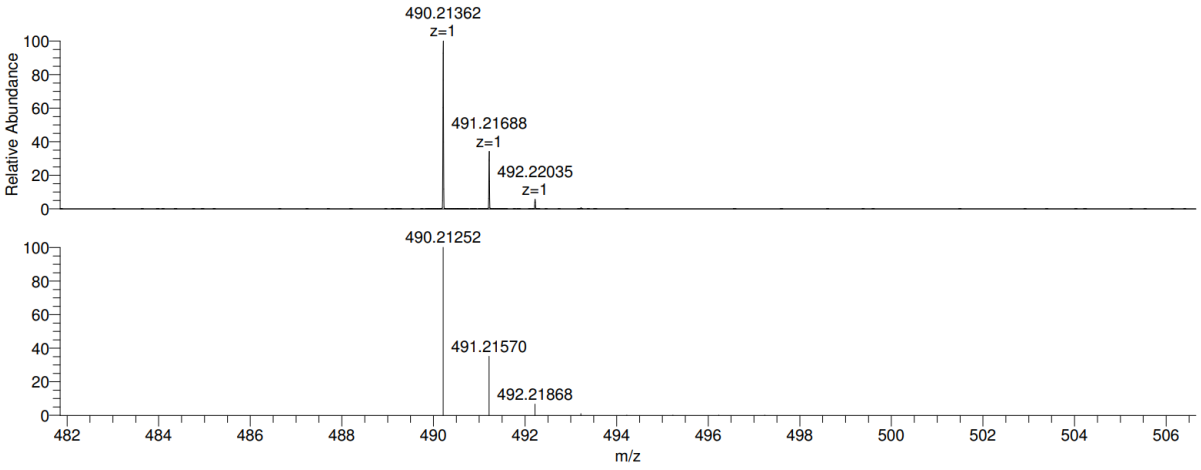

Figure S9. ESI-MS (MeOH) of $\mathbf{L_{OMe}}$.

N,N-bis(2-(4-hexyloxyphenyl)pyrid-6-yl)-4-methoxyaniline (L_{OHex}).

N,N-bis(2-bromopyrid-6-yl)-4-methoxyaniline (0.503 g, 1.16 mmol), $Pd(PPh_3)_4$ (0.170 g, 0.15 mmol) and 4-hydroxyphenylboronic acid (0.400 g, 2.89 mmol) were placed in a 250 mL two-neck flask and dissolved in 60 mL of THF. The solution was degassed by bubbling with Ar at room temperature and heated to reflux. Then, K_2CO_3 as a 2 M solution (4 mL, 8.0 mmol) was added with a syringe. The resulting yellow solution was stirred at 75 °C overnight. THF was evaporated and the excess of K_2CO_3 neutralized with 4 mL of HCl (1:4); then, 20 mL of water were added and the mixture centrifuged. The

solid was washed twice with 5 mL of acetone. The solid was dried and transferred to a 100 mL two-necked flask with K_2CO_3 (0.333 g, 2.41 mmol) and suspended in 50 mL of butanone. The mixture was degassed at room temperature by bubbling with Ar and after 10 min heated up to reflux under Ar flux and $C_6H_{13}Br$ was added (0.3 mL, 2.14 mmol). The mixture was reacted for 48 h. The solvent was evaporated, the crude product dissolved in CH_2Cl_2 (50 mL) and washed with water (25 mL), brine (25 mL), dried with Na_2SO_4 and adsorbed onto silica gel. This was loaded onto a column packed with silica gel to perform a column chromatography separation with cyclohexane/ethyl acetate as the eluent (100:1 to 20:1) to yield a white solid (0.381 g, 52 %).

^{1}H NMR (500 MHz, CD_2Cl_2): δ = 7.85 – 7.77 (m, 4H), 7.59 (t, *J* = 7.9 Hz, 2H), 7.32 (dd, *J* = 7.6, 0.8 Hz, 2H), 7.03 – 6.93 (m, 4H), 6.93 – 6.85 (m, 4H), 3.98 (t, *J* = 6.6 Hz, 5H), 3.86 (s, 3H), 1.82 – 1.71 (m, 3H), 1.51 – 1.41 (m, 1H), 1.35 (dq, *J* = 7.0, 3.4 Hz, 4H), 0.97 – 0.88 (m, 2H).

^{13}C NMR (126 MHz, CD_2Cl_2): δ = 159.9, 157.7, 157.6, 154.9, 137.7, 131.6, 129.6, 127.8, 114.5, 114.3 113.7, 112.7, 68.1, 55.4, 31.6, 29.2, 25.7, 22.6, 13.8.

EM (ESI+, MeOH, m/z): calcd. for $[M + H]^+$, 630.36902; found, 630.36902.

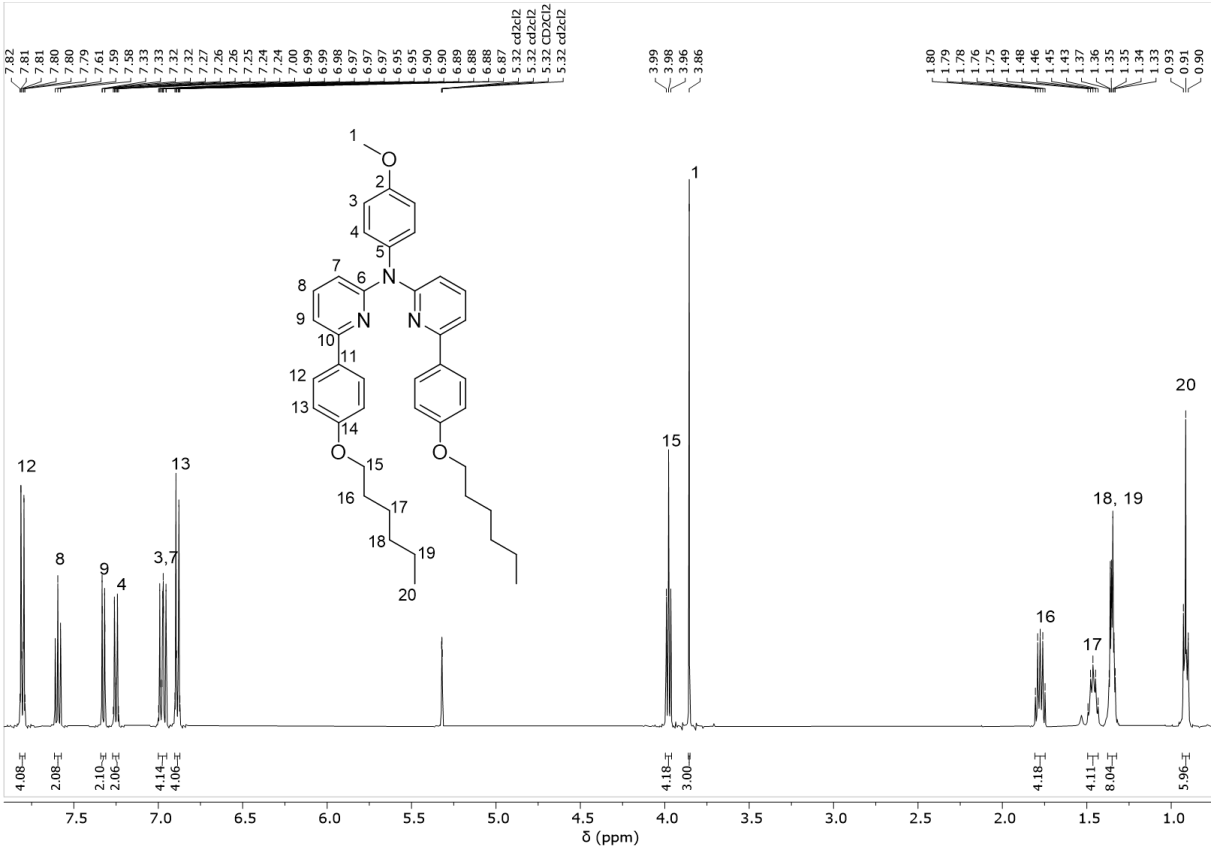

Figure S10. ^{1}H-NMR spectrum (500 MHz, CD_2Cl_2) of $\mathbf{L_{OHex}}$.

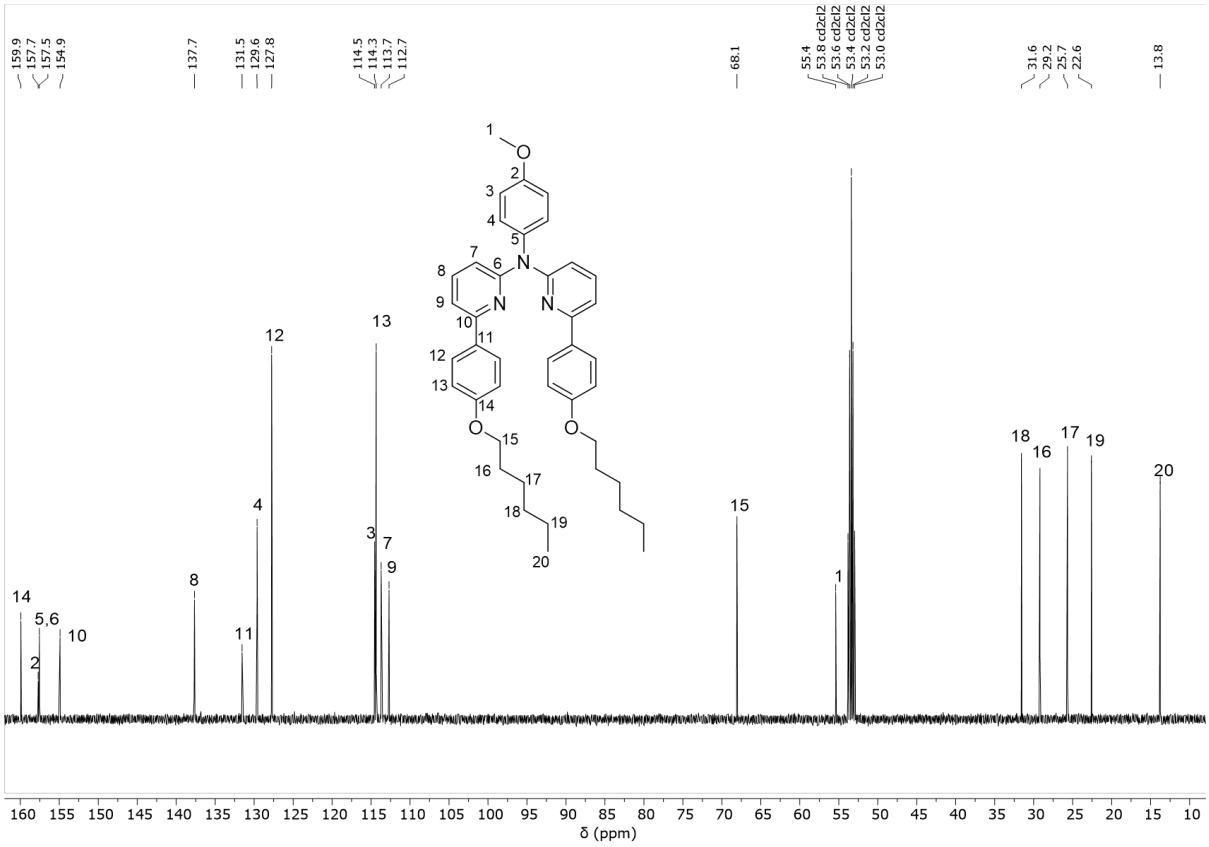

Figure S11. ^{13}C-{^{1}H}-NMR spectrum (126 MHz, CD_2Cl_2) of $\mathbf{L_{OHex}}$.

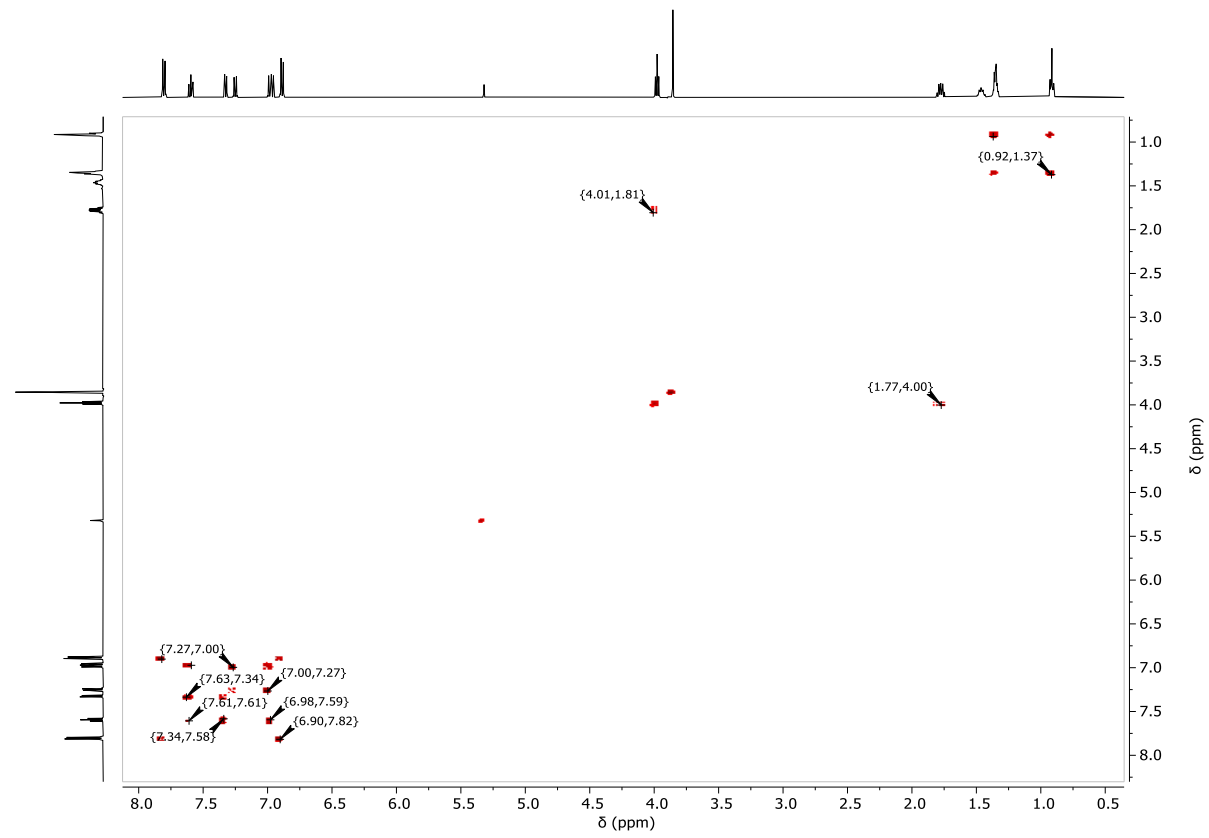

Figure S12. $^{1}H/^{1}H$-COSY-NMR spectrum (500 MHz/500 MHz, CD_2Cl_2) of $\mathbf{L_{OHex}}$.

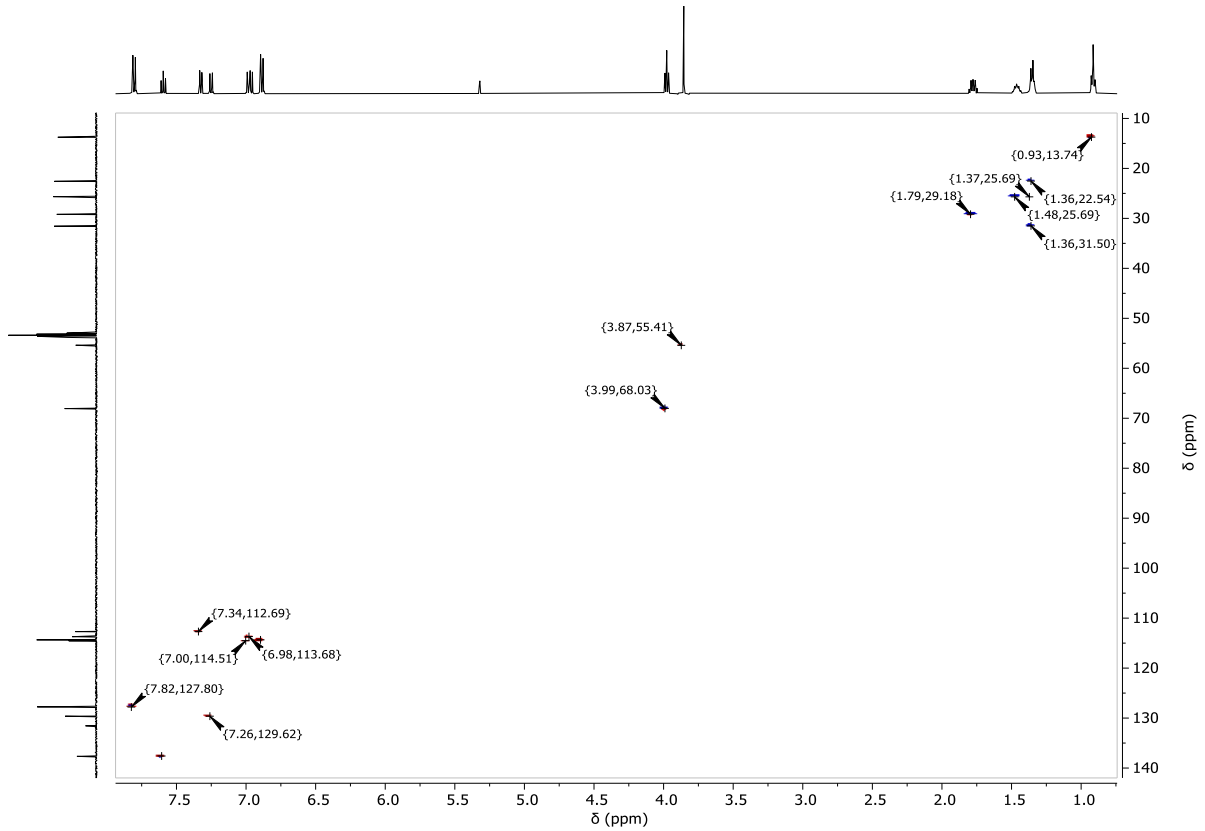

Figure S13. $^{1}H/^{13}C$-gHSQC-NMR spectrum (500 MHz/126 MHZ, CD_2Cl_2) of $\mathbf{L_{OHex}}$.

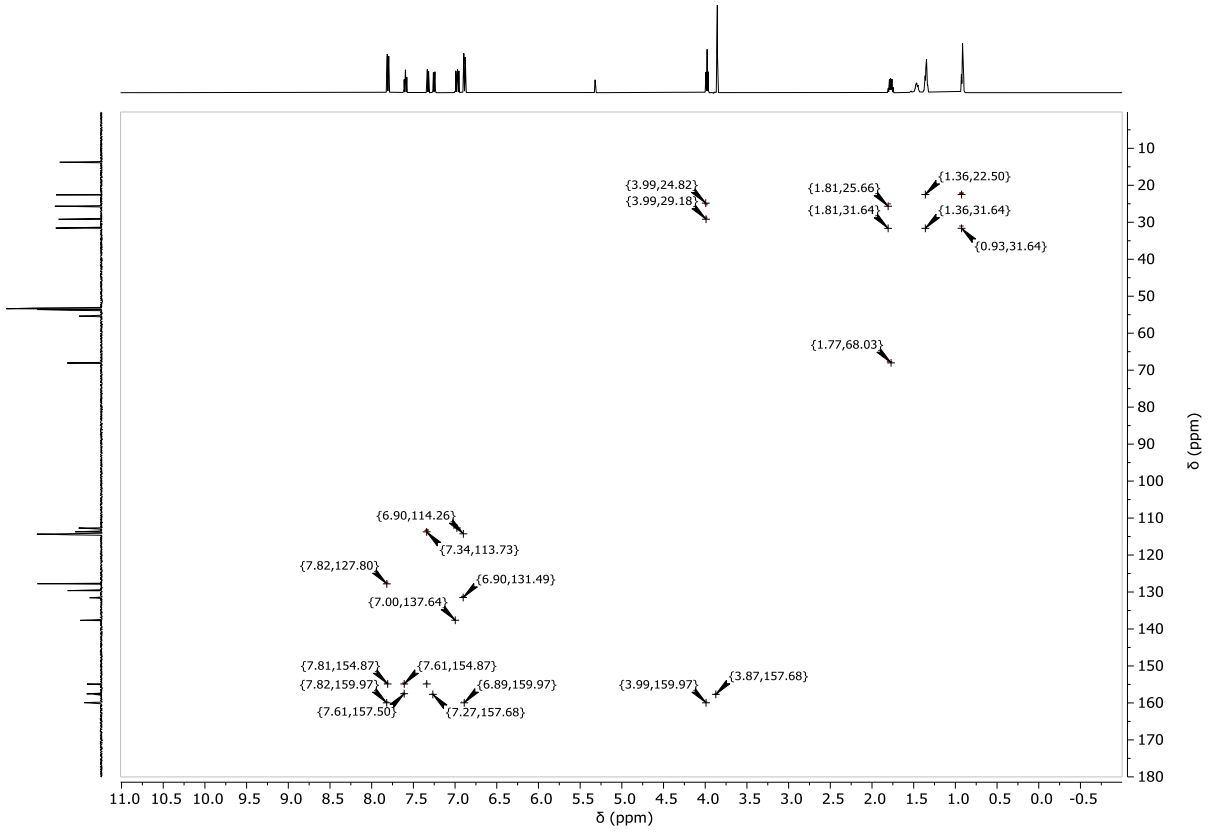

Figure S14. $^{1}H/^{13}C$-gHMBC-NMR spectrum (500 MHz/126 MHz, CD_2Cl_2) of $\mathbf{L_{OHex}}$.

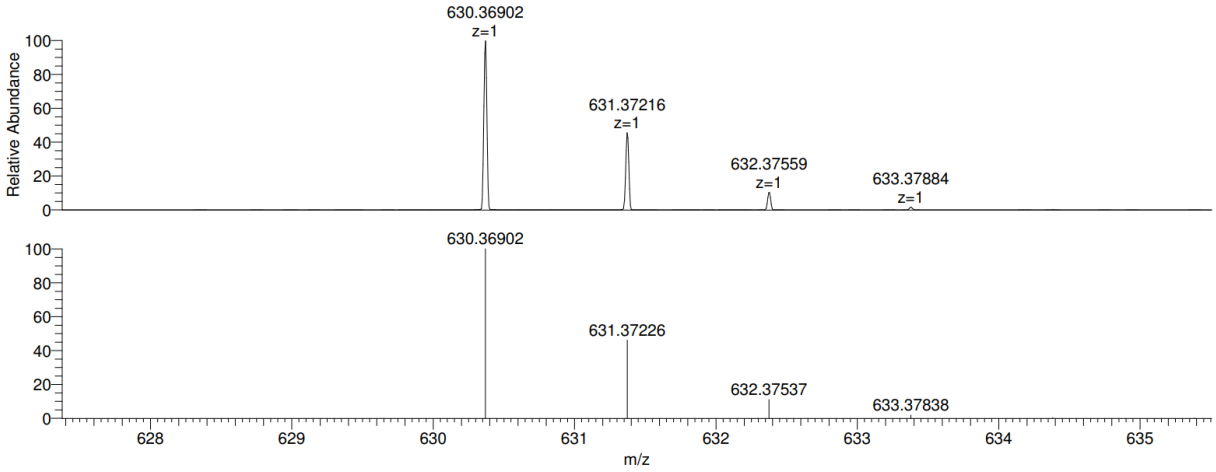

Figure S15. ESI-MS (MeOH) of $\mathbf{L_{OHex}}$.

$\mathbf{PtL_{OMe}}$

In a 50 mL two-necked flask, $\mathbf{L_{OMe}}$ (100.7 mg, 0.21 mmol) and K_2PtCl_4 (107.0 mg, 0.26 mmol) were suspended using 35 mL of acetic acid. The mixture was degassed by bubbling with Ar at room temperature for 15 min, then heated up to 130 °C under Ar flux and reacted for 72 h. The mixture was cooled down to room temperature and the solvent was evaporated. The crude product was adsorbed onto silica gel and purified by column chromatography using cyclohexane/CH_2Cl_2 as the eluent (1:1 to 1:3) to yield a yellow solid (58 mg, 40 %). Single crystals suitable for X-ray diffractometric analysis were obtained by slow evaporation from a CH_2Cl_2/*n*-heptane solution.

^{1}H NMR (400 MHz, CD_2Cl_2): δ = 7.84 (d, *J* = 2.6 Hz, 2H), 7.76 (d, *J* = 8.6 Hz, 2H), 7.71 (dd, *J* = 8.7, 7.7 Hz, 2H), 7.51 (dd, *J* = 7.9, 0.9 Hz, 2H), 7.33 (m, 2H), 7.19 (m, 2H), 6.76 (dd, *J* = 8.6, 2.6 Hz, 2H), 6.49 (dd, *J* = 8.7, 0.9 Hz, 1H), 3.98 (s, 6H), 3.94 (s, 3H).

^{13}C NMR (126 MHz, CD_2Cl_2): δ = 164.2, 161.0, 160.8, 152.3, 149.7, 140.5, 137.4, 136.4, 131.9, 125.9, 119.9, 117.1, 113.5, 111.5, 110.3, 56.3, 55.7.

EM (ESI+, MeOH, m/z): calcd. for $[M + H]^+$, 683.16192; found, 683.16256.

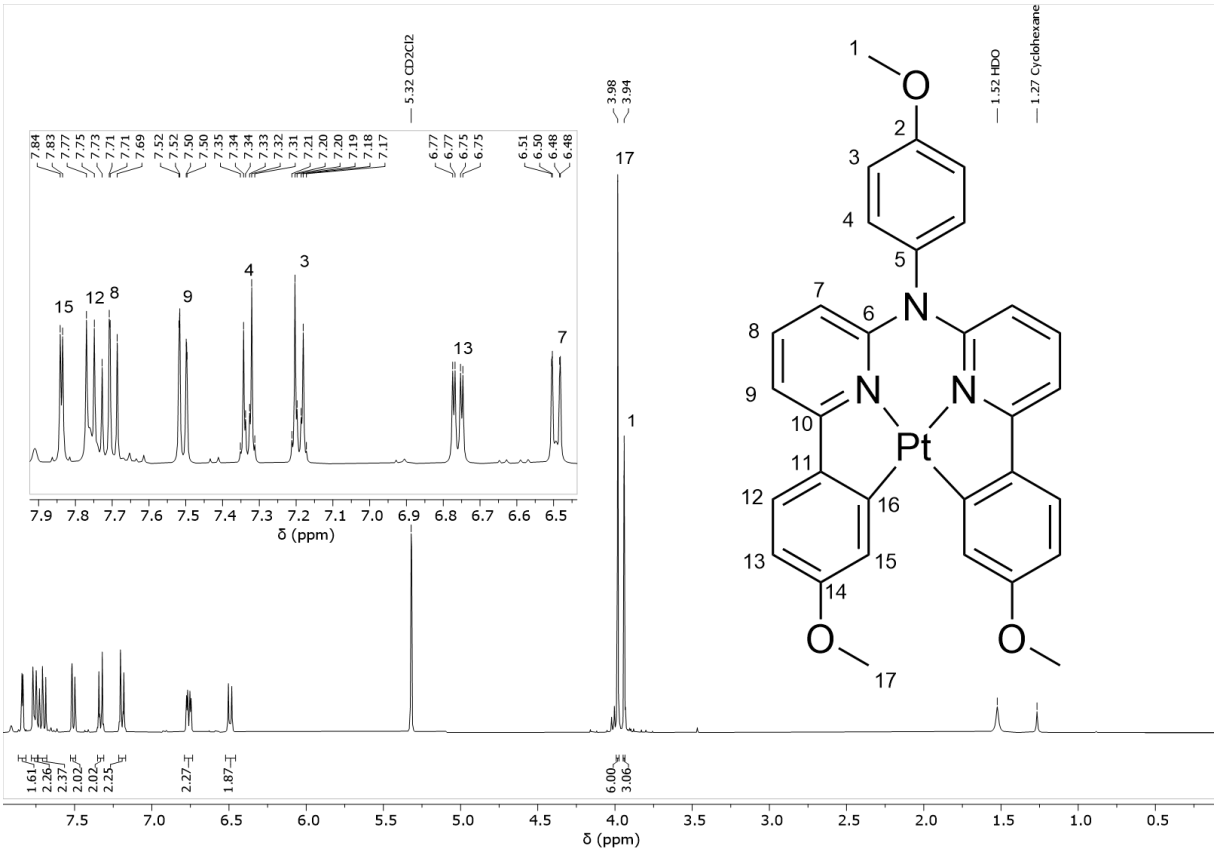

Figure S16. ^{1}H-NMR spectrum (400 MHz, CD_2Cl_2) of **PtL_{OMe}**.

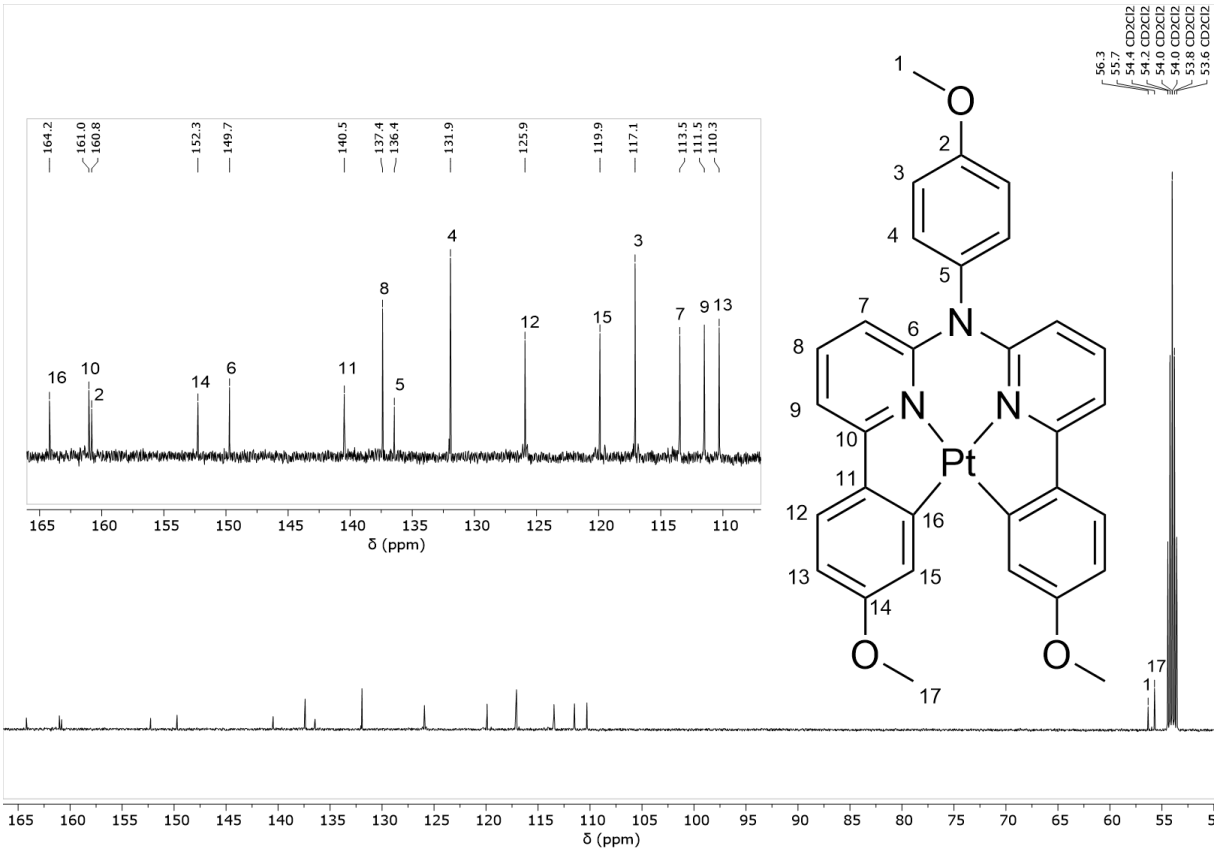

Figure S17. ^{13}C-{^{1}H}-NMR spectrum (126 MHz, CD_2Cl_2) of **PtL_{OMe}**.

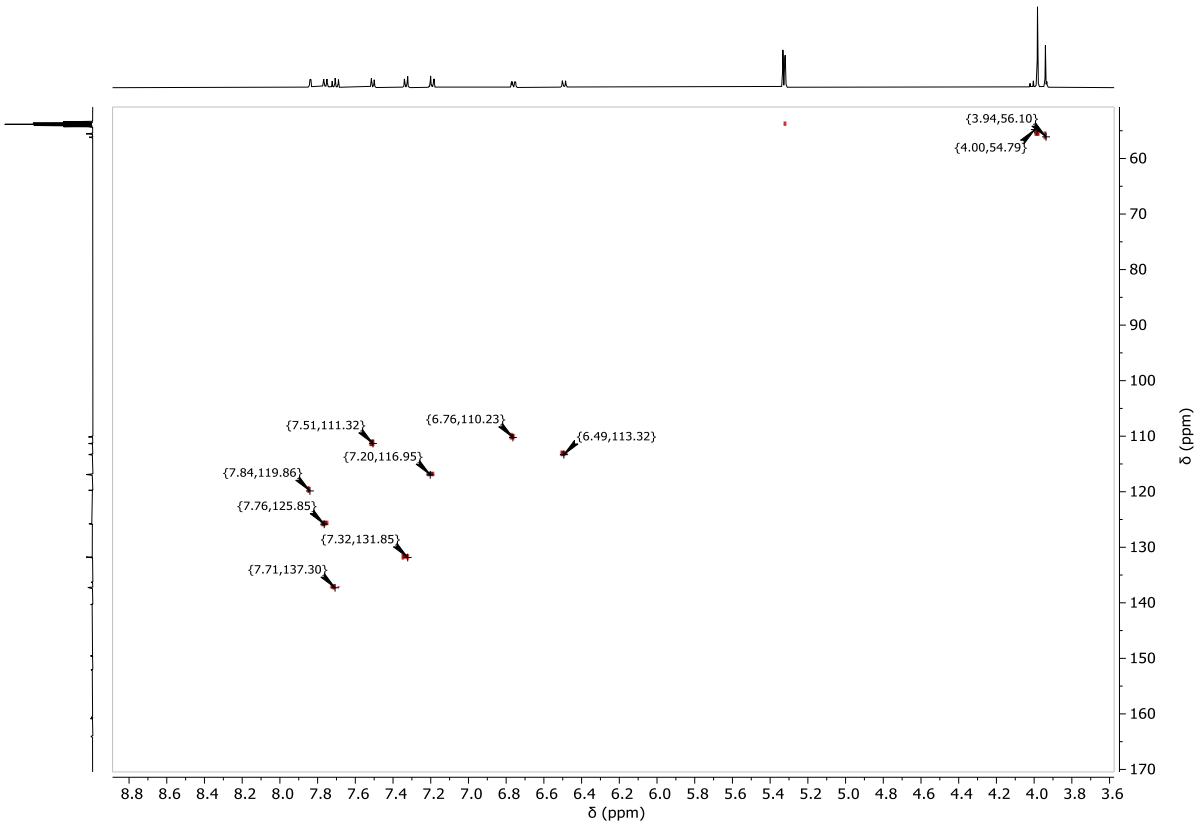

Figure S18. $^{1}H/^{13}C$-gHSQC-NMR spectrum (400 MHz/126 MHZ, CD_2Cl_2) of **PtL_{OMe}**.

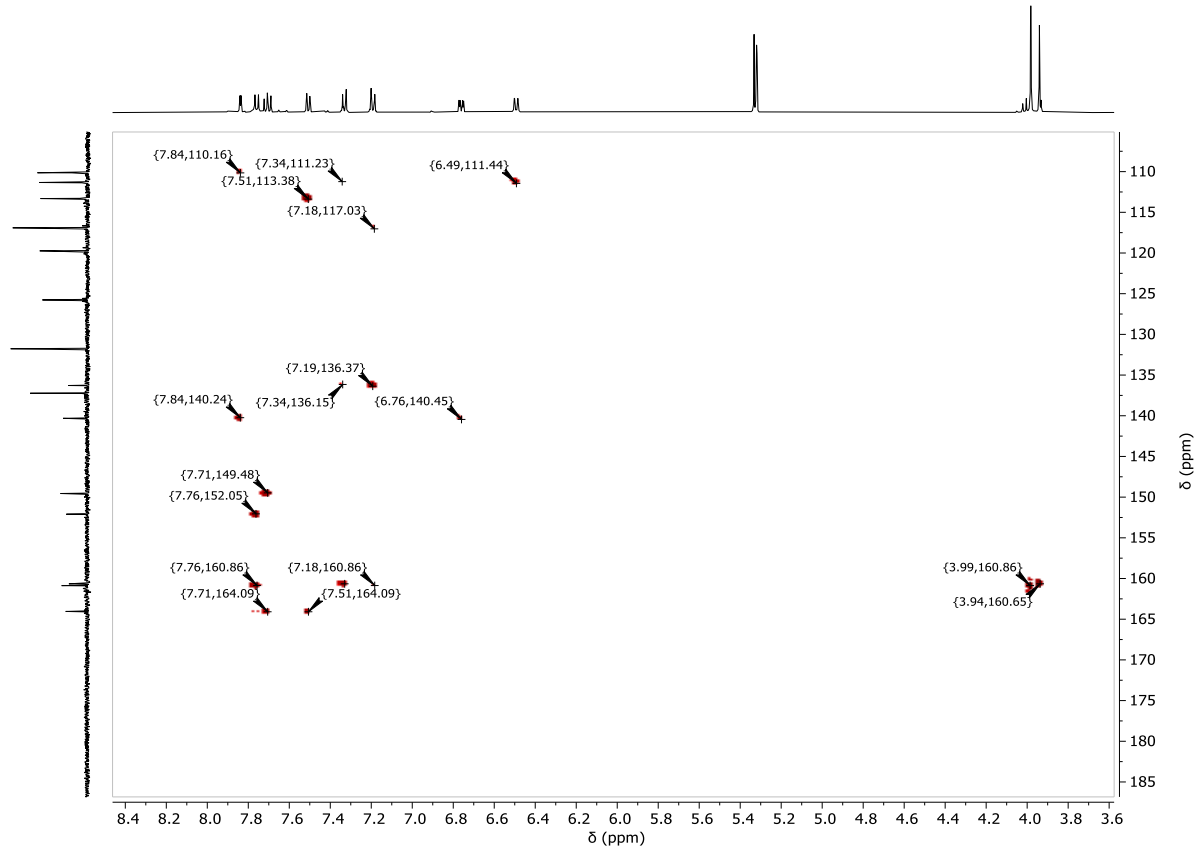

Figure S19. $^{1}H/^{13}C$-gHMBC-NMR spectrum (400 MHz/126 MHz, CD_2Cl_2) of **PtL_{OMe}**.

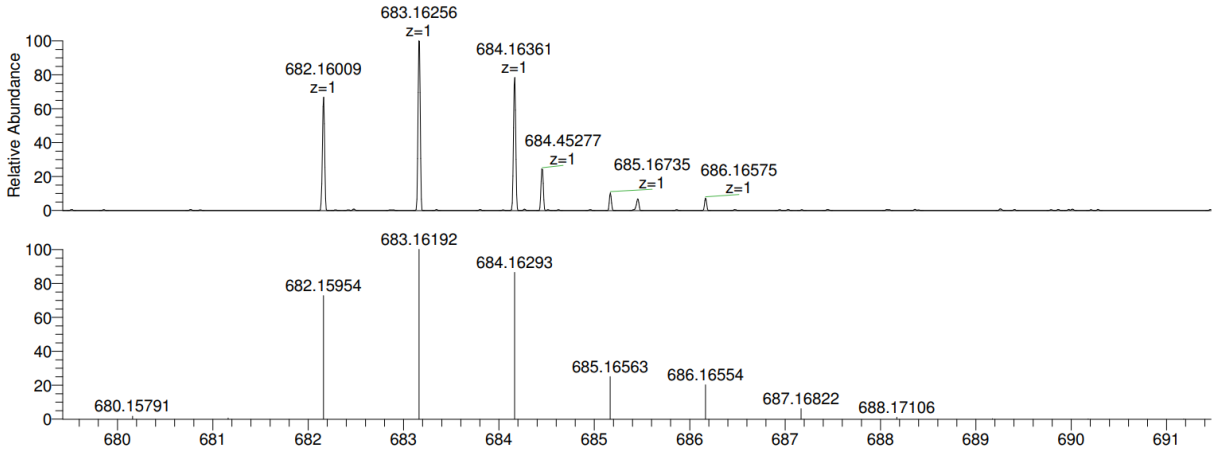

Figure S20. ESI-MS (MeOH) of **PtL$_{OMe}$**.

PdL$_{OMe}$

In a 50 mL two-necked flask, **L$_{OMe}$** (102.5 mg, 0.21 mmol) and $Pd(OAc)_2$ (45.7 mg, 0.20 mmol) were suspended using 25 mL of acetic acid. The mixture was degassed by bubbling with Ar at room temperature and the mixture was stirred at room temperature for 24 h. The temperature of the mixture was raised up to 80 °C and reacted for 48 h. Finally, the temperature was increased up to 130 °C and the mixture reacted for 1 h. Then, the mixture was cooled down to room temperature and the solvent was evaporated. The crude product was adsorbed onto silica gel and purified by column chromatography using cyclohexane/CH_2Cl_2 as the eluent (1:1 to 1:3) to yield a pale brown solid (21 mg, 16 %). Single crystals suitable for X-ray diffractometric analysis were obtained by slow evaporation from a CH_2Cl_2/*n*-heptane solution.

^{1}H NMR (400 MHz, CD_2Cl_2): δ = 7.72 (d, *J* = 8.6 Hz, 2H), 7.71 (d, *J* = 2.6 Hz, 2H), 7.60 (dd, *J* = 8.6, 7.7 Hz, 2H), 7.48 (dd, *J* = 7.9, 0.9 Hz, 2H), 7.30 (d, *J* = 8.9 Hz, 2H), 7.17 (d, *J* = 8.9 Hz, 2H), 6.75 (dd, *J* = 8.5, 2.6 Hz, 2H), 6.34 (dd, *J* = 8.6, 0.8 Hz, 2H), 3.96 (s, 6H), 3.93 (s, 3H).

^{13}C NMR (101 MHz, CD_2Cl_2): δ = 163.9, 163.2, 160.6, 160.5, 152.0, 140.9, 138.3, 136.2, 131.8, 125.5, 120.1, 116.9, 113.1, 111.3, 110.6, 56.1, 55.5.

EM (ESI+, MeOH, m/z): calcd. for $[M + H]^+$, 594.10153; found, 594.10122.

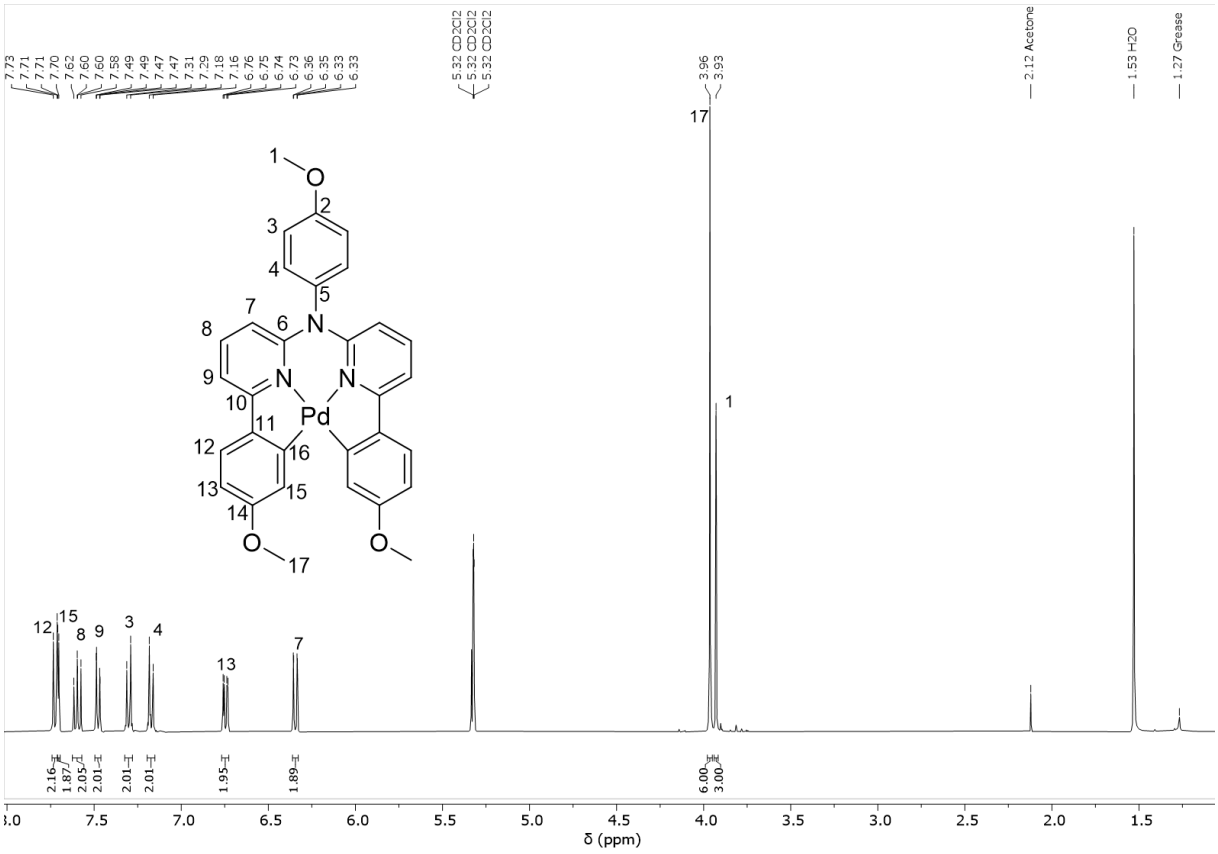

Figure S21. ^{1}H-NMR spectrum (400 MHz, CD_2Cl_2) of **PdL_{OMe}**.

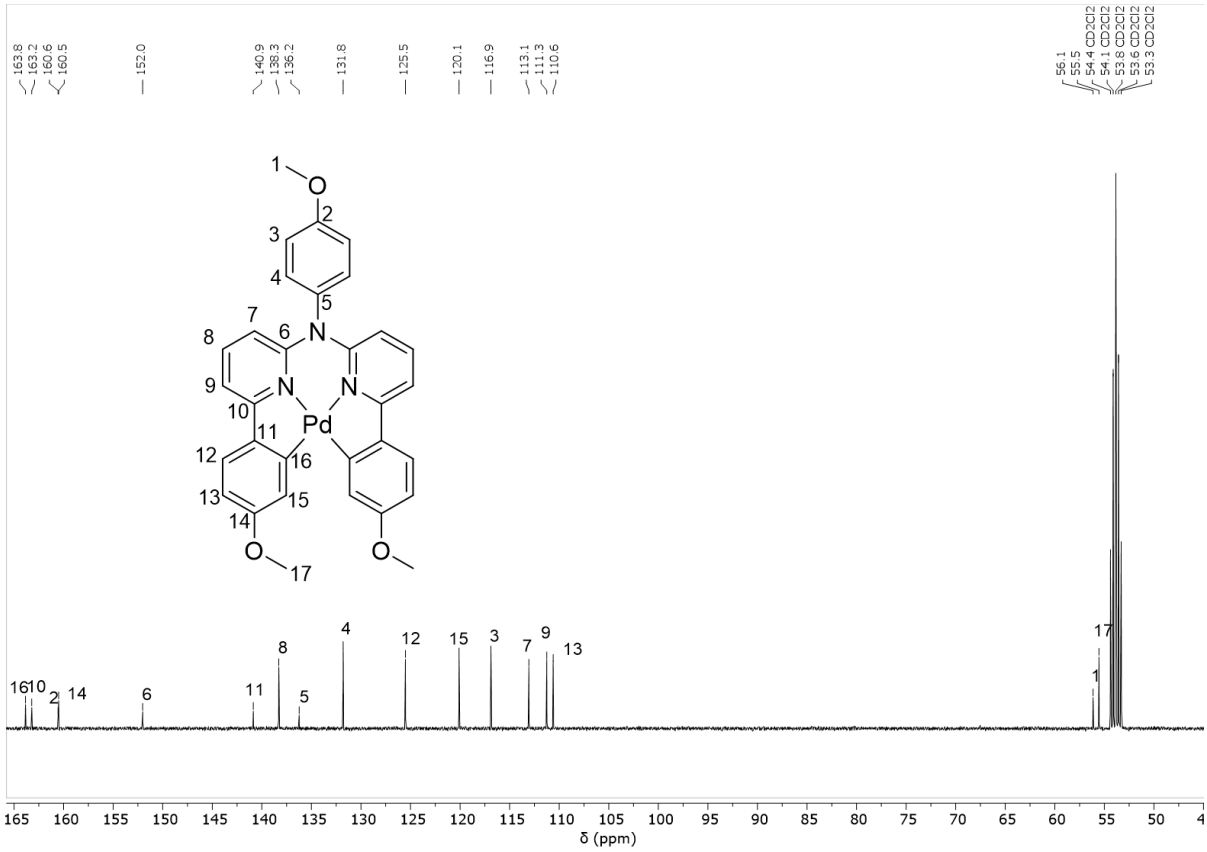

Figure S22. ^{13}C-{^{1}H}-NMR spectrum (126 MHz, CD_2Cl_2) of **PdL_{OMe}**.

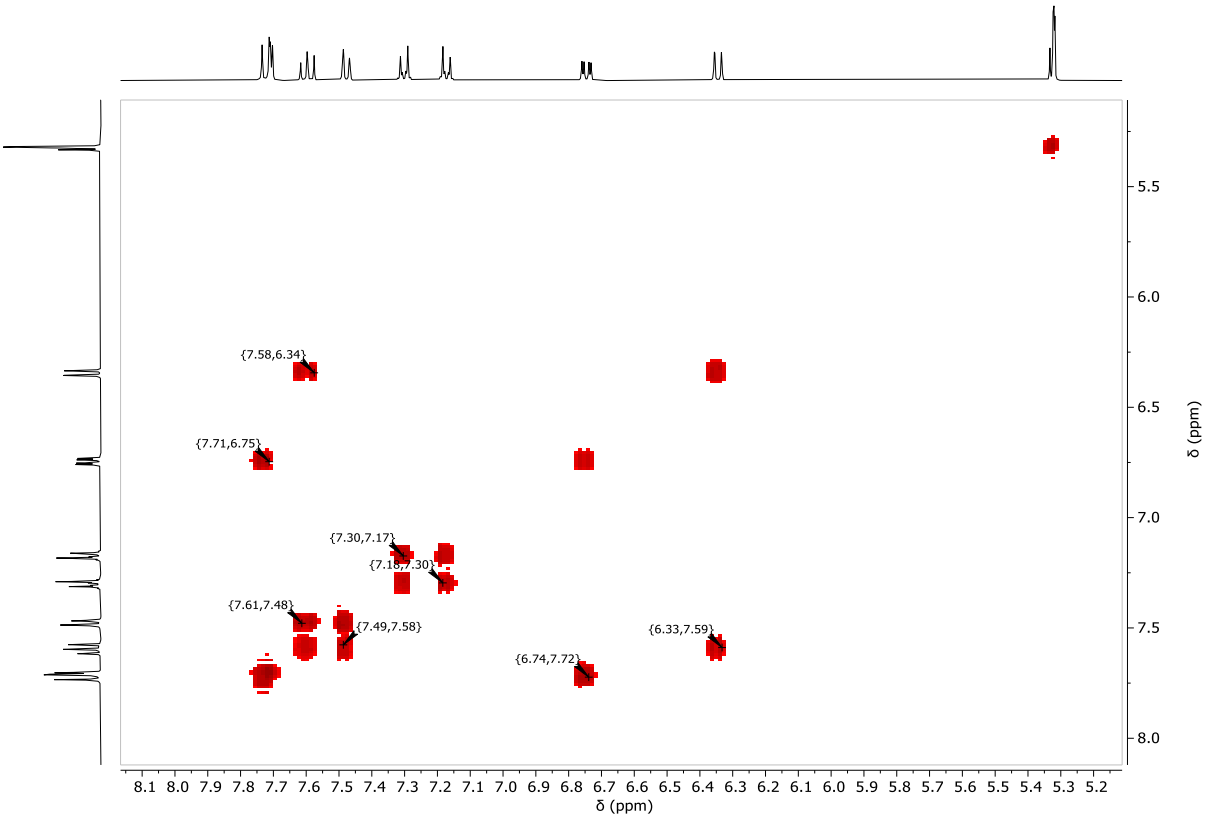

Figure S23. $^{1}H/^{1}H$-COSY-NMR spectrum (400 MHz/400 MHz, CD_2Cl_2) of **PdL_{OMe}**.

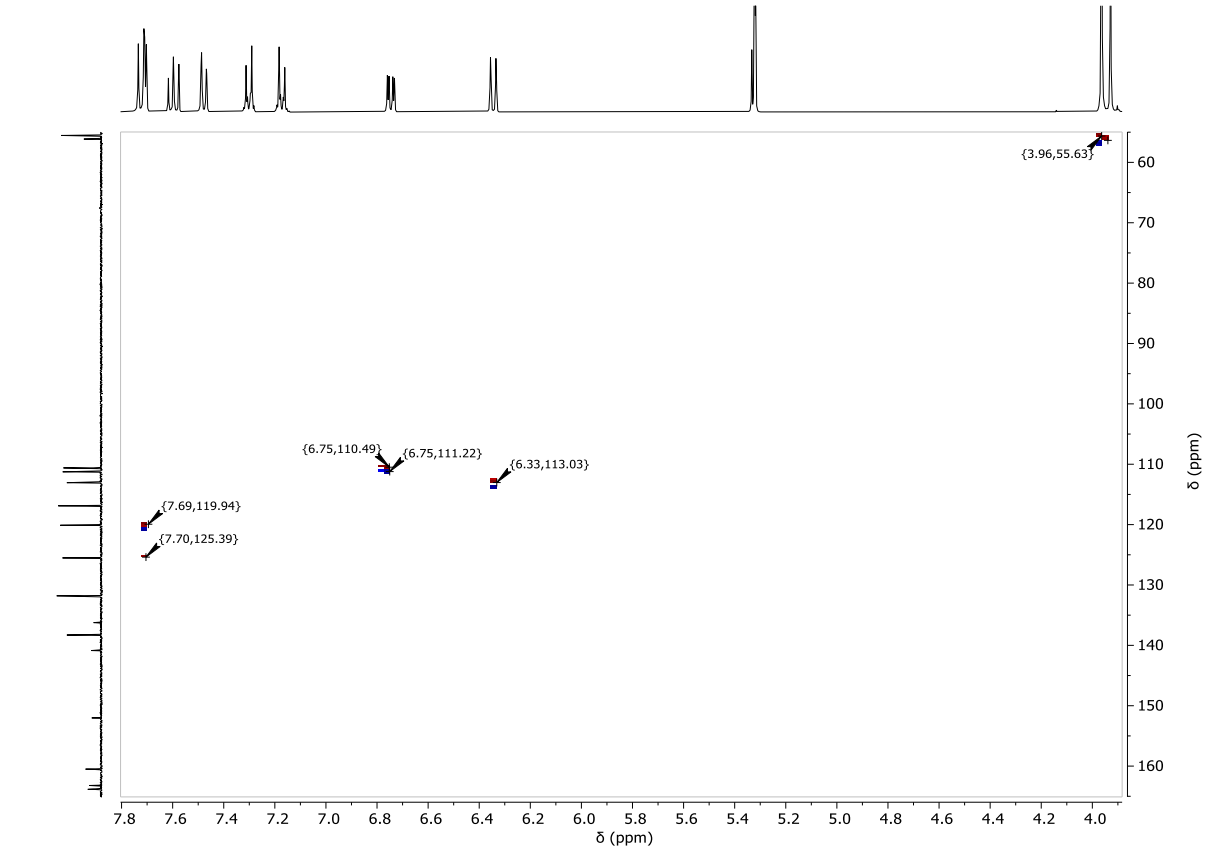

Figure S24. $^{1}H/^{13}C$-gHSQC-NMR spectrum (400 MHz/126 MHZ, CD_2Cl_2) of **PdL_{OMe}**.

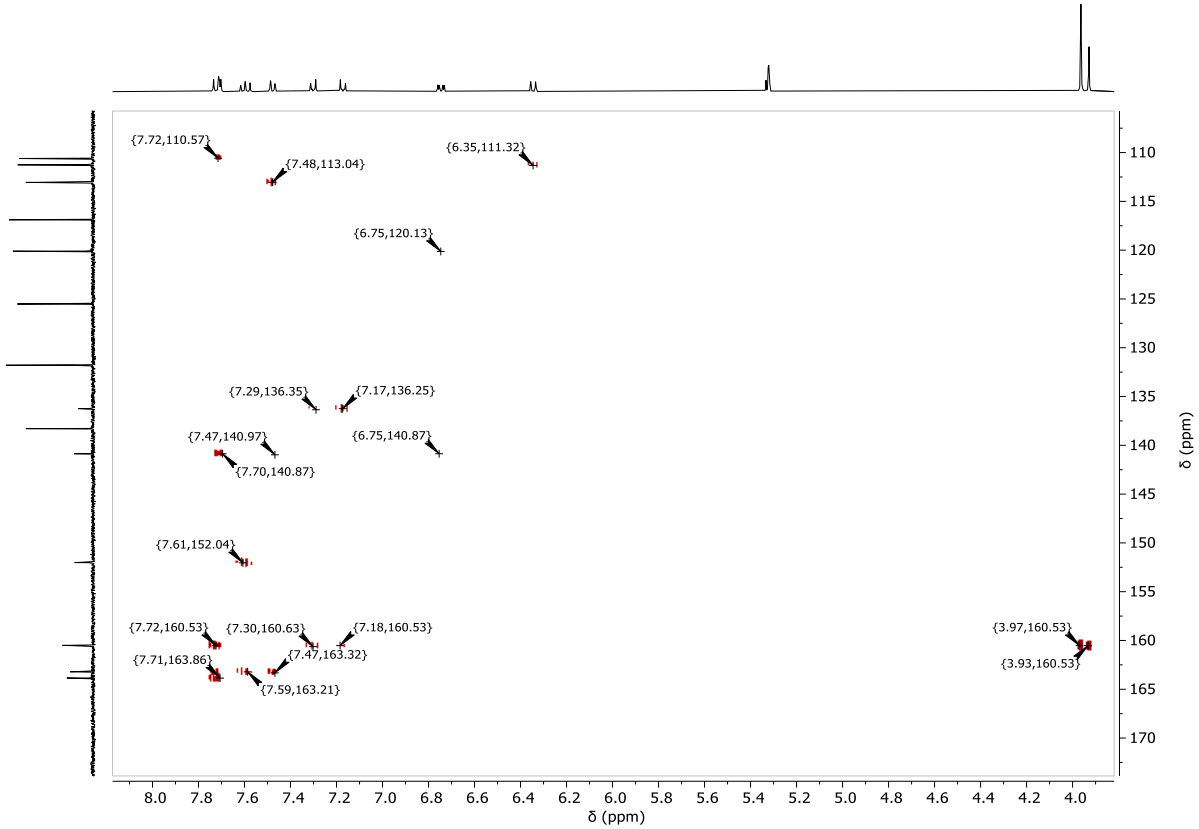

Figure S25. $^{1}H/^{13}C$-gHMBC-NMR spectrum (400 MHz/126 MHz, CD_2Cl_2) of **PdL_{OMe}**.

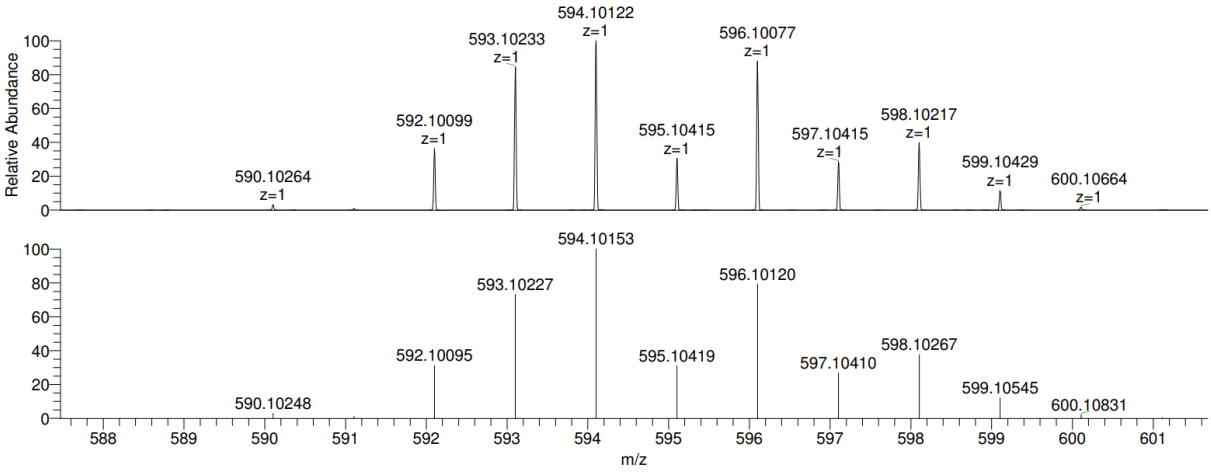

Figure S26. ESI-MS (MeOH) of **PdL_{OMe}**.

PtL_{OHex}

In a 50 mL two-necked flask, **L_{OHex}** (62 mg, 0.10 mmol) and K_2PtCl_4 (42 mg, 42 mmol) were suspended using 35 mL of acetic acid. The mixture was degassed by bubbling with Ar at room temperature for 15 min, then heated up to 130 °C under Ar flux and reacted for 72 h. The mixture was cooled down to room temperature and the solvent evaporated. The crude product was adsorbed onto silica gel and purified by column chromatography using cyclohexane/CH_2Cl_2 as eluent (1:1 to 1:3) to yield a yellow solid (35 mg, 43 %).

^{1}H NMR (500 MHz, CD_2Cl_2): δ = 7.84 (d, *J* = 2.6 Hz, 2H), 7.74 (d, *J* = 8.8 Hz, 2H), 7.67 (dd, *J* = 8.8, 7.7 Hz, 2H), 7.47 (d, *J* = 7.3 Hz, 2H), 7.35 – 7.28 (m, 2H), 7.23 – 7.14 (m, 2H), 6.75 (dd, *J* = 8.5, 2.6 Hz, 2H), 6.45 (dd, *J* = 8.6, 1.0 Hz, 2H), 4.20 (t, *J* = 6.6 Hz, 4H), 3.94 (s, 3H), 1.93 – 1.84 (m, 4H), 1.62 – 1.50 (m, 4H), 1.42 (td, *J* = 7.7, 3.8 Hz, 8H), 1.01 – 0.90 (m, 6H).

^{13}C NMR (126 MHz, CD_2Cl_2): δ = 163.6, 160.1, 160.0, 151.7, 149.0, 139.6, 136.7, 135.8, 131.3, 125.3, 119.8, 116.4, 112.8, 110.8, 110.3, 67.8, 55.7, 31.7, 29.6, 25.9, 22.7, 13.8.

EM (ESI+, MeOH, m/z): calcd. for $[M + H]^+$, 823.31849; found, 823.31991; calcd. for $[M+Na]^+$, 835.30044; found, 835.30190.

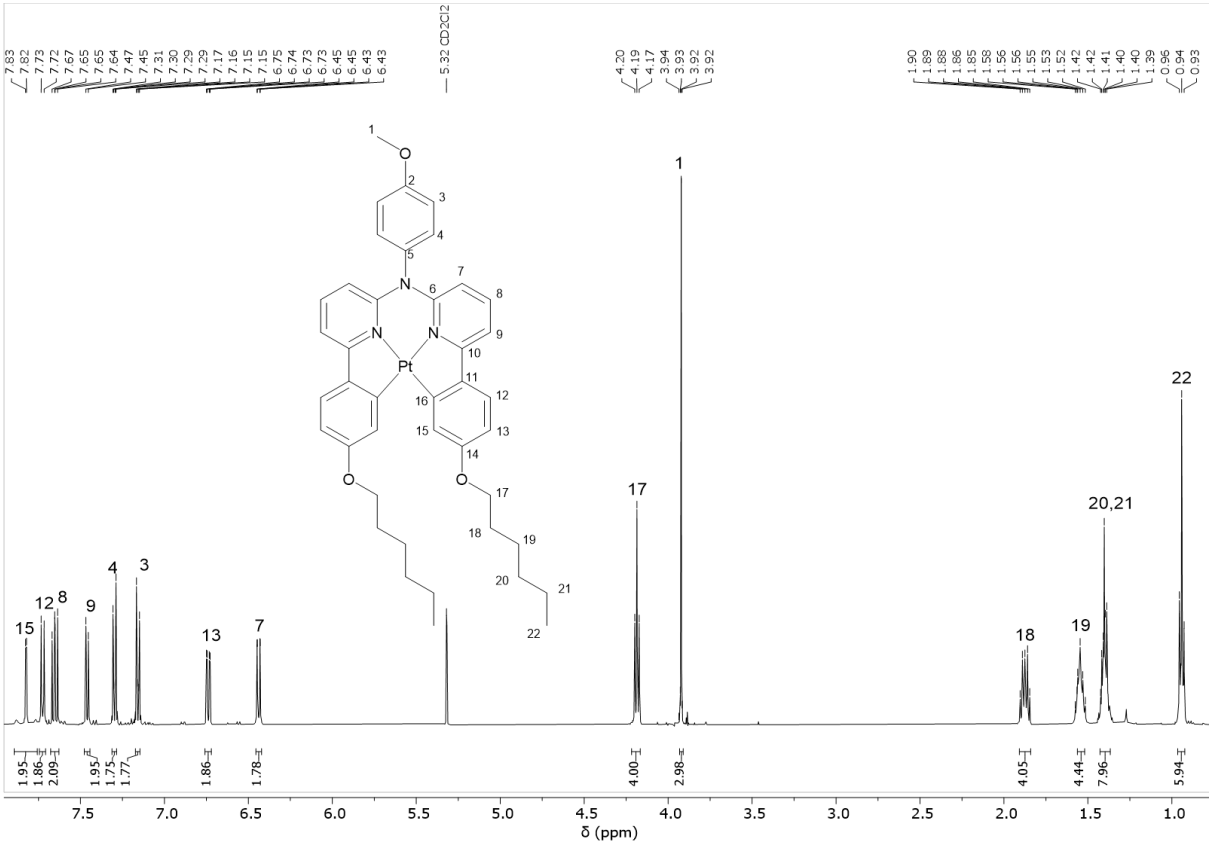

Figure S27. ^{1}H-NMR spectrum (500 MHz, CD_2Cl_2) of **PtL_{OHex}**.

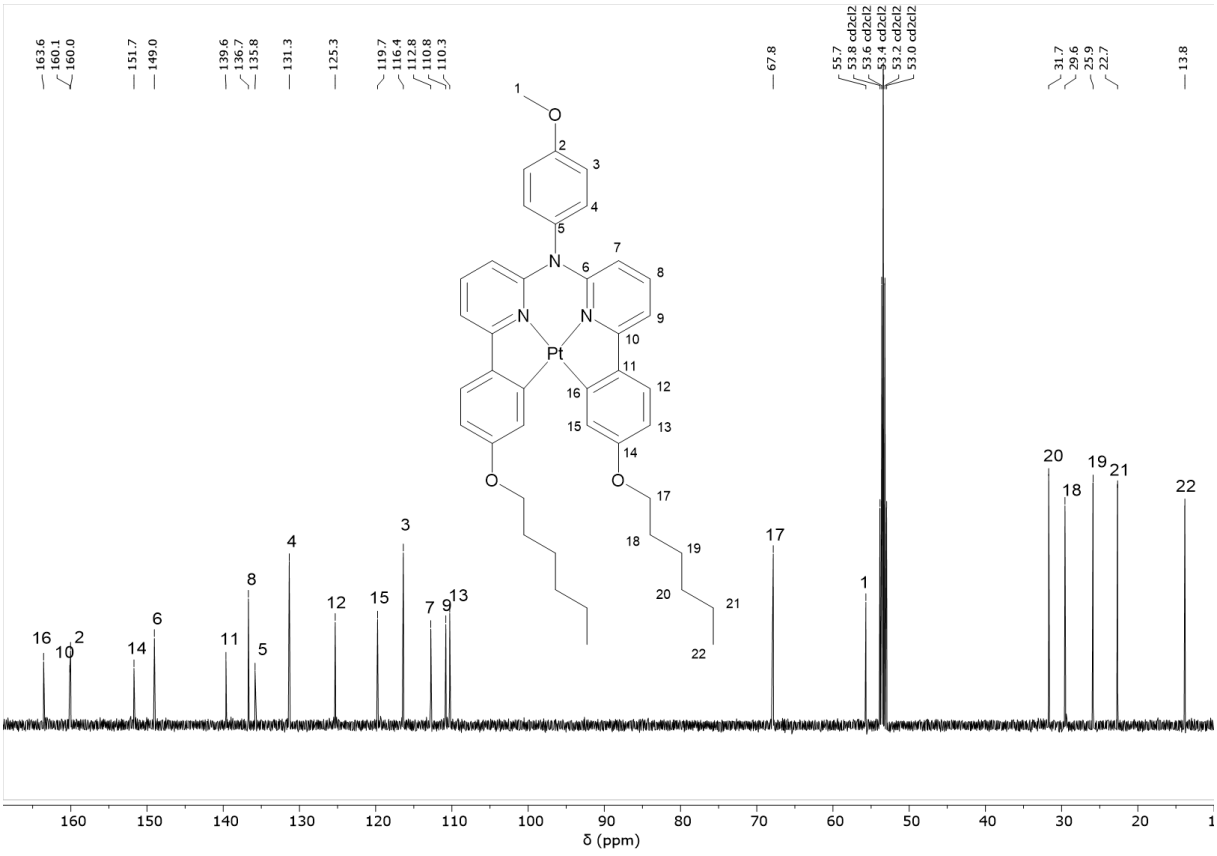

Figure S28. ^{13}C-{^{1}H}-NMR spectrum (126 MHz, CD_2Cl_2) of **PtL_{OHex}**.

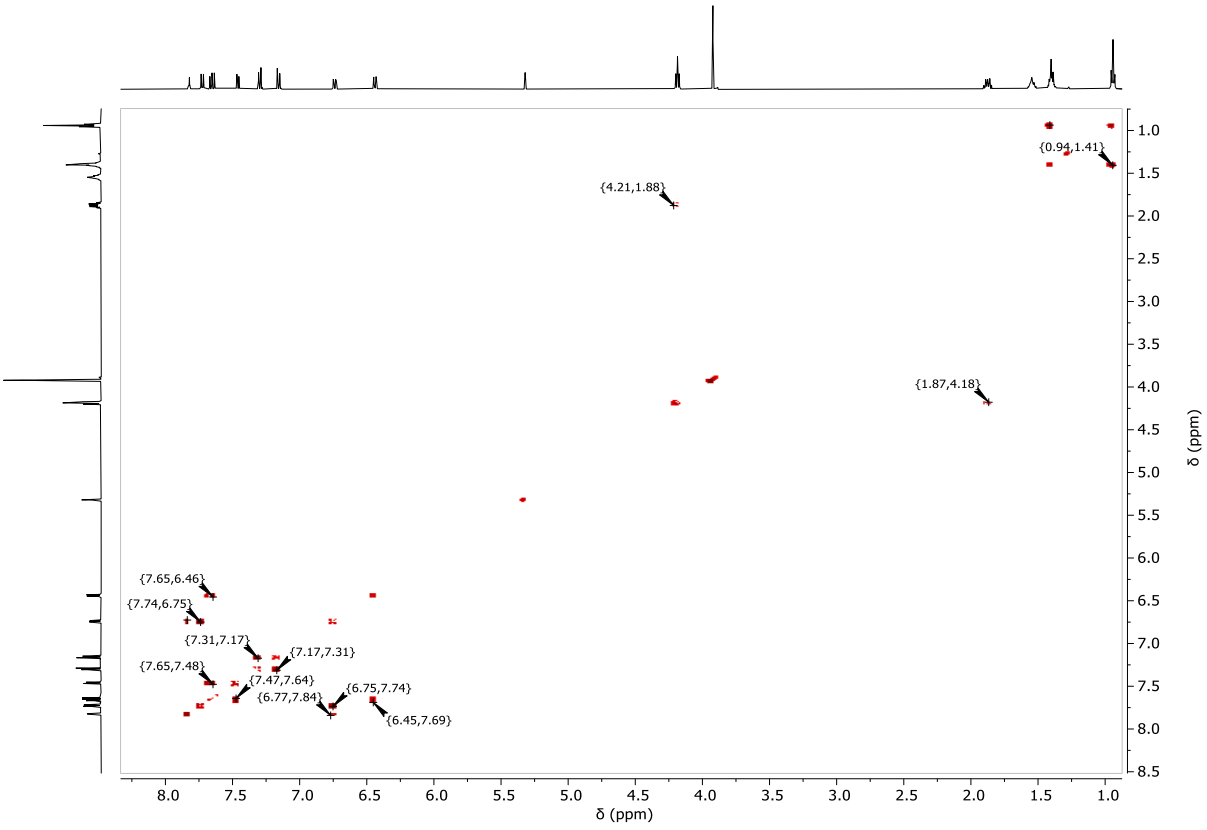

Figure S29. $^{1}H/^{1}H$-COSY-NMR spectrum (500 MHz/500 MHz, CD_2Cl_2) of **PtL_{OHex}**.

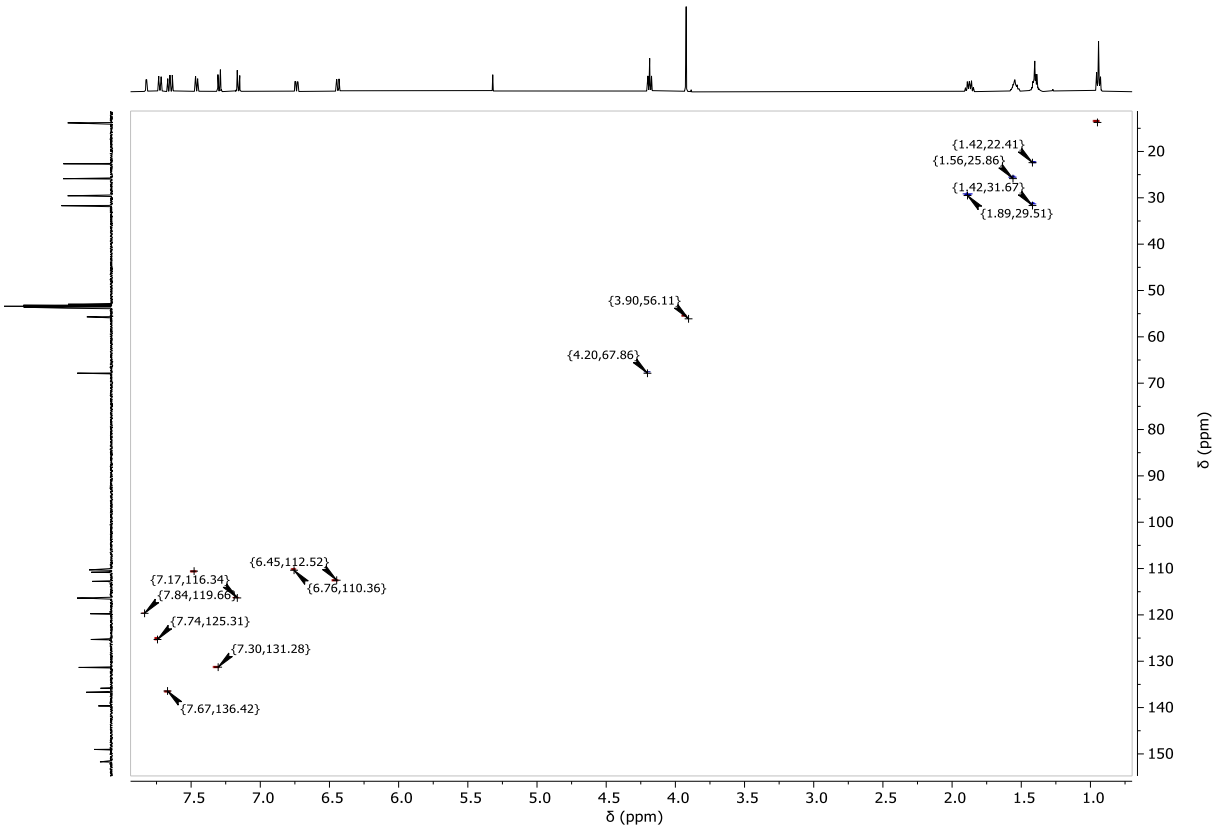

Figure S30. $^{1}H/^{13}C$-gHSQC-NMR spectrum (500 MHz/126 MHZ, CD_2Cl_2) of **PtL_{OHex}**.

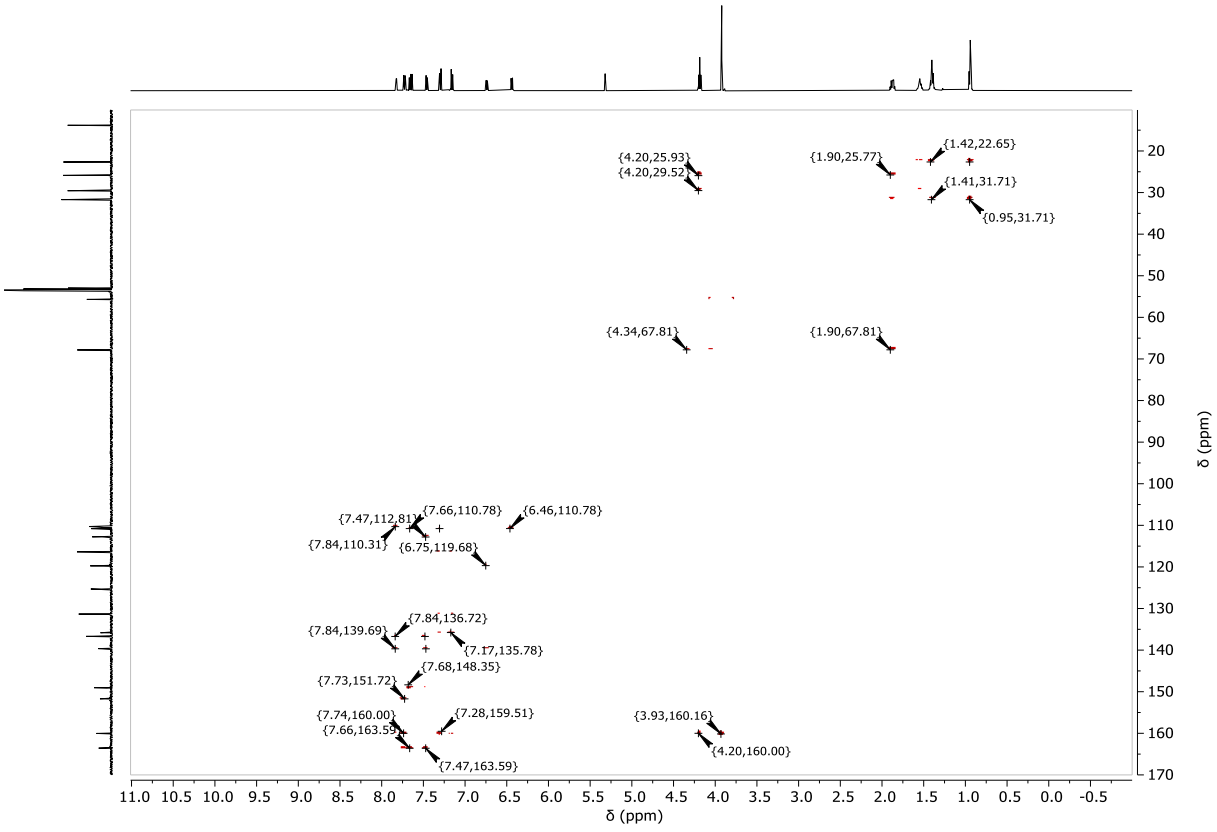

Figure S31. $^{1}H/^{13}C$-gHMBC-NMR spectrum (500 MHz/126 MHz, CD_2Cl_2) of **PtL_{OHex}**.

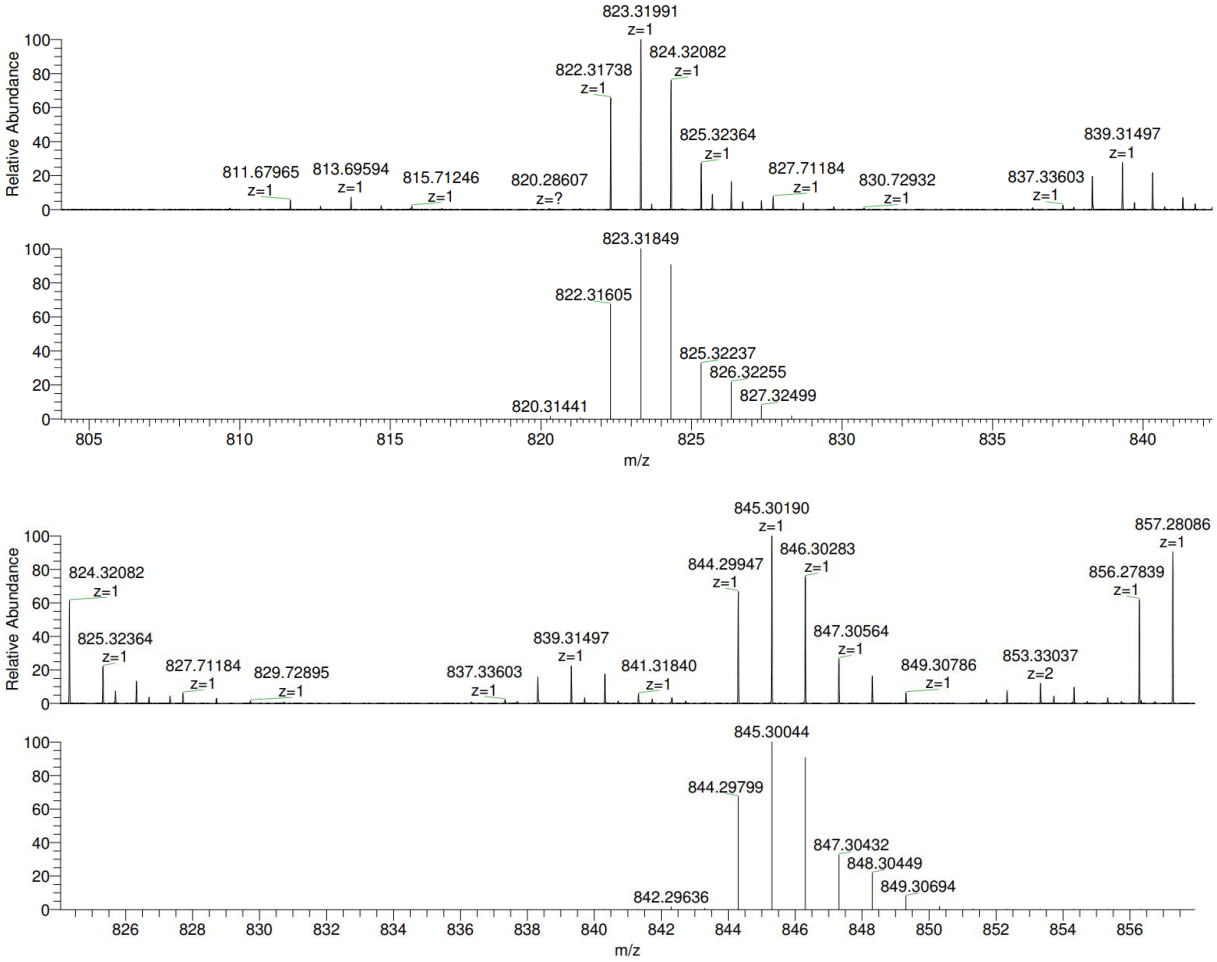

Figure S32. ESI-MS (MeOH) of **PtL_{OHex}**.

PdL_{OHex}

In a 50 mL two-necked flask, **L_{OHex}** (188.5 mg, 0.30 mmol) and $Pd(OAc)_2$ (67.7 mg, 0.30 mmol) were suspended using 25 mL of acetic acid. The mixture was degassed by bubbling with Ar at room temperature and the mixture was stirred at room temperature for 24 h. The temperature was raised up to 80 °C and reacted for 48 h. Finally, the temperature was increased up to 130 °C and the mixture reacted for 1 h. Then the mixture was cooled down to room temperature and the solvent evaporated. The crude product was adsorbed onto silica gel and purified by column chromatography using cyclohexane/CH_2Cl_2 as the eluent (1:1 to 1:3) to yield a pale brown solid (31 mg, 14 %).

^{1}H NMR (500 MHz, CD_2Cl_2): δ = 7.70 (d, J = 2.6 Hz, 2H), 7.68 (d, J = 8.6 Hz, 2H), 7.55 – 7.48 (m, 1H), 7.41 (d, J = 7.5 Hz, 2H), 7.24 (d, J = 8.8 Hz, 1H), 7.11 (d, J = 8.9 Hz, 1H), 6.72 (dd, J = 8.5, 2.5 Hz, 2H), 6.27 (d, J = 8.6 Hz, 1H), 4.17 (t, J = 6.6 Hz, 3H), 3.89 (s, 3H), 1.92 – 1.82 (m, 2H), 1.54 (q, J = 7.3 Hz, 2H), 1.46 – 1.34 (m, 4H), 0.95 (t, J = 6.8 Hz 3H).

^{13}C NMR (126 MHz, CD_2Cl_2): δ = 164.1, 163.3, 160.6, 160.2, 152.1, 140.8, 138.3, 136.4, 132.0, 125.7, 120.7, 116.9, 113.1, 111.3, 111.3, 68.4, 56.2, 54.4, 54.2, 54.0, 53.8, 53.6, 32.3, 30.2, 26.5, 23.3, 14.4.

EM (ESI+, MeOH, m/z): calcd. for $[M + H]^+$, 734.25835; found, 734.25769; calcd. for $[M+Na]^+$, 756.24030; found, 756.24005.

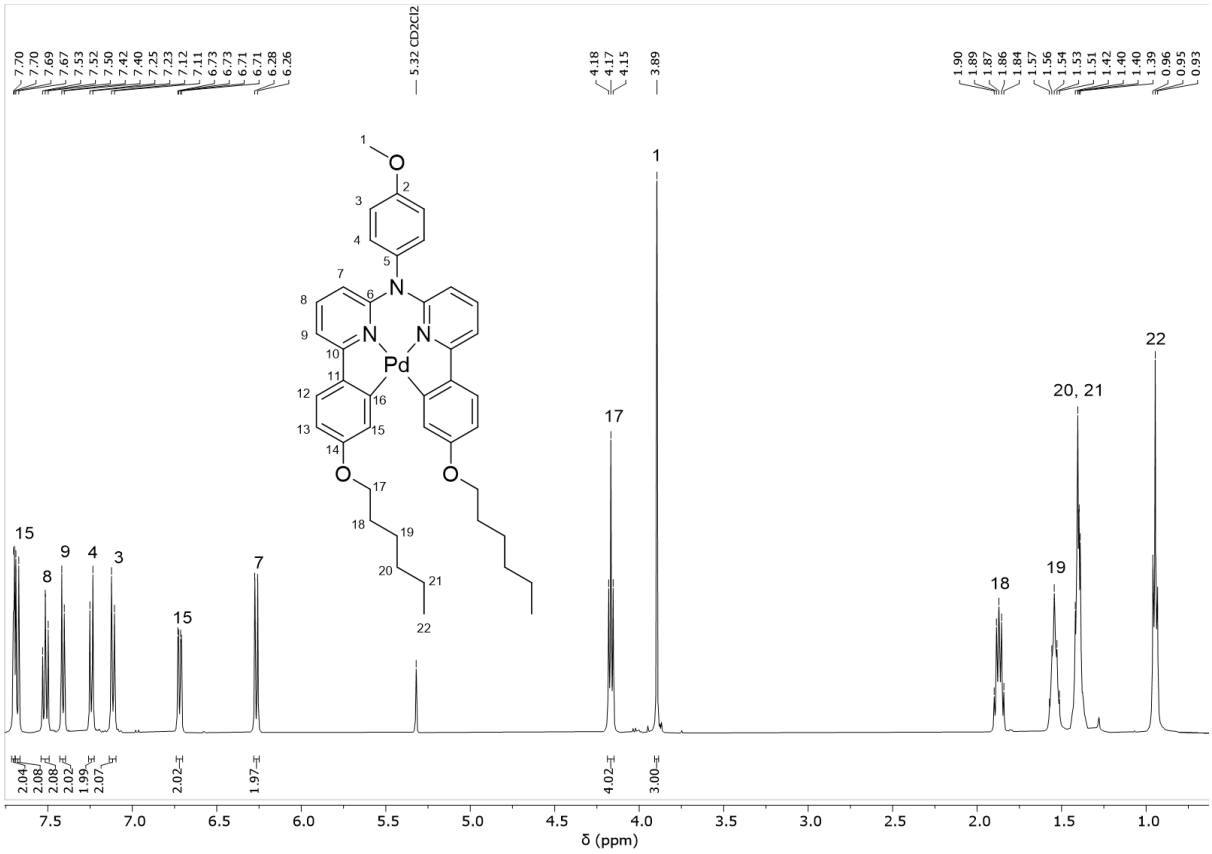

Figure S33. ^{1}H-NMR spectrum (500 MHz, CD_2Cl_2) of **PdL_{OHex}**.

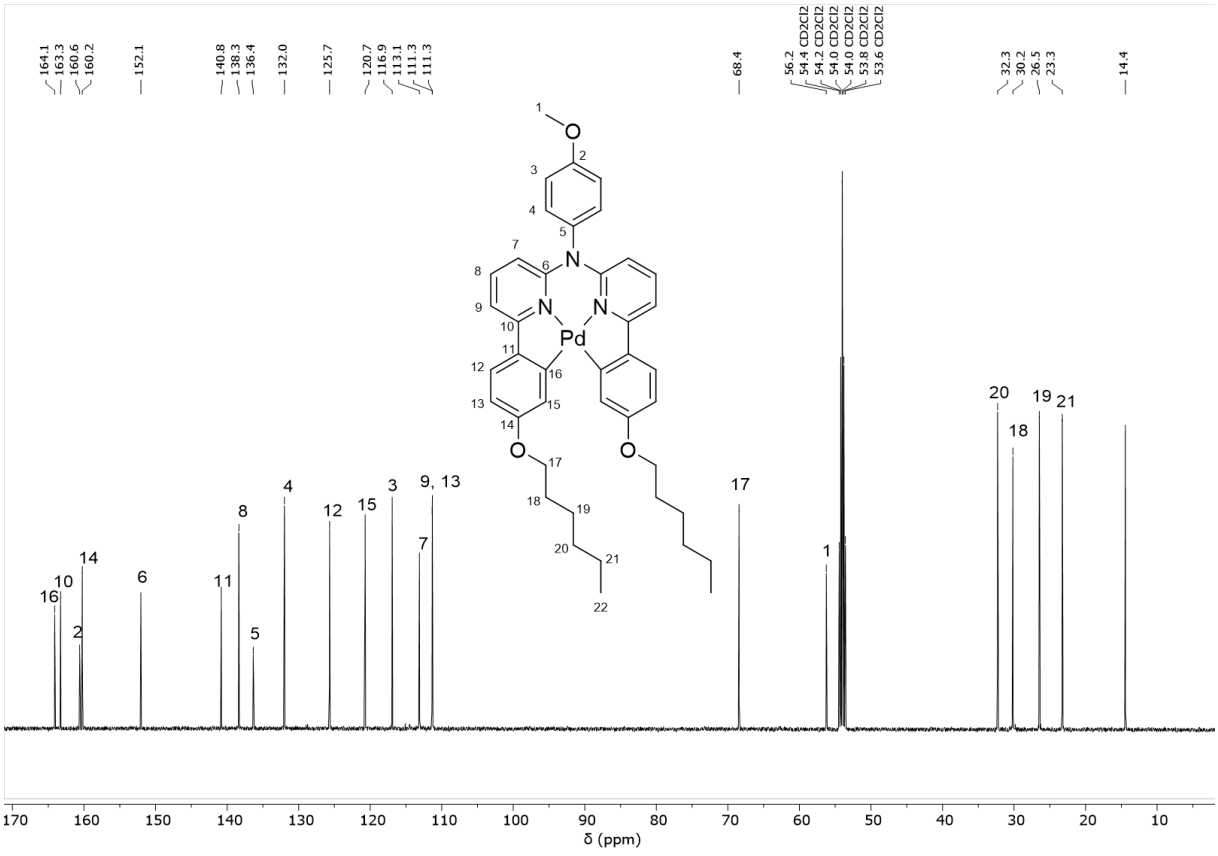

Figure S34. ^{13}C-{^{1}H}-NMR spectrum (126 MHz, CD_2Cl_2) of **PdL_{OHex}**.

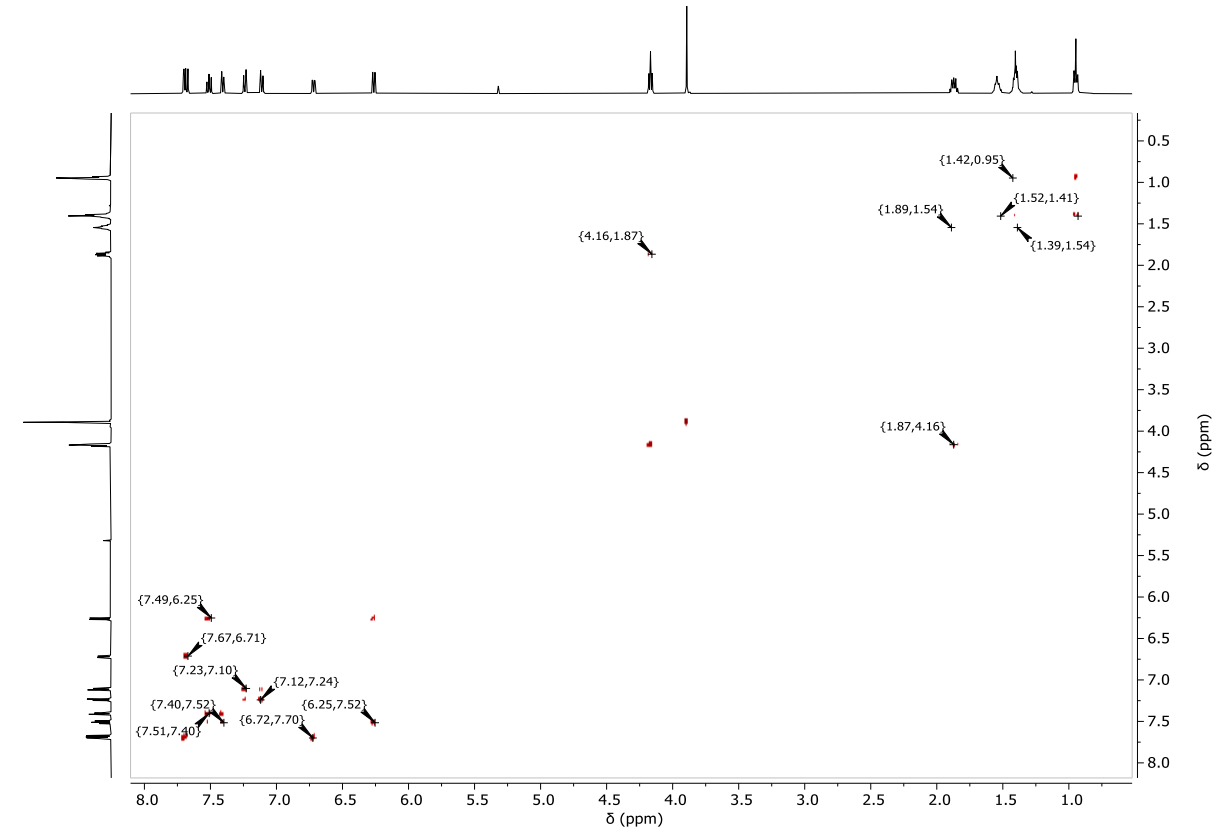

Figure S35. $^{1}H/^{1}H$-COSY-NMR spectrum (500 MHz/500 MHz, CD_2Cl_2) of **PdL_{OHex}.**

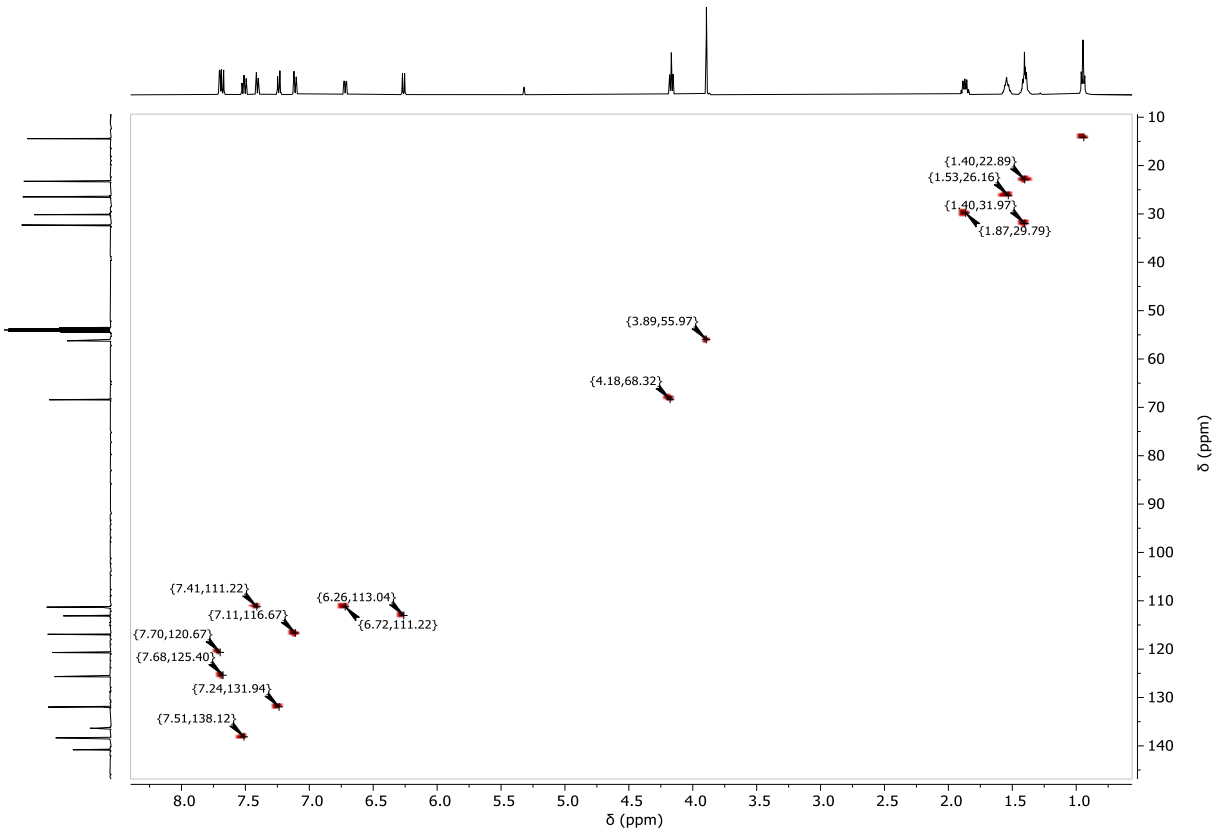

Figure S36. $^{1}H/^{13}C$-gHSQC-NMR spectrum (500 MHz/126 MHZ, CD_2Cl_2) of **PdL_{OHex}.**

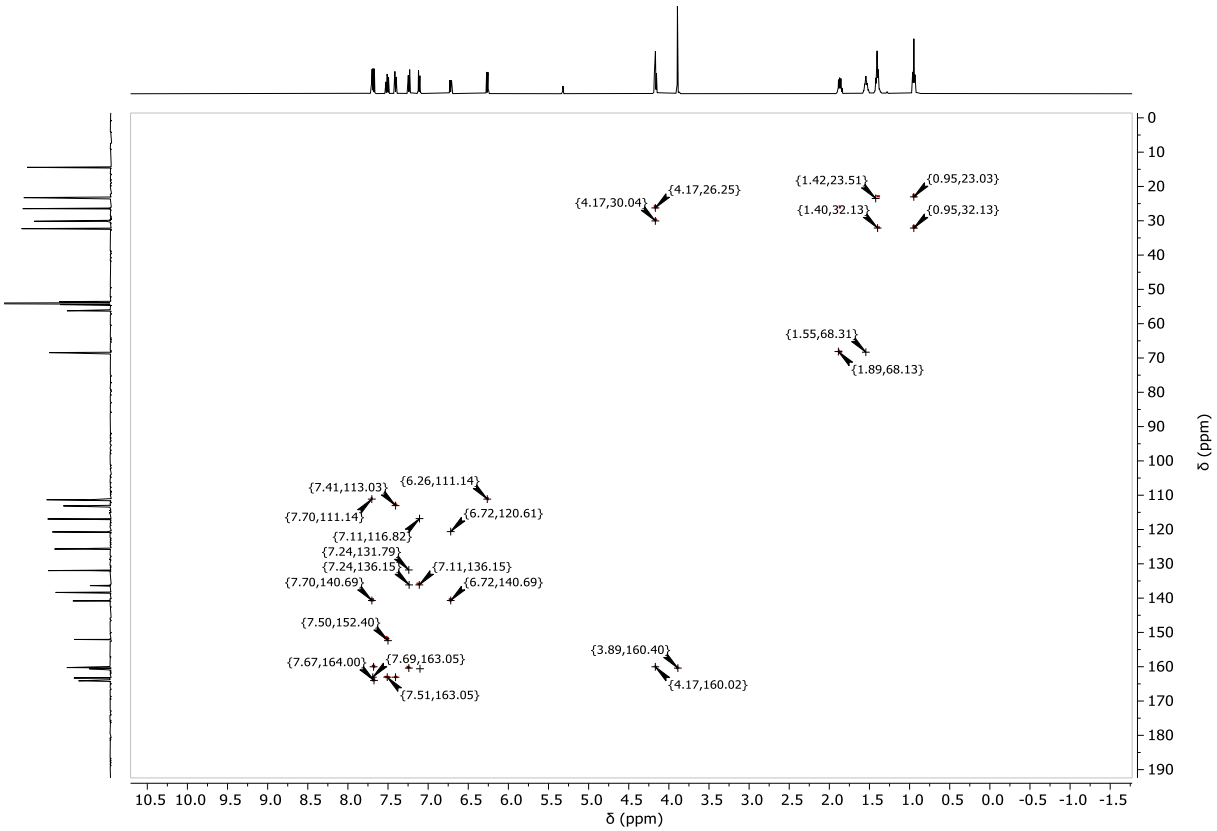

Figure S37. $^{1}H/^{13}C$-gHMBC-NMR spectrum (500 MHz/126 MHz, CD_2Cl_2) of **PdL_{OHex}**.

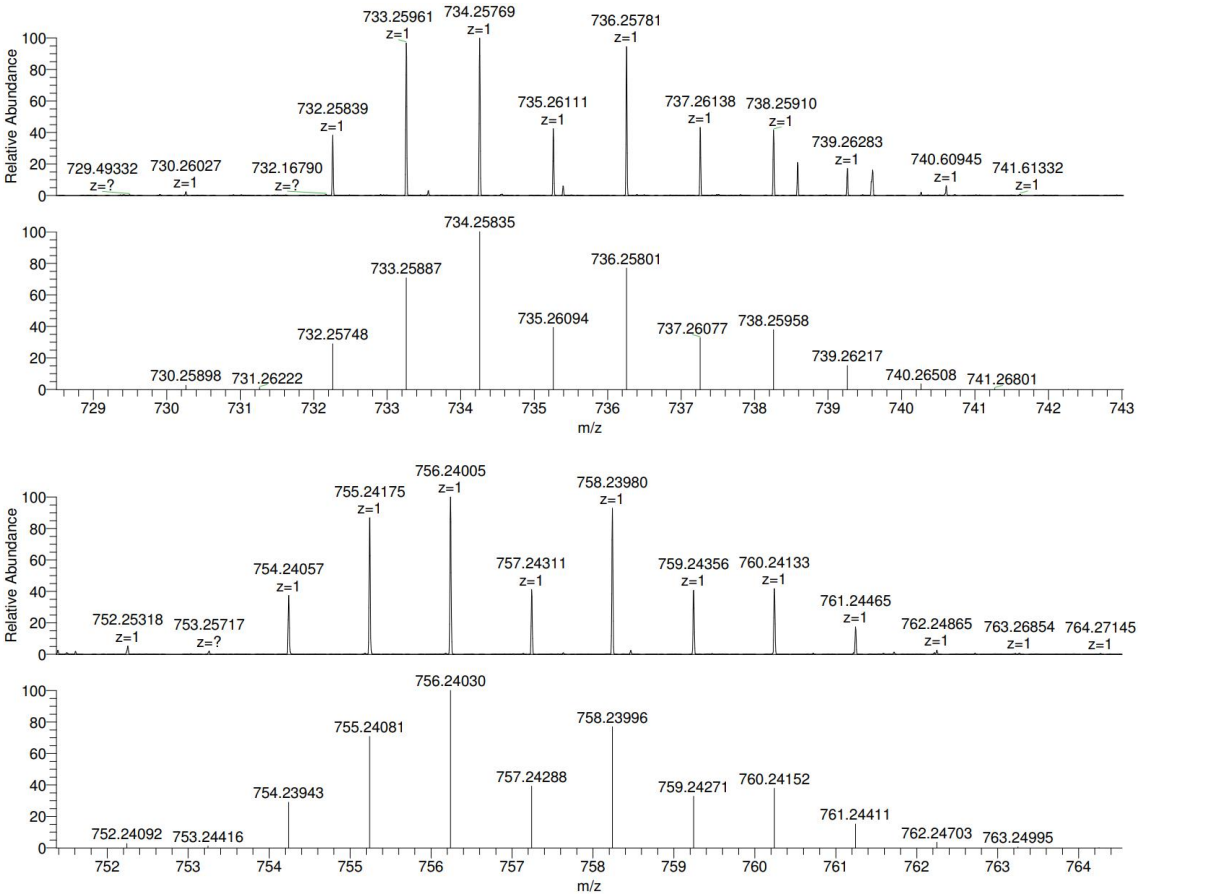

Figure S38. ESI-MS (MeOH) of **PdL_{OHex}**.

2) Crystallography

The data for X-ray diffractometric analysis was collected using graphite-monochromated Mo Kα radiation (λ = 0.71073 Å) on a Bruker Quazar diffractometer. The structures were solved by Direct Methods and refined by full-matrix least squares on F2 by using the programs *Shelxtl* and *Shelxl97*.

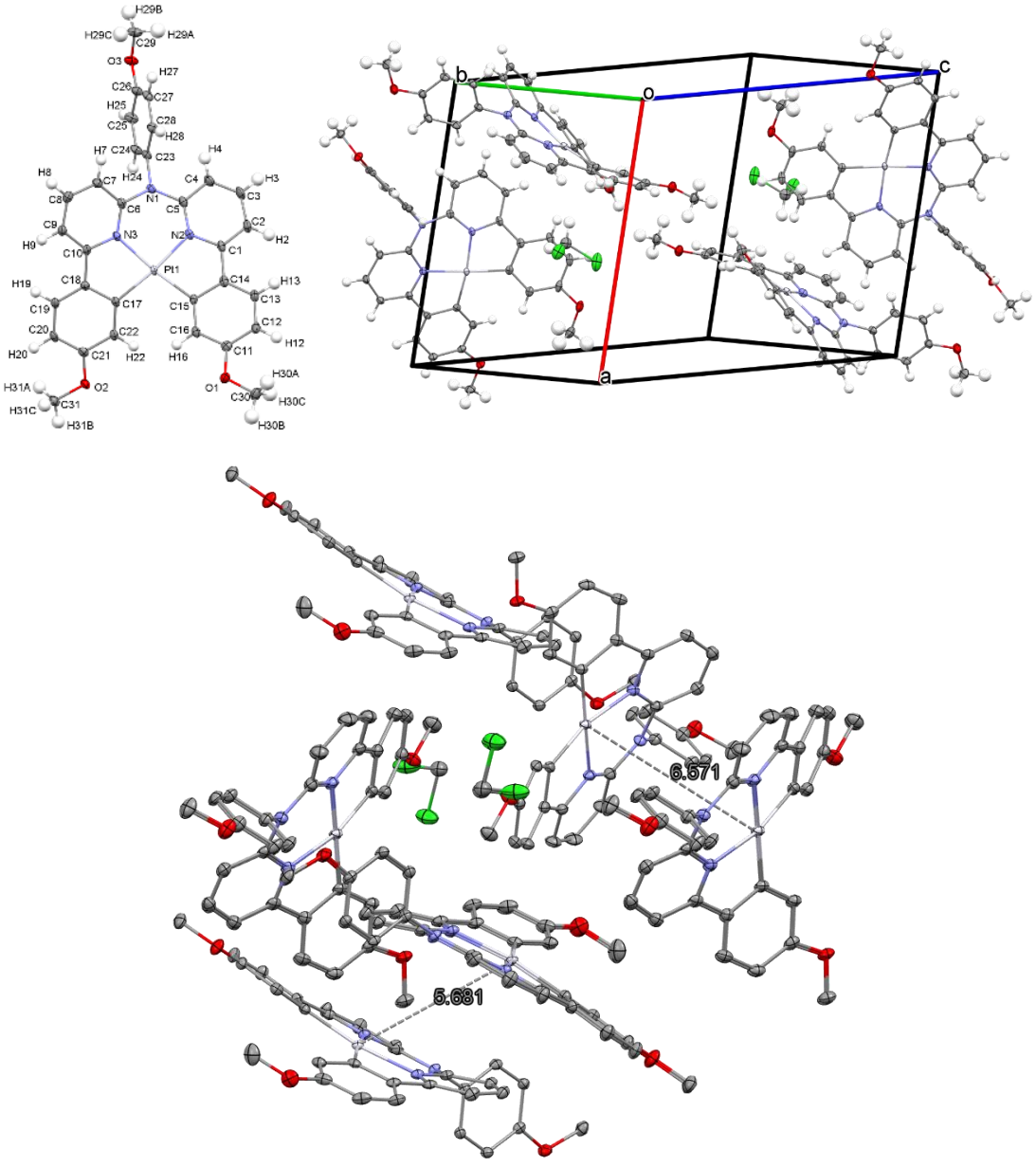

Figure S39. PtL_{OMe}: Molecular structure in the crystal (top left), unit cell (top right) and Pt-Pt distances (bottom; H atoms were omitted for clarity). Thermal displacement ellipsoids are drawn at a 50 % probability.

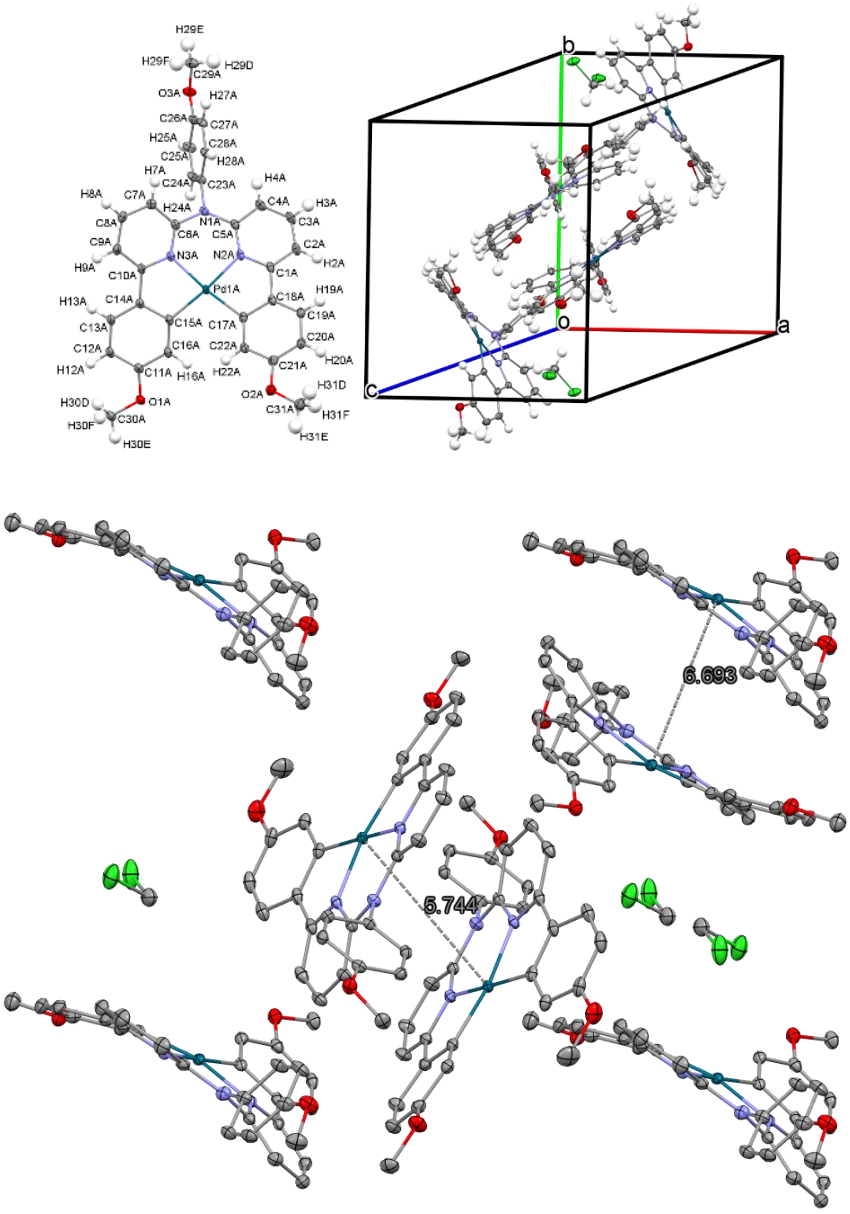

Figure S40. PdL_{OMe}: Molecular structure in the crystal (top left), unit cell (top right) and Pd-Pd distances (bottom; H atoms were omitted for clarity). Thermal displacement ellipsoids are drawn at a 50 % probability.

3) Photophysical characterization

Absorption spectra were measured with a Shimadzu UV-3600 I plus UV-VIS-NIR spectrophotometer. In all measurements, matched quartz (Hellma®) cuvettes were used. Photoluminescence quantum yields were measured with a Hamamatsu Photonics absolute PL quantum yield measurement system (C9920-02) equipped with a L9799-01 CW Xe light source (150 W), a monochromator, a C7473 photonic multi-channel analyzer, an integrating sphere and employing U6039-05 software (Hamamatsu Photonics, Ltd., Shizuoka, Japan).

Steady-state excitation and emission spectra were recorded on a FluoTime 300 spectrometer from PicoQuant equipped with: a 300 W ozone-free Xe lamp (250-900 nm), a 10 W Xe flash-lamp (250-900 nm, pulse width *ca*. 1 µs) with repetition rates of 0.1 – 300 Hz, double excitation monocromators (Czerny-Turner type, grating with 1200 lines/mm, blaze wavelength: 300 nm), diode lasers (pulse width < 80 ps) operated by a computer-controlled laser driver PDL-828 "Sepia II" (repetition rate up to 80 MHz, burst mode for slow and weak decays), two double-grating emission monochromators (Czerny-Turner, selectable gratings blazed at 500 nm with 2.7 nm/mm dispersion and 1200 lines/mm, or blazed at 1200 nm with 5.4 nm/mm dispersion and 600 lines/mm) with adjustable slit width between 25 µm and 7 mm, Glan-Thompson polarizers for excitation (after the Xe-lamps) and emission (after the sample). Different sample holders (Peltier-cooled mounting unit ranging from -15 to 110 °C or an adjustable front-face sample holder), along with two detectors (namely a PMA Hybrid-07 from PicoQuant with transit time spread FWHM < 50 ps, 200 – 850 nm, or a H10330C-45-C3 NIR detector with transit time spread FWHM 0.4 ns, 950-1700 nm from Hamamatsu) were used. Steady-state spectra and photoluminescence lifetimes were recorded in TCSPC mode by a PicoHarp 300 (minimum base resolution 4 ps) or in MCS mode by a TimeHarp 260 (where up to several ms can be traced). Emission and excitation spectra were corrected for source intensity (lamp and grating) by standard correction curves. For samples with lifetimes in the ns order, an instrument response function calibration (IRF) was performed using a diluted Ludox® dispersion. Lifetime analysis was performed using the commercial EasyTau 2 software (PicoQuant). The quality of the fit was assessed by minimizing the reduced chi squared function (χ^2) and visual inspection of the weighted residuals and their autocorrelation.

Photoluminescence lifetime imaging microscopy (PLIM) was recorded on a fluorescence microscope (IX 73 from Olympus) with a complete confocal system and a laser combining unit (LCU), an inverted microscope body and a multichannel detection unit (MicroTime 200, PicoQuant) equipped with diode lasers (providing adjustable output power and repetition rates up to 80 MHz inside a compact fibre couple unit with wavelengths between 375 and 900 nm). For beam diagnostics, a charge-couple device (CCD) camera and a photodiode were available in the main optical unit (MOU) of the microscope. The MOU is equipped with two detectors, namely a hybrid photomultiplier-based single photon counting module (PMA Hybrid 40, PicoQuant) and a SPAD-based photon counting module (SPCM-AQR-14, Perkin-Elmer). Different band-pass (BP) and low-pass (LP) filters were placed before these detectors on demand to acquire lifetime maps. Data acquisition is based on the unique time-tagged time-resolved (TTTR) measurement mode, where simultaneous data acquisition on two channels is possible. Data were processed and analysed with the SymphoTime 64 (PicoQuant) software. In order to couple the MicroTime 200 and the FluoTime 300 instruments, a fiber coupler was employed. In this way, the spectrometer can be used to record either steady-state or time-resolved luminescence spectra and decays from a sample mounted on the microscope. Luminescence micrographs were acquired using the same microscope mentioned above, equipped with a X-CiteQ Lamp module (Excelitas Technologies) as excitation source and a UI-5580SE (IDS) digital camera. Different band pass (BP) and low pass (LP) cubes were using accordingly.

All solvents used were of spectrometric grade (Uvasol, Merck).

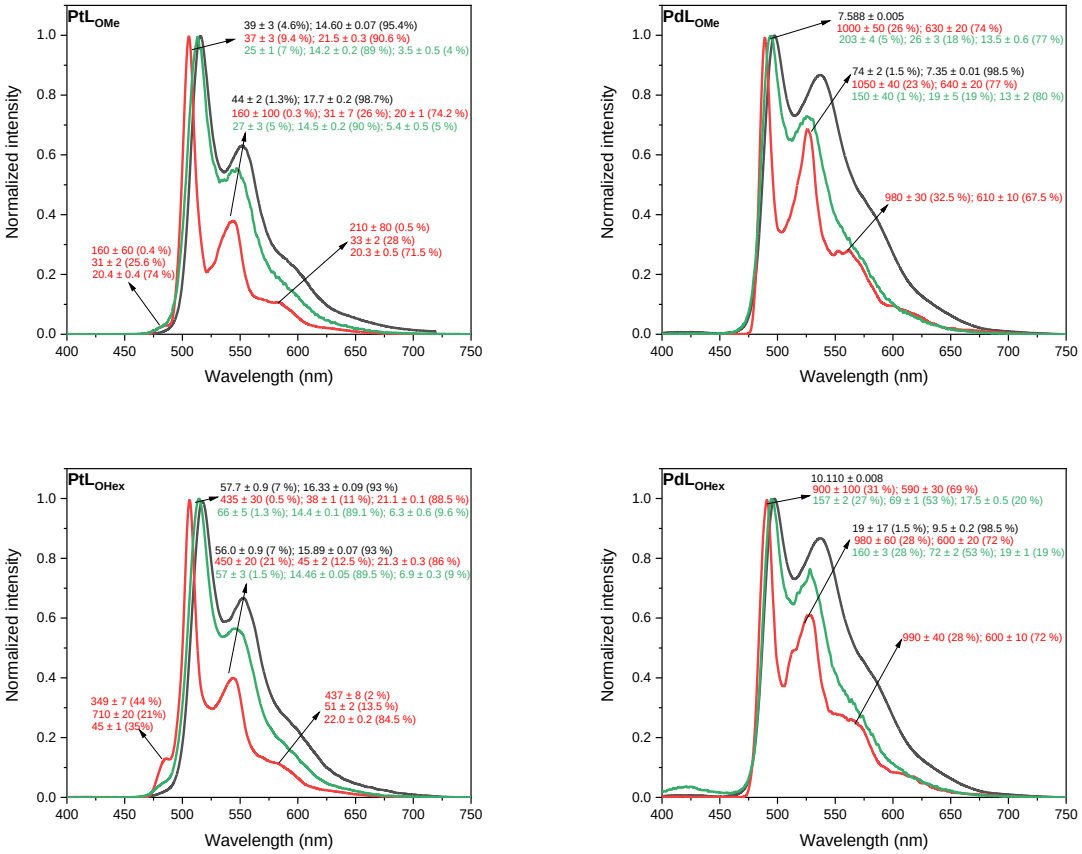

Condition	Maximum	PtL$_{OMe}$	PdL$_{OMe}$	PtL$_{OHex}$	PdL$_{OHex}$
Ar-purged	1st	15.75 ± 0.03	7.588 ± 0.005	19.21 ± 0.03	10.110 ± 0.008
	2nd	18.1 ± 0.1	8.34 ± 0.04	18.74 ± 0.04	9.69 ± 0.04
DCM/MeOH (1:1) glassy matrix at 77 K	1st	291 ± 2	724 ± 1	319 ± 1	765 ± 2
	2nd	22.94 ± 0.04	733 ± 1	25.0 ± 0.1	709 ± 2
	3rd	23.6 ± 0.1	732.4 ± 0.6	30.7 ± 0.2	709 ± 2
	4th	24.6 ± 0.2	-	34.5 ± 0.2	-
PMMA film at r.t.	1st	14.58 ± 0.02	96.7 ± 0.5	14.30 ± 0.04	83.1 ± 0.2
	2nd	14.68 ± 0.01	103.1 ± 0.3	14.29 ± 0.02	85.9 ± 0.2

Figure S41. Photoluminescence spectra in fluid DCM solutions at room temperature ($c = 10^{-5}$ M, black), in frozen DCM/MeOH 1:1 glassy matrices at 77 K ($c = 10^{-5}$ M, red) and in PMMA films at r.t.(c = 0.4 mg / 100 mg, green) for **PtL$_{OMe}$** (top left), **PdL$_{OMe}$** (top right), **PtL$_{OHex}$** (bottom left) and **PdL$_{OHex}$** (bottom right), λ_{exc} = 350 nm. Individual components of the amplitude-weighted average lifetimes (in µs) at each maximum and shoulders along with their relative amplitudes are shown. Table: amplitude-weighted average lifetimes (in µs) at each maximum and shoulders.

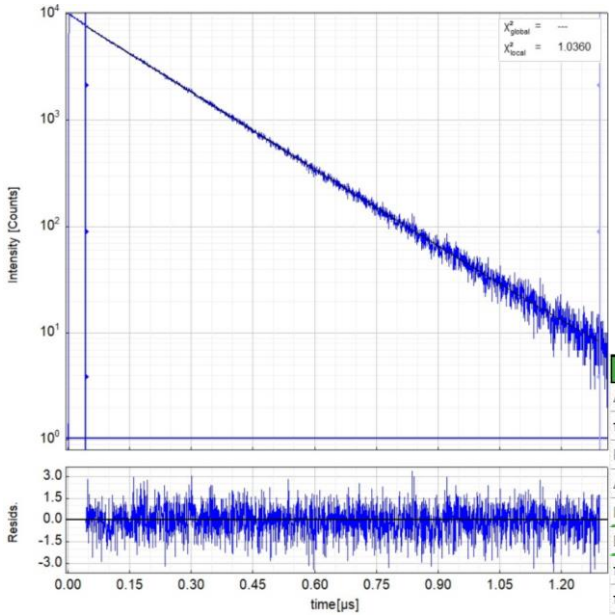

Parameter	Value	Error
A_1[kCnts/Chnl]	7.6517	± 0.0100
τ_1[ns]	179.74	± 0.20
I_1[kCnts]	2686.2	± 3.2
$A_{Rel\,1}$[%]	100.0000	± 0.0000
$I_{Rel\,1}$[%]	100.0000	± 0.0000
$Bkgr_{Dec}$[kCnts]	0.0010	± 0.0004
$\tau_{Av\,Int}$[ns]	179.74	± 0.20
$\tau_{Av\,Amp}$[ns]	179.74	± 0.20

Figure S42. Left: Time-resolved photoluminescence decay of **PtL_{OMe}** (10^{-5} M) in fluid air-equilibrated DCM at r.t., including the residuals (λ_{exc} = 376.7 nm, λ_{em} = 515 nm). Right: Fitting parameters including pre-exponential factors and confidence limits.

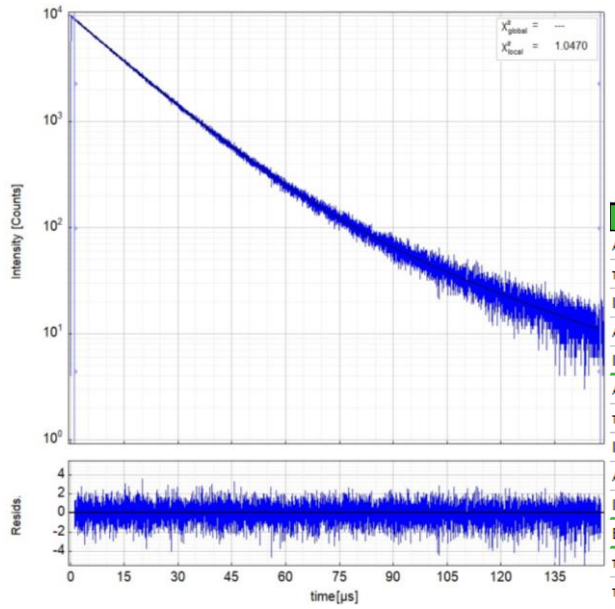

Parameter	Value	Error
A_1[kCnts/Chnl]	0.428	± 0.063
τ_1[ns]	39618	± 2489
I_1[kCnts]	1059	± 80
$A_{Rel\,1}$[%]	4.61	± 0.68
$I_{Rel\,1}$[%]	11.60	± 0.90
A_2[kCnts/Chnl]	8.844	± 0.059
τ_2[ns]	14597	± 72
I_2[kCnts]	8068	± 93
$A_{Rel\,2}$[%]	95.39	± 0.68
$I_{Rel\,2}$[%]	88.40	± 0.90
$Bkgr_{Dec}$[kCnts]	-0.0001	± 0.0015
$\tau_{Av\,Int}$[ns]	17499	± 168
$\tau_{Av\,Amp}$[ns]	15751	± 33

Figure S43. Left: Time-resolved photoluminescence decay of **PtL_{OMe}** in (10^{-5} M) in fluid Ar-purged DCM at r.t., including the residuals (λ_{exc} = 376.7 nm, λ_{em} = 515 nm). Right: Fitting parameters including pre-exponential factors and confidence limits.

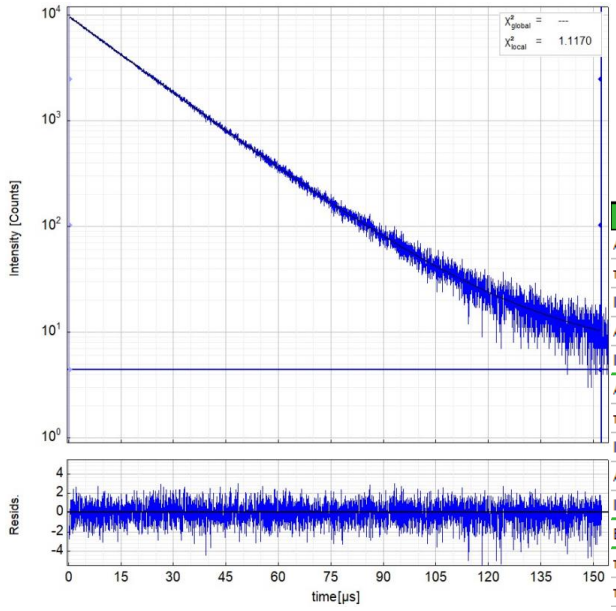

Parameter	Value	Error
A_1[kCnts/Chnl]	0.13	± 0.23
τ_1[ns]	44189	± 24445
I_1[kCnts]	173	± 168
$A_{Rel\,1}$[%]	1.3	± 2.4
$I_{Rel\,1}$[%]	3.2	± 3.2
A_2[kCnts/Chnl]	9.43	± 0.21
τ_2[ns]	17732	± 225
I_2[kCnts]	5228	± 181
$A_{Rel\,2}$[%]	98.7	± 2.4
$I_{Rel\,2}$[%]	96.8	± 3.2
$Bkgr_{Dec}$[kCnts]	0.0044	± 0.0033
$\tau_{Av\,Int}$[ns]	18582	± 544
$\tau_{Av\,Amp}$[ns]	18080	± 107

Figure S44. Left: Time-resolved photoluminescence decay of **PtL_{OMe}** in in fluid Ar-purged DCM at r.t., including the residuals (λ_{exc} = 376.7 nm, λ_{em} = 550 nm). Right: Fitting parameters including pre-exponential factors and confidence limits.

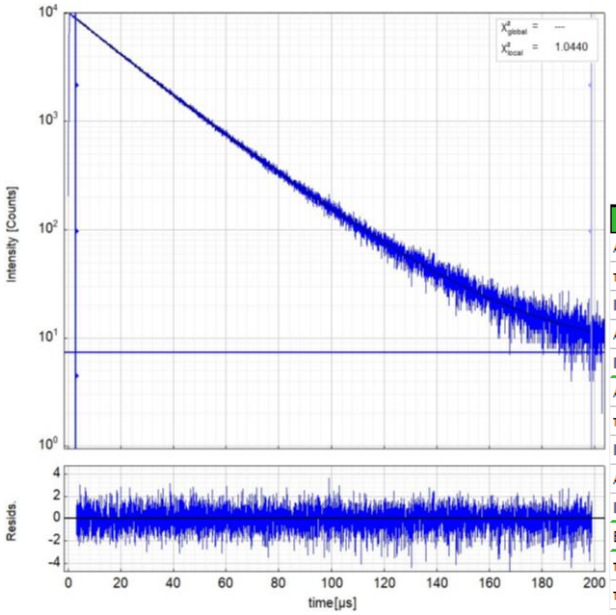

Parameter	Value	Error
A_1[kCnts/Chnl]	0.90	± 0.33
τ_1[ns]	37202	± 2823
I_1[kCnts]	1046	± 291
$A_{Rel\,1}$[%]	9.4	± 3.4
$I_{Rel\,1}$[%]	15.2	± 4.3
A_2[kCnts/Chnl]	8.70	± 0.32
τ_2[ns]	21466	± 314
I_2[kCnts]	5839	± 294
$A_{Rel\,2}$[%]	90.6	± 3.4
$I_{Rel\,2}$[%]	84.8	± 4.3
$Bkgr_{Dec}$[kCnts]	0.0056	± 0.0004
$\tau_{Av\,Int}$[ns]	23857	± 54
$\tau_{Av\,Amp}$[ns]	22941	± 44

Figure S45. Left: Time-resolved photoluminescence decay of **PtL_{OMe}** (10^{-5} M) in a frozen glassy matrix of DCM/MeOH (1:1) at 77 K, including the residuals (λ_{exc} = 376.7 nm, λ_{em} = 505 nm). Right: Fitting parameters including pre-exponential factors and confidence limits.

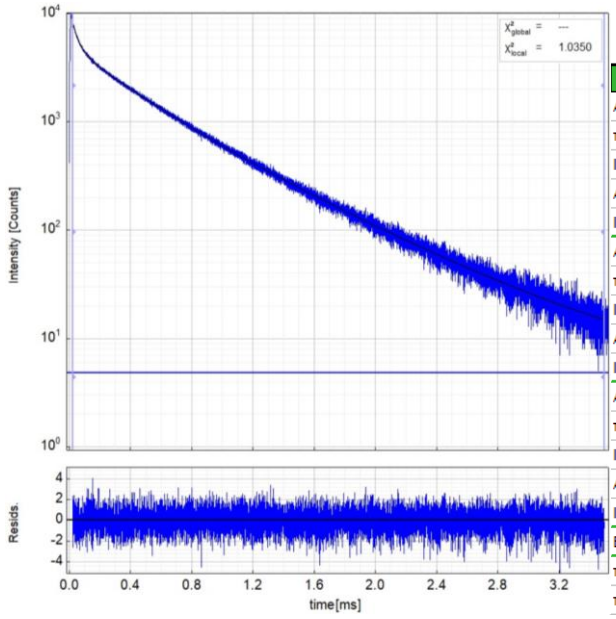

Parameter	Value	Error
A_1[kCnts/Chnl]	1.95	± 0.28
τ_1[µs]	658	± 25
I_1[kCnts]	5016	± 507
$A_{Rel\,1}$[%]	24.2	± 3.4
$I_{Rel\,1}$[%]	54.6	± 5.7
A_2[kCnts/Chnl]	2.76	± 0.25
τ_2[µs]	338	± 20
I_2[kCnts]	3647	± 509
$A_{Rel\,2}$[%]	34.2	± 3.2
$I_{Rel\,2}$[%]	39.7	± 5.5
A_3[kCnts/Chnl]	3.354	± 0.020
τ_3[µs]	39.84	± 0.91
I_3[kCnts]	522	± 14
$A_{Rel\,3}$[%]	41.57	± 0.27
$I_{Rel\,3}$[%]	5.68	± 0.14
$Bkgr_{Dec}$[kCnts]	0.0048	± 0.0010
$\tau_{Av\,Int}$[µs]	495.6	± 2.8
$\tau_{Av\,Amp}$[µs]	291.4	± 1.7

Figure S46. Left: Time-resolved photoluminescence decay of **PtL_{OMe}** in a frozen glassy matrix of DCM/MeOH (1:1) at 77 K, including the residuals (λ_{exc} = 376.7 nm, λ_{em} = 485 nm). Right: Fitting parameters including pre-exponential factors and confidence limits.

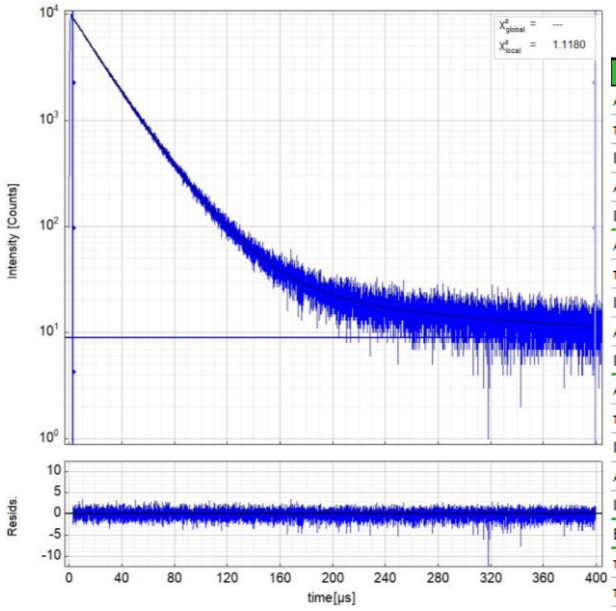

Parameter	Value	Error
A_1[kCnts/Chnl]	0.0318	± 0.0080
τ_1[ns]	161204	± 57184
I_1[kCnts]	160	± 20
$A_{Rel\,1}$[%]	0.341	± 0.086
$I_{Rel\,1}$[%]	2.33	± 0.28
A_2[kCnts/Chnl]	2.38	± 0.60
τ_2[ns]	30960	± 1859
I_2[kCnts]	2306	± 461
$A_{Rel\,2}$[%]	25.6	± 6.4
$I_{Rel\,2}$[%]	33.6	± 6.9
A_3[kCnts/Chnl]	6.89	± 0.59
τ_3[ns]	20429	± 425
I_3[kCnts]	4399	± 483
$A_{Rel\,3}$[%]	74.0	± 6.4
$I_{Rel\,3}$[%]	64.1	± 6.7
$Bkgr_{Dec}$[kCnts]	0.0089	± 0.0016
$\tau_{Av\,Int}$[ns]	27248	± 1625
$\tau_{Av\,Amp}$[ns]	23608	± 117

Figure S47. Left: Time-resolved photoluminescence decay of **PtL_{OMe}** in a frozen glassy matrix of DCM/MeOH (1:1) at 77 K, including the residuals (λ_{exc} = 376.7 nm, λ_{em} = 545 nm). Right: Fitting parameters including pre-exponential factors and confidence limits.

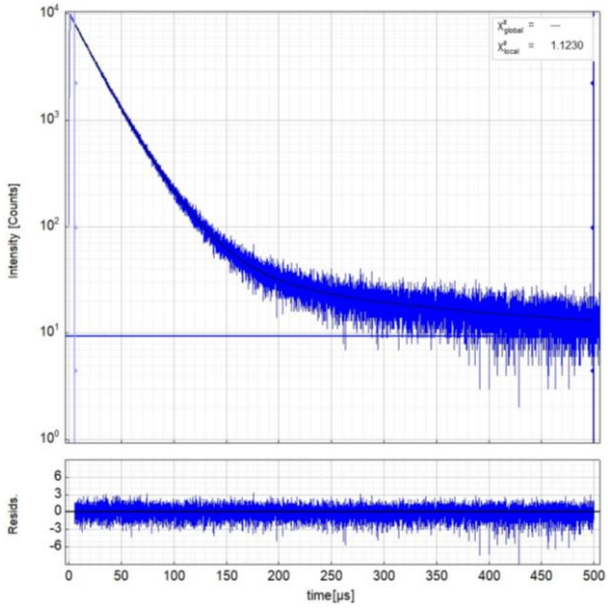

Parameter	Value	Error
A_1[kCnts/Chnl]	0.0401	± 0.0087
τ_1[ns]	213773	± 82220
I_1[kCnts]	268	± 38
$A_{Rel\,1}$[%]	0.449	± 0.097
$I_{Rel\,1}$[%]	3.89	± 0.51
A_2[kCnts/Chnl]	2.51	± 0.63
τ_2[ns]	32565	± 2314
I_2[kCnts]	2552	± 487
$A_{Rel\,2}$[%]	28.0	± 7.0
$I_{Rel\,2}$[%]	37.0	± 7.5
A_3[kCnts/Chnl]	6.40	± 0.63
τ_3[ns]	20381	± 541
I_3[kCnts]	4074	± 520
$A_{Rel\,3}$[%]	71.5	± 7.1
$I_{Rel\,3}$[%]	59.1	± 6.8
$Bkgr_{Dec}$[kCnts]	0.0092	± 0.0023
$\tau_{Av\,Int}$[ns]	32411	± 4794
$\tau_{Av\,Amp}$[ns]	24664	± 244

Figure S48. Left: Time-resolved photoluminescence decay of **PtL_{OMe}** in a frozen glassy matrix of DCM/MeOH (1:1) at 77 K, including the residuals (λ_{exc} = 376.7 nm, λ_{em} = 580 nm). Right: Fitting parameters including pre-exponential factors and confidence limits.

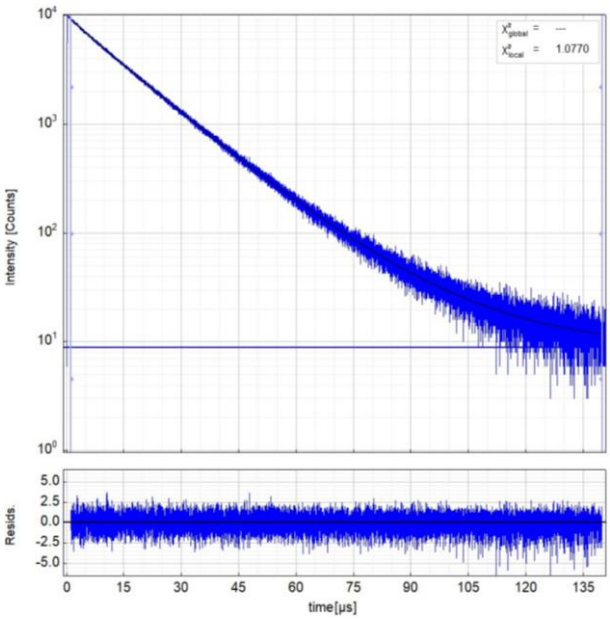

Parameter	Value	Error
A_1[kCnts/Chnl]	0.65	± 0.18
τ_1[ns]	24970	± 1286
I_1[kCnts]	2041	± 425
$A_{Rel\,1}$[%]	7.1	± 2.0
$I_{Rel\,1}$[%]	12.2	± 2.6
A_2[kCnts/Chnl]	8.17	± 0.15
τ_2[ns]	14184	± 140
I_2[kCnts]	14491	± 402
$A_{Rel\,2}$[%]	89.3	± 1.6
$I_{Rel\,2}$[%]	86.9	± 2.4
A_3[kCnts/Chnl]	0.323	± 0.037
τ_3[ns]	3499	± 556
I_3[kCnts]	141	± 36
$A_{Rel\,3}$[%]	3.53	± 0.40
$I_{Rel\,3}$[%]	0.85	± 0.22
$Bkgr_{Dec}$[kCnts]	0.0088	± 0.0005
$\tau_{Av\,Int}$[ns]	15414	± 32
$\tau_{Av\,Amp}$[ns]	14578	± 21

Figure S49. Left: Time-resolved photoluminescence decay of **PtL_{OMe}** in a PMMA film at r.t., including the residuals (λ_{exc} = 376.7 nm, λ_{em} = 515 nm). Right: Fitting parameters including pre-exponential factors and confidence limits.

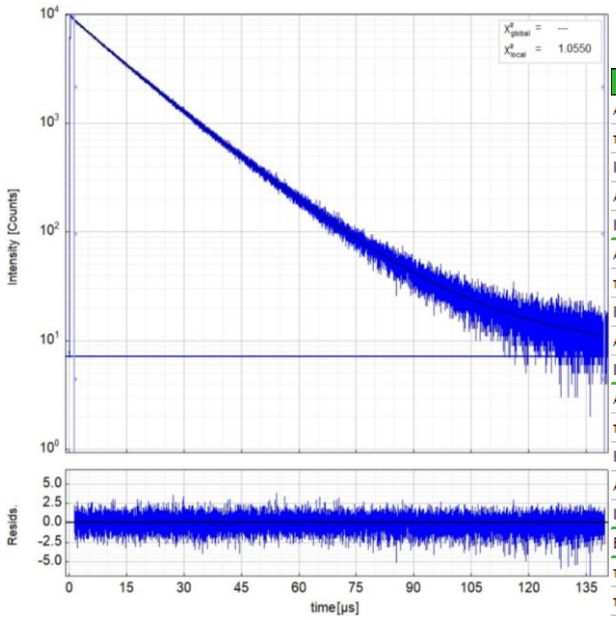

Parameter	Value	Error
A_1[kCnts/Chnl]	0.46	± 0.15
τ_1[ns]	26803	± 2477
I_1[kCnts]	1554	± 381
$A_{Rel\,1}$[%]	5.2	± 1.6
$I_{Rel\,1}$[%]	9.5	± 2.4
A_2[kCnts/Chnl]	8.054	± 0.064
τ_2[ns]	14489	± 196
I_2[kCnts]	14588	± 315
$A_{Rel\,2}$[%]	89.89	± 0.71
$I_{Rel\,2}$[%]	88.7	± 1.9
A_3[kCnts/Chnl]	0.442	± 0.076
τ_3[ns]	5405	± 447
I_3[kCnts]	298	± 74
$A_{Rel\,3}$[%]	4.93	± 0.85
$I_{Rel\,3}$[%]	1.82	± 0.45
$Bkgr_{Dec}$[kCnts]	0.0079	± 0.0003
$\tau_{Av\,Int}$[ns]	15488	± 37
$\tau_{Av\,Amp}$[ns]	14679	± 13

Figure S50. Left: Time-resolved photoluminescence decay of **PtL_{OMe}** in a PMMA film at r.t., including the residuals (λ_{exc} = 376.7 nm, λ_{em} = 550 nm). Right: Fitting parameters including pre-exponential factors and confidence limits.

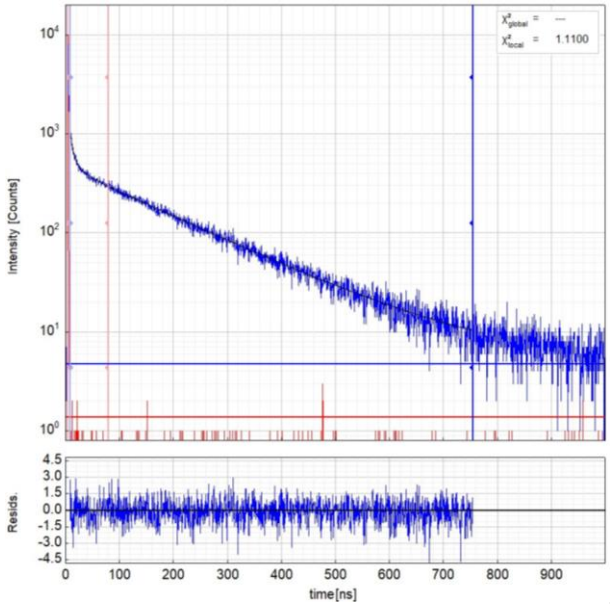

Parameter	Value	Error
A_1[kCnts/Chnl]	2.257	± 0.099
τ_1[ns]	170.9	± 3.5
I_1[kCnts]	753	± 44
$A_{Rel\,1}$[%]	37.1	± 2.4
$I_{Rel\,1}$[%]	94.83	± 0.44
A_2[kCnts/Chnl]	3.83	± 0.35
τ_2[ns]	5.48	± 0.60
I_2[kCnts]	41.0	± 2.4
$A_{Rel\,2}$[%]	62.9	± 2.4
$I_{Rel\,2}$[%]	5.17	± 0.44
$Bkgr_{Dec}$[kCnts]	0.0047	± 0.0007
$Bkgr_{IRF}$[Cnts/Chnl]	1.37	± 0.61
$Shift_{IRF}$[ps]	511.5602	± 0.0035
$\tau_{Av\,Int}$[ns]	162.4	± 3.7
$\tau_{Av\,Amp}$[ns]	66.8	± 5.2

Figure S51. Left: Time-resolved photoluminescence decay of **PdL_{OMe}** (10^{-5} M) in air-equilibrated DCM at r.t. (blue) and IRF (red), including the residuals (λ_{exc} = 376.7 nm, λ_{em} = 500 nm). Right: Fitting parameters including pre-exponential factors and confidence limits.

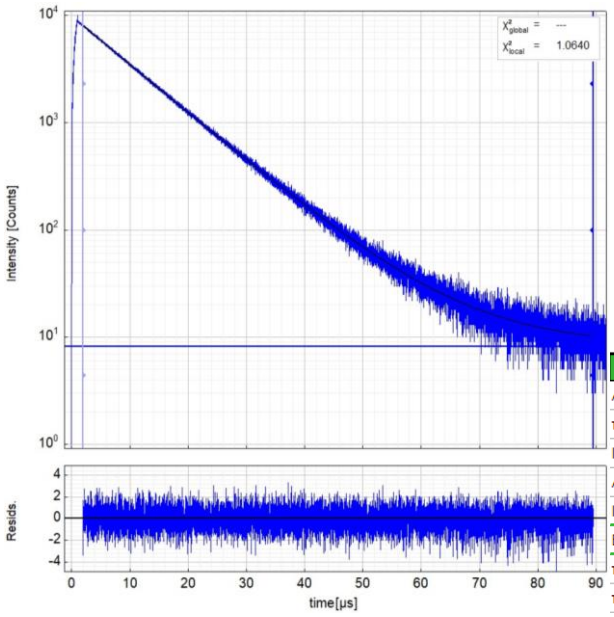

Parameter	Value	Error
A_1[kCnts/Chnl]	7.4630	± 0.0068
τ_1[ns]	7587.9	± 5.2
I_1[kCnts]	14157.1	± 8.7
$A_{Rel\,1}$[%]	100.0000	± 0.0000
$I_{Rel\,1}$[%]	100.0000	± 0.0000
$Bkgr_{Dec}$[kCnts]	0.0022	± 0.0002
$\tau_{Av\,Int}$[ns]	7587.9	± 5.2
$\tau_{Av\,Amp}$[ns]	7587.9	± 5.2

Figure S52. Left: Time-resolved photoluminescence decay of **PdL_{OMe}** in in fluid Ar-purged DCM at r.t., including the residuals (λ_{exc} = 376.7 nm, λ_{em} = 500 nm). Right: Fitting parameters including pre-exponential factors and confidence limits.

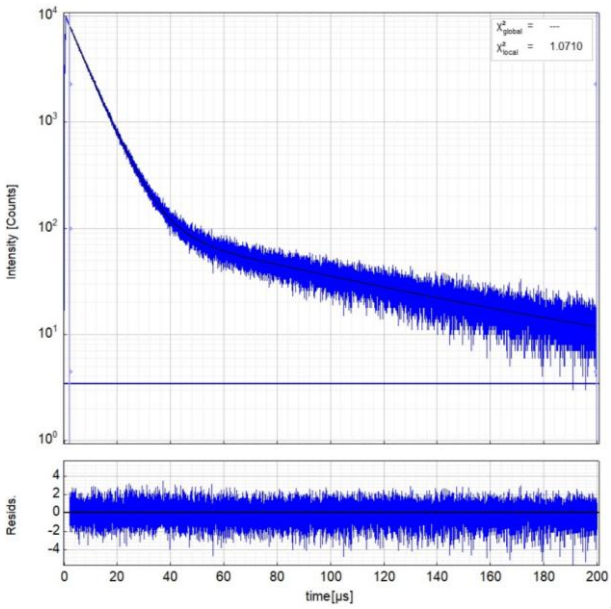

Parameter	Value	Error
A_1[kCnts/Chnl]	0.1192	± 0.0011
τ_1[ns]	74497	± 2248
I_1[kCnts]	1110	± 25
$A_{Rel\,1}$[%]	1.481	± 0.014
$I_{Rel\,1}$[%]	13.22	± 0.25
A_2[kCnts/Chnl]	7.9327	± 0.0080
τ_2[ns]	7353	± 13
I_2[kCnts]	7290.9	± 7.2
$A_{Rel\,2}$[%]	98.519	± 0.014
$I_{Rel\,2}$[%]	86.78	± 0.25
$Bkgr_{Dec}$[kCnts]	0.0034	± 0.0008
$\tau_{Av\,Int}$[ns]	16227	± 472
$\tau_{Av\,Amp}$[ns]	8347	± 38

Figure S53. Left: Time-resolved photoluminescence decay of **PdL_{OMe}** in in fluid Ar-purged DCM at r.t., including the residuals (λ_{exc} = 376.7 nm, λ_{em} = 535 nm). Right: Fitting parameters including pre-exponential factors and confidence limits.

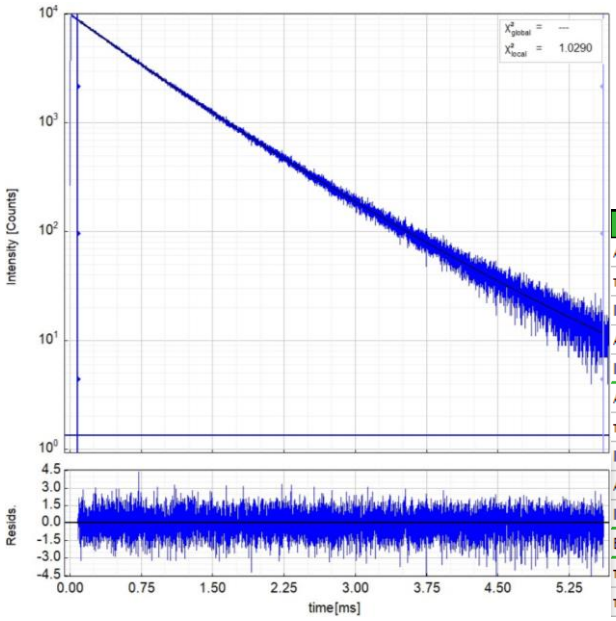

Parameter	Value	Error
A_1[kCnts/Chnl]	2.30	± 0.65
τ_1[µs]	1003	± 50
I_1[kCnts]	4505	± 984
$A_{Rel\,1}$[%]	26.0	± 7.4
$I_{Rel\,1}$[%]	36.1	± 8.0
A_2[kCnts/Chnl]	6.54	± 0.65
τ_2[µs]	625	± 19
I_2[kCnts]	7983	± 995
$A_{Rel\,2}$[%]	74.0	± 7.4
$I_{Rel\,2}$[%]	63.9	± 8.0
$Bkgr_{Dec}$[kCnts]	0.0013	± 0.0009
$\tau_{Av\,Int}$[µs]	761.4	± 2.2
$\tau_{Av\,Amp}$[µs]	723.5	± 1.4

Figure S54. Left: Time-resolved photoluminescence decay of **PdL_{OMe}** in a frozen glassy matrix of DCM/MeOH (1:1) at 77 K, including the residuals (λ_{exc} = 376.7 nm, λ_{em} = 490 nm). Right: Fitting parameters including pre-exponential factors and confidence limits.

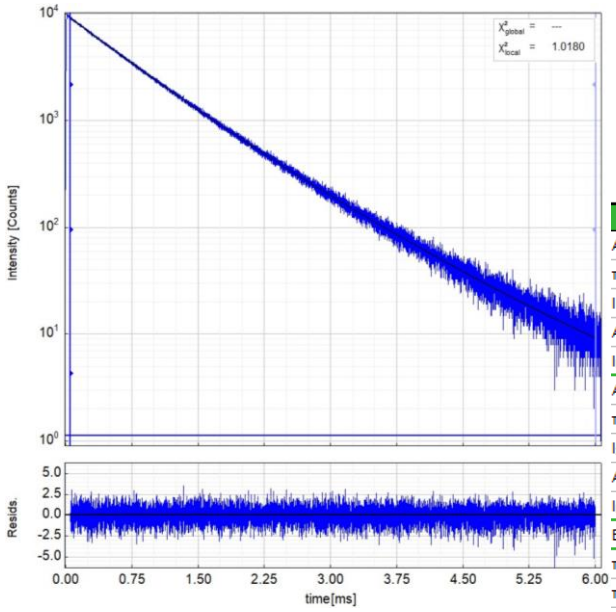

Parameter	Value	Error
A_1[kCnts/Chnl]	2.10	± 0.36
τ_1[µs]	1054	± 37
I_1[kCnts]	4329	± 564
$A_{Rel\,1}$[%]	23.0	± 3.9
$I_{Rel\,1}$[%]	33.0	± 4.4
A_2[kCnts/Chnl]	7.05	± 0.35
τ_2[µs]	637	± 11
I_2[kCnts]	8776	± 573
$A_{Rel\,2}$[%]	77.0	± 3.9
$I_{Rel\,2}$[%]	67.0	± 4.4
$Bkgr_{Dec}$[kCnts]	0.0011	± 0.0007
$\tau_{Av\,Int}$[µs]	774.8	± 2.2
$\tau_{Av\,Amp}$[µs]	732.9	± 1.4

Figure S55. Left: Time-resolved photoluminescence decay of **PdL_{OMe}** in a frozen glassy matrix of DCM/MeOH (1:1) at 77 K, including the residuals (λ_{exc} = 376.7 nm, λ_{em} = 525 nm). Right: Fitting parameters including pre-exponential factors and confidence limits.

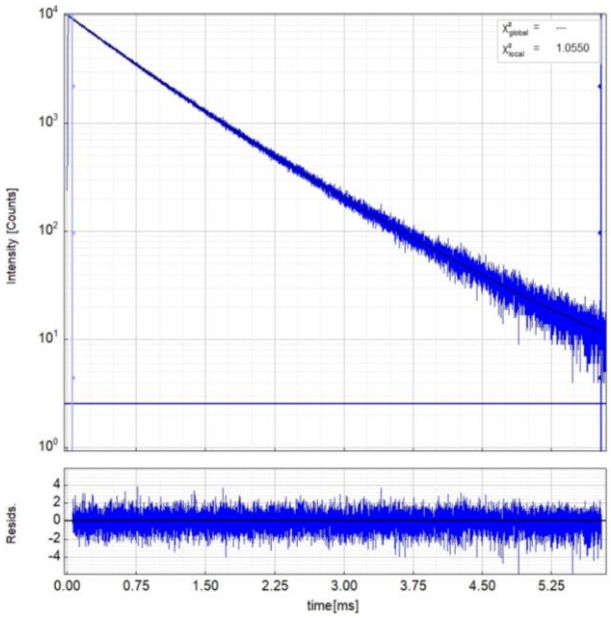

Parameter	Value	Error
A_1[kCnts/Chnl]	3.00	± 0.43
τ_1[µs]	984	± 29
I_1[kCnts]	5765	± 639
$A_{Rel\,1}$[%]	32.6	± 4.7
$I_{Rel\,1}$[%]	43.7	± 4.9
A_2[kCnts/Chnl]	6.21	± 0.43
τ_2[µs]	611	± 12
I_2[kCnts]	7416	± 645
$A_{Rel\,2}$[%]	67.4	± 4.7
$I_{Rel\,2}$[%]	56.3	± 4.9
$Bkgr_{Dec}$[kCnts]	0.0025	± 0.0006
$\tau_{Av\,Int}$[µs]	774.1	± 1.4
$\tau_{Av\,Amp}$[µs]	732.43	± 0.63

Figure S56. Left: Time-resolved photoluminescence decay of **PdL_{OMe}** in a frozen glassy matrix of DCM/MeOH (1:1) at 77 K, including the residuals (λ_{exc} = 376.7 nm, λ_{em} = 560 nm). Right: Fitting parameters including pre-exponential factors and confidence limits.

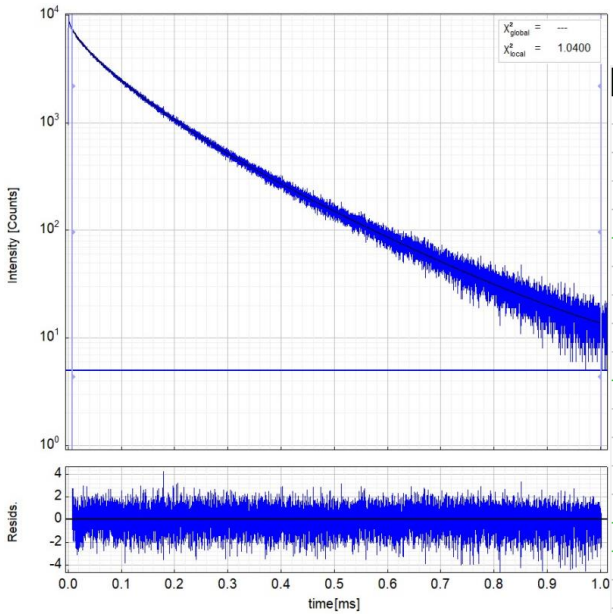

Parameter	Value	Error
A_1[kCnts/Chnl]	2.09	± 0.22
τ_1[ns]	181109	± 5759
I_1[kCnts]	5918	± 407
$A_{Rel\,1}$[%]	28.6	± 3.0
$I_{Rel\,1}$[%]	53.4	± 3.8
A_2[kCnts/Chnl]	3.836	± 0.089
τ_2[ns]	78661	± 4256
I_2[kCnts]	4714	± 359
$A_{Rel\,2}$[%]	52.4	± 1.3
$I_{Rel\,2}$[%]	42.6	± 3.2
A_3[kCnts/Chnl]	1.40	± 0.13
τ_3[ns]	20228	± 1498
I_3[kCnts]	442	± 70
$A_{Rel\,3}$[%]	19.1	± 1.8
$I_{Rel\,3}$[%]	3.99	± 0.63
$Bkgr_{Dec}$[kCnts]	0.0050	± 0.0011
$\tau_{Av\,Int}$[ns]	131079	± 780
$\tau_{Av\,Amp}$[ns]	96759	± 446

Figure S57. Left: Time-resolved photoluminescence decay of **PdL_{OMe}** in a PMMA film at r.t., including the residuals (λ_{exc} = 376.7 nm, λ_{em} = 495 nm). Right: Fitting parameters including pre-exponential factors and confidence limits.

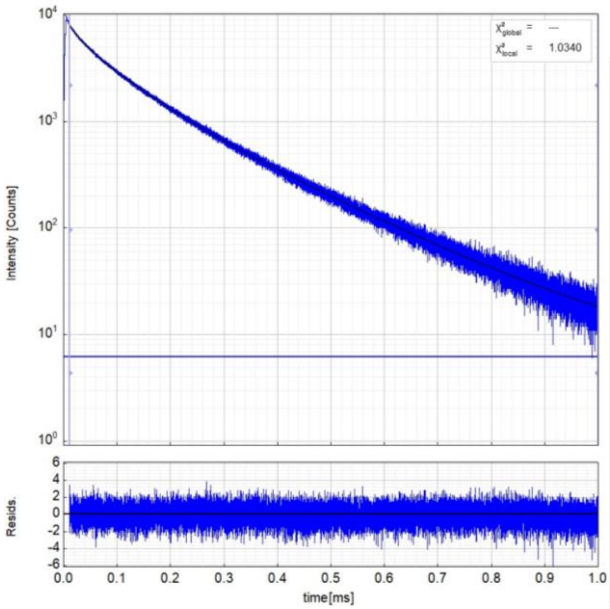

Parameter	Value	Error
A_1[kCnts/Chnl]	2.64	± 0.12
τ_1[ns]	183977	± 2629
I_1[kCnts]	15151	± 462
$A_{Rel\,1}$[%]	32.9	± 1.5
$I_{Rel\,1}$[%]	58.6	± 1.9
A_2[kCnts/Chnl]	3.907	± 0.064
τ_2[ns]	80165	± 2562
I_2[kCnts]	9787	± 388
$A_{Rel\,2}$[%]	48.70	± 0.81
$I_{Rel\,2}$[%]	37.9	± 1.5
A_3[kCnts/Chnl]	1.480	± 0.074
τ_3[ns]	19777	± 1268
I_3[kCnts]	915	± 104
$A_{Rel\,3}$[%]	18.45	± 0.95
$I_{Rel\,3}$[%]	3.54	± 0.40
$Bkgr_{Dec}$[kCnts]	0.0062	± 0.0008
$\tau_{Av\,Int}$[ns]	138869	± 514
$\tau_{Av\,Amp}$[ns]	103128	± 297

Figure S58. Left: Time-resolved photoluminescence decay of **PdL_{OMe}** in a PMMA film at r.t., including the residuals (λ_{exc} = 376.7 nm, λ_{em} = 525 nm). Right: Fitting parameters including pre-exponential factors and confidence limits.

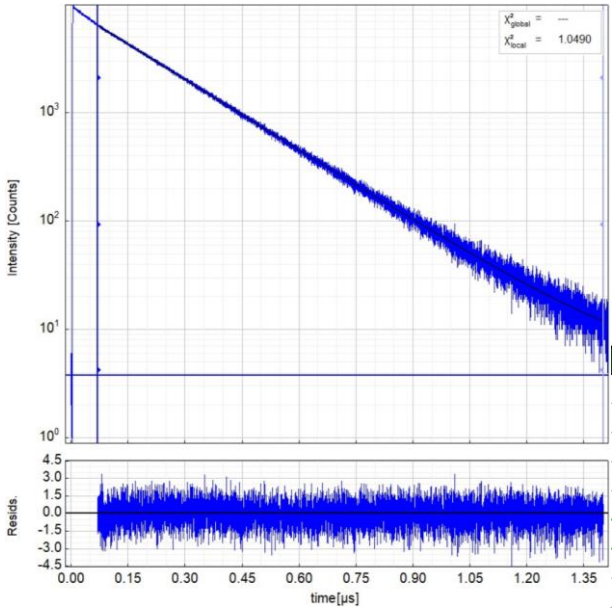

Parameter	Value	Error
A_1[kCnts/Chnl]	6.4399	± 0.0088
τ_1[ns]	199.32	± 0.16
I_1[kCnts]	10028.2	± 7.8
$A_{Rel\,1}$[%]	100.0000	± 0.0000
$I_{Rel\,1}$[%]	100.0000	± 0.0000
$Bkgr_{Dec}$[kCnts]	0.0038	± 0.0003
$\tau_{Av\,Int}$[ns]	199.32	± 0.16
$\tau_{Av\,Amp}$[ns]	199.32	± 0.16

Figure S59. Left: Time-resolved photoluminescence decay of **PtL_{OHex}** (10^{-5} M) in air-equilibrated DCM at r.t., including the residuals (λ_{exc} = 376.7 nm, λ_{em} = 520 nm). Right: Fitting parameters including pre-exponential factors and confidence limits.

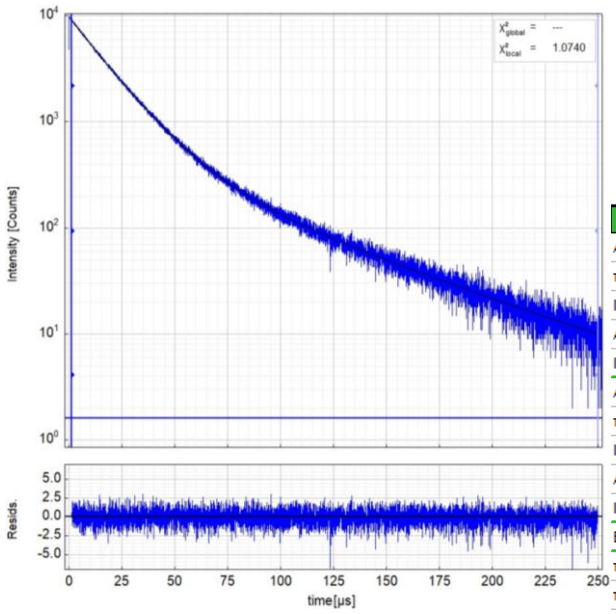

Parameter	Value	Error
A_1[kCnts/Chnl]	0.626	± 0.016
τ_1[ns]	57679	± 944
I_1[kCnts]	1129	± 11
$A_{Rel\,1}$[%]	6.96	± 0.17
$I_{Rel\,1}$[%]	20.90	± 0.21
A_2[kCnts/Chnl]	8.376	± 0.016
τ_2[ns]	16329	± 41
I_2[kCnts]	4274	± 16
$A_{Rel\,2}$[%]	93.04	± 0.17
$I_{Rel\,2}$[%]	79.10	± 0.21
$Bkgr_{Dec}$[kCnts]	0.0016	± 0.0006
$\tau_{Av\,Int}$[ns]	24969	± 141
$\tau_{Av\,Amp}$[ns]	19206	± 32

Figure S60. Left: Time-resolved photoluminescence decay of **PtL_{OHex}** (10^{-5} M) in fluid Ar-purged DCM at r.t., including the residuals (λ_{exc} = 376.7 nm, λ_{em} = 515 nm). Right: Fitting parameters including pre-exponential factors and confidence limits.

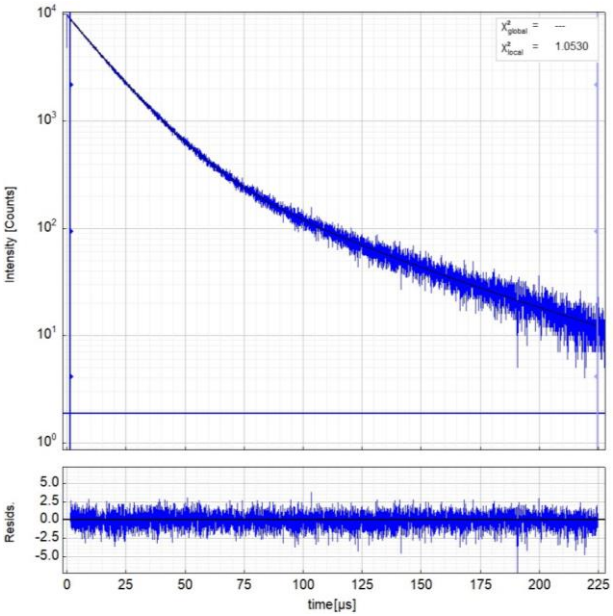

Parameter	Value	Error
A_1[kCnts/Chnl]	0.572	± 0.019
τ_1[ns]	55995	± 921
I_1[kCnts]	1002	± 16
$A_{Rel\,1}$[%]	7.12	± 0.22
$I_{Rel\,1}$[%]	21.27	± 0.34
A_2[kCnts/Chnl]	7.467	± 0.017
τ_2[ns]	15888	± 69
I_2[kCnts]	3707	± 19
$A_{Rel\,2}$[%]	92.88	± 0.22
$I_{Rel\,2}$[%]	78.73	± 0.34
$Bkgr_{Dec}$[kCnts]	0.0011	± 0.0004
$\tau_{Av\,Int}$[ns]	24419	± 116
$\tau_{Av\,Amp}$[ns]	18744	± 42

Figure S61. Left: Time-resolved photoluminescence decay of **PtL_{OHex}** (10^{-5} M) in fluid Ar-purged DCM at r.t., including the residuals (λ_{exc} = 376.7 nm, λ_{em} = 550 nm). Right: Fitting parameters including pre-exponential factors and confidence limits.

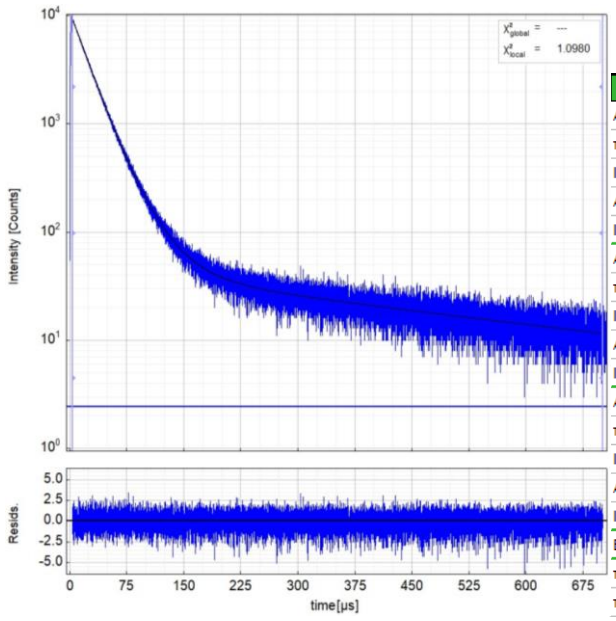

Parameter	Value	Error
A_1[kCnts/Chnl]	0.0456	± 0.0007
τ_1[ns]	435098	± 30060
I_1[kCnts]	620	± 41
$A_{Rel\,1}$[%]	0.4913	± 0.0069
$I_{Rel\,1}$[%]	8.55	± 0.50
A_2[kCnts/Chnl]	1.01	± 0.11
τ_2[ns]	38200	± 1025
I_2[kCnts]	1205	± 96
$A_{Rel\,2}$[%]	10.9	± 1.2
$I_{Rel\,2}$[%]	16.6	± 1.3
A_3[kCnts/Chnl]	8.23	± 0.11
τ_3[ns]	21108	± 113
I_3[kCnts]	5430	± 97
$A_{Rel\,3}$[%]	88.6	± 1.2
$I_{Rel\,3}$[%]	74.8	± 1.5
$Bkgr_{Dec}$[kCnts]	0.0024	± 0.0011
$\tau_{Av\,Int}$[ns]	59346	± 4528
$\tau_{Av\,Amp}$[ns]	25000	± 141

Figure S62. Left: Time-resolved photoluminescence decay of **PtL_{OHex}** (10^{-5} M) in a frozen glassy matrix of DCM/MeOH (1:1) at 77 K, including the residuals (λ_{exc} = 376.7 nm, λ_{em} = 505 nm). Right: Fitting parameters including pre-exponential factors and confidence limits.

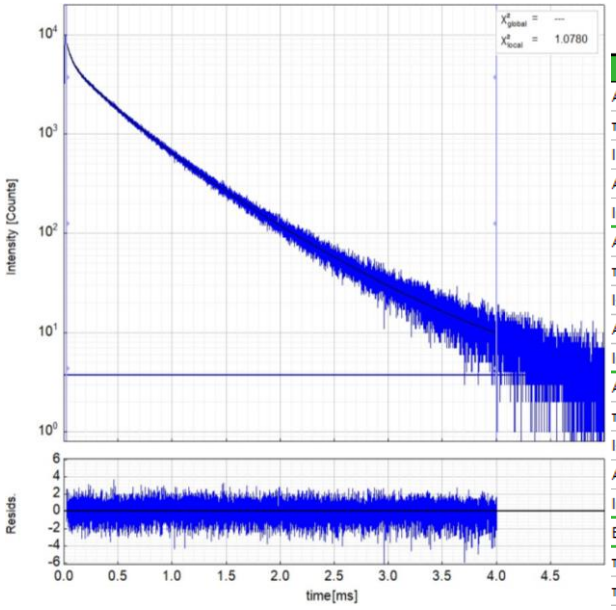

Parameter	Value	Error
A_1[kCnts/Chnl]	1.66	± 0.12
τ_1[µs]	710	± 18
I_1[kCnts]	4606	± 219
$A_{Rel\,1}$[%]	20.8	± 1.5
$I_{Rel\,1}$[%]	46.4	± 2.3
A_2[kCnts/Chnl]	3.54	± 0.12
τ_2[µs]	349.1	± 6.7
I_2[kCnts]	4829	± 233
$A_{Rel\,2}$[%]	44.4	± 1.5
$I_{Rel\,2}$[%]	48.7	± 2.3
A_3[kCnts/Chnl]	2.766	± 0.017
τ_3[µs]	45.2	± 1.1
I_3[kCnts]	488	± 12
$A_{Rel\,3}$[%]	34.71	± 0.20
$I_{Rel\,3}$[%]	4.92	± 0.12
$Bkgr_{Dec}$[kCnts]	0.0037	± 0.0006
$\tau_{Av\,Int}$[µs]	501.7	± 2.3
$\tau_{Av\,Amp}$[µs]	318.9	± 1.1

Figure S63. Left: Time-resolved photoluminescence decay of **PtL_{OHex}** (10^{-5} M) in a frozen glassy matrix of DCM/MeOH (1:1) at 77 K, including the residuals (λ_{exc} = 376.7 nm, λ_{em} = 485 nm). Right: Fitting parameters including pre-exponential factors and confidence limits.

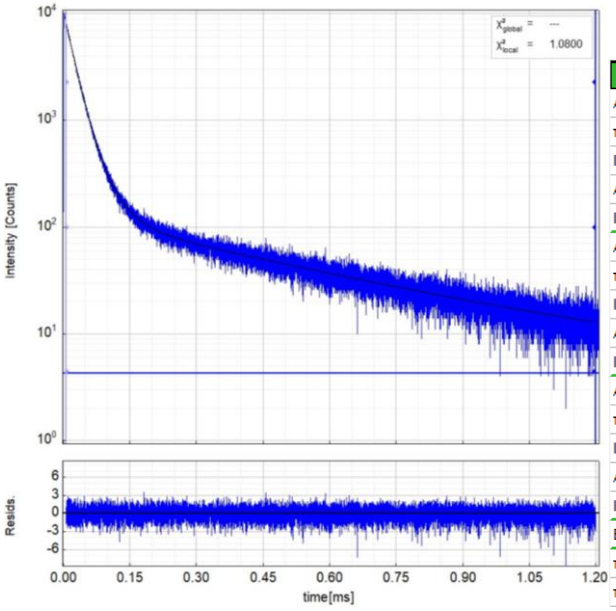

Parameter	Value	Error
A_1[kCnts/Chnl]	0.1230	± 0.0021
τ_1[ns]	447377	± 16596
I_1[kCnts]	860	± 19
$A_{Rel\,1}$[%]	1.538	± 0.026
$I_{Rel\,1}$[%]	22.40	± 0.34
A_2[kCnts/Chnl]	0.98	± 0.15
τ_2[ns]	44759	± 2093
I_2[kCnts]	687	± 70
$A_{Rel\,2}$[%]	12.3	± 1.8
$I_{Rel\,2}$[%]	17.9	± 1.9
A_3[kCnts/Chnl]	6.89	± 0.13
τ_3[ns]	21272	± 279
I_3[kCnts]	2291	± 71
$A_{Rel\,3}$[%]	86.2	± 1.9
$I_{Rel\,3}$[%]	59.7	± 1.9
$Bkgr_{Dec}$[kCnts]	0.0043	± 0.0009
$\tau_{Av\,Int}$[ns]	120940	± 5189
$\tau_{Av\,Amp}$[ns]	30708	± 188

Figure S64. Left: Time-resolved photoluminescence decay of **PtL_{OHex}** (10^{-5} M) in a frozen glassy matrix of DCM/MeOH (1:1) at 77 K, including the residuals (λ_{exc} = 376.7 nm, λ_{em} = 545 nm). Right: Fitting parameters including pre-exponential factors and confidence limits.

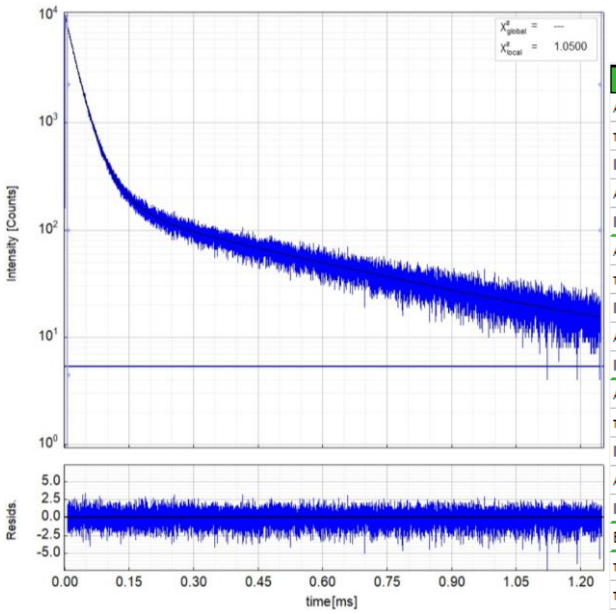

Parameter	Value	Error
A_1[kCnts/Chnl]	1.10	± 0.13
τ_1[ns]	50715	± 2400
I_1[kCnts]	868	± 59
$A_{Rel\,1}$[%]	13.4	± 1.5
$I_{Rel\,1}$[%]	19.7	± 1.5
A_2[kCnts/Chnl]	6.88	± 0.12
τ_2[ns]	21893	± 228
I_2[kCnts]	2353	± 64
$A_{Rel\,2}$[%]	84.4	± 1.5
$I_{Rel\,2}$[%]	53.5	± 1.3
A_3[kCnts/Chnl]	0.1724	± 0.0021
τ_3[ns]	436953	± 8352
I_3[kCnts]	1177	± 11
$A_{Rel\,3}$[%]	2.117	± 0.029
$I_{Rel\,3}$[%]	26.77	± 0.15
$Bkgr_{Dec}$[kCnts]	0.0053	± 0.0006
$\tau_{Av\,Int}$[ns]	138684	± 2997
$\tau_{Av\,Amp}$[ns]	34554	± 157

Figure S65. Left: Time-resolved photoluminescence decay of **PtL_{OHex}** (10^{-5} M) in a frozen glassy matrix of DCM/MeOH (1:1) at 77 K, including the residuals (λ_{exc} = 376.7 nm, λ_{em} = 580 nm). Right: Fitting parameters including pre-exponential factors and confidence limits.

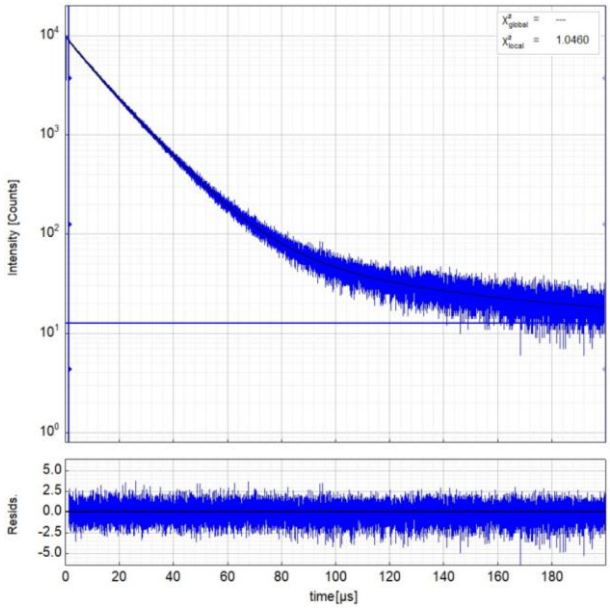

Parameter	Value	Error
A_1[kCnts/Chnl]	0.112	± 0.012
τ_1[ns]	66382	± 5109
I_1[kCnts]	928	± 17
$A_{Rel\,1}$[%]	1.25	± 0.13
$I_{Rel\,1}$[%]	5.81	± 0.12
A_2[kCnts/Chnl]	7.97	± 0.15
τ_2[ns]	14429	± 118
I_2[kCnts]	14366	± 138
$A_{Rel\,2}$[%]	89.1	± 1.6
$I_{Rel\,2}$[%]	90.0	± 1.1
A_3[kCnts/Chnl]	0.86	± 0.16
τ_3[ns]	6300	± 593
I_3[kCnts]	676	± 182
$A_{Rel\,3}$[%]	9.6	± 1.7
$I_{Rel\,3}$[%]	4.2	± 1.2
$Bkgr_{Dec}$[kCnts]	0.0126	± 0.0010
$\tau_{Av\,Int}$[ns]	17104	± 263
$\tau_{Av\,Amp}$[ns]	14298	± 42

Figure S66. Left: Time-resolved photoluminescence decay of **PtL_{OHex}** in a PMMA film at r.t., including the residuals (λ_{exc} = 376.7 nm, λ_{em} = 515 nm). Right: Fitting parameters including pre-exponential factors and confidence limits.

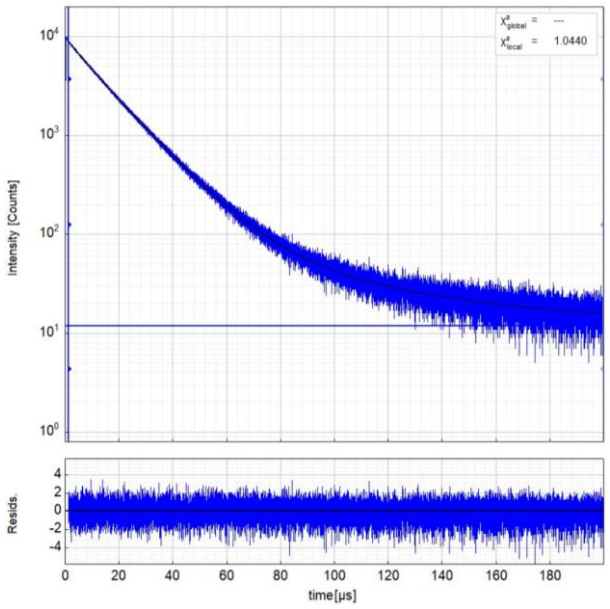

Parameter	Value	Error
A_1[kCnts/Chnl]	0.1265	± 0.0093
τ_1[ns]	57263	± 3068
I_1[kCnts]	906	± 18
$A_{Rel\,1}$[%]	1.41	± 0.11
$I_{Rel\,1}$[%]	5.65	± 0.12
A_2[kCnts/Chnl]	8.023	± 0.053
τ_2[ns]	14463	± 51
I_2[kCnts]	14504	± 39
$A_{Rel\,2}$[%]	89.48	± 0.55
$I_{Rel\,2}$[%]	90.56	± 0.31
A_3[kCnts/Chnl]	0.816	± 0.049
τ_3[ns]	5949	± 261
I_3[kCnts]	607	± 72
$A_{Rel\,3}$[%]	9.11	± 0.57
$I_{Rel\,3}$[%]	3.79	± 0.45
$Bkgr_{Dec}$[kCnts]	0.0118	± 0.0006
$\tau_{Av\,Int}$[ns]	16560	± 145
$\tau_{Av\,Amp}$[ns]	14292	± 23

Figure S67. Left: Time-resolved photoluminescence decay of **PtL_{OHex}** in a PMMA film at r.t., including the residuals (λ_{exc} = 376.7 nm, λ_{em} = 550 nm). Right: Fitting parameters including pre-exponential factors and confidence limits.

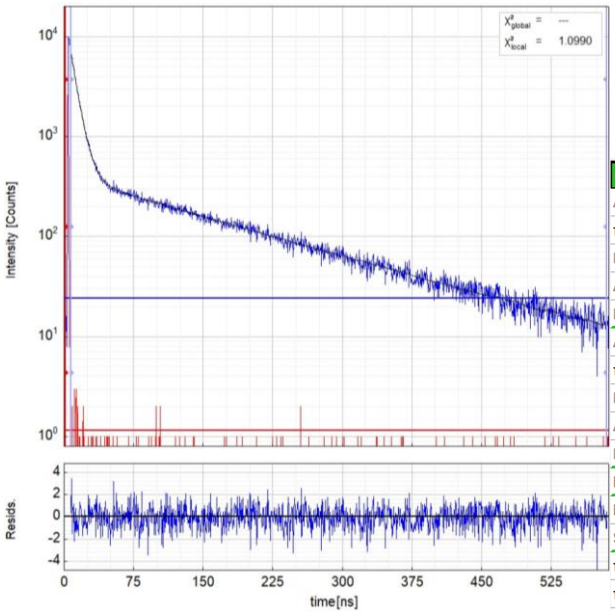

Parameter	Value	Error
A_1[kCnts/Chnl]	0.384	± 0.021
τ_1[ns]	158.6	± 2.9
I_1[kCnts]	118.9	± 5.4
$A_{Rel\,1}$[%]	3.343	± 0.060
$I_{Rel\,1}$[%]	43.08	± 0.29
A_2[kCnts/Chnl]	11.10	± 0.41
τ_2[ns]	7.248	± 0.097
I_2[kCnts]	157.1	± 6.1
$A_{Rel\,2}$[%]	96.657	± 0.060
$I_{Rel\,2}$[%]	56.92	± 0.29
$Bkgr_{Dec}$[kCnts]	0.0241	± 0.0007
$Bkgr_{IRF}$[Cnts/Chnl]	1.148	± 0.069
$Shift_{IRF}$[ps]	0	± 44
$\tau_{Av\,Int}$[ns]	72.5	± 1.6
$\tau_{Av\,Amp}$[ns]	12.31	± 0.16

Figure S68. Left: Time-resolved photoluminescence decay of **PdL_{OHex}** (10^{-5} M) in fluid air-equilibrated DCM at r.t. (blue) and IRF (red), including the residuals (λ_{exc} = 376.7 nm, λ_{em} = 500 nm). Right: Fitting parameters including pre-exponential factors and confidence limits.

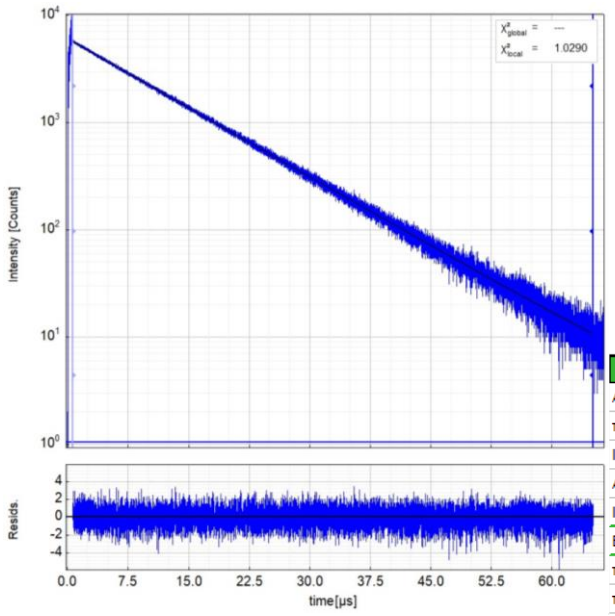

Parameter	Value	Error
A_1[kCnts/Chnl]	5.6712	± 0.0067
τ_1[ns]	10109.9	± 7.8
I_1[kCnts]	14333.9	± 9.8
$A_{Rel\,1}$[%]	100.0000	± 0.0000
$I_{Rel\,1}$[%]	100.0000	± 0.0000
$Bkgr_{Dec}$[kCnts]	0.0011	± 0.0002
$\tau_{Av\,Int}$[ns]	10109.9	± 7.8
$\tau_{Av\,Amp}$[ns]	10109.9	± 7.8

Figure S69. Left: Time-resolved photoluminescence decay of **PdL_{OHex}** (10^{-5} M) in fluid Ar-purged DCM at r.t., including the residuals (λ_{exc} = 376.7 nm, λ_{em} = 500 nm). Right: Fitting parameters including pre-exponential factors and confidence limits.

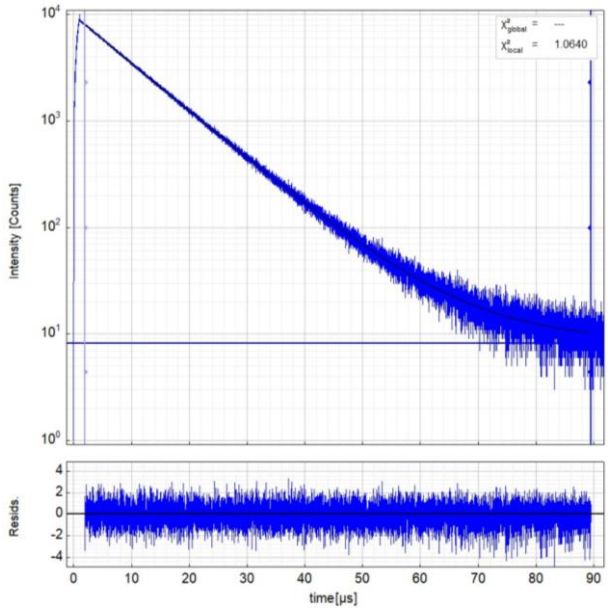

Parameter	Value	Error
A_1[kCnts/Chnl]	0.12	± 0.48
τ_1[ns]	19256	± 17489
I_1[kCnts]	279	± 707
$A_{Rel\,1}$[%]	1.4	± 5.9
$I_{Rel\,1}$[%]	2.9	± 7.3
A_2[kCnts/Chnl]	7.95	± 0.47
τ_2[ns]	9551	± 171
I_2[kCnts]	9487	± 719
$A_{Rel\,2}$[%]	98.6	± 5.9
$I_{Rel\,2}$[%]	97.1	± 7.3
$Bkgr_{Dec}$[kCnts]	0.0082	± 0.0030
$\tau_{Av\,Int}$[ns]	9829	± 275
$\tau_{Av\,Amp}$[ns]	9691	± 45

Figure S70. Left: Time-resolved photoluminescence decay of **PdL_{OHex}** (10^{-5} M) in fluid Ar-purged DCM at r.t., including the residuals (λ_{exc} = 376.7 nm, λ_{em} = 535 nm). Right: Fitting parameters including pre-exponential factors and confidence limits.

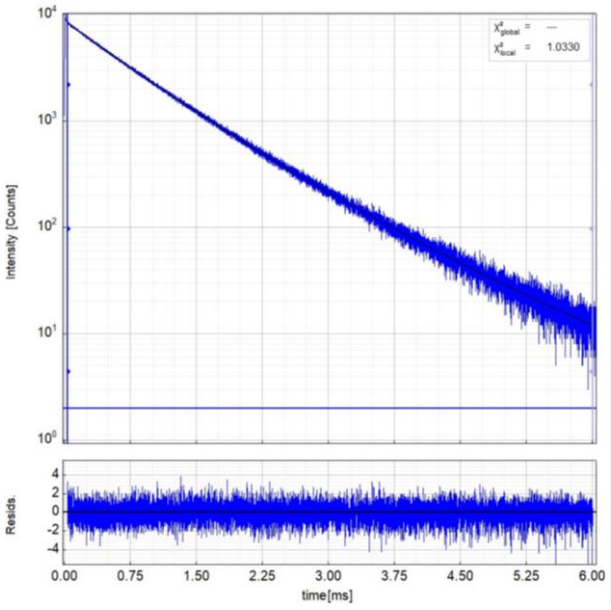

Parameter	Value	Error
A_1[kCnts/Chnl]	2.61	± 0.48
τ_1[µs]	1066	± 46
I_1[kCnts]	5439	± 748
$A_{Rel\,1}$[%]	31.3	± 5.8
$I_{Rel\,1}$[%]	43.6	± 6.1
A_2[kCnts/Chnl]	5.74	± 0.48
τ_2[µs]	627	± 18
I_2[kCnts]	7035	± 766
$A_{Rel\,2}$[%]	68.7	± 5.8
$I_{Rel\,2}$[%]	56.4	± 6.1
$Bkgr_{Dec}$[kCnts]	0.0020	± 0.0011
$\tau_{Av\,Int}$[µs]	818.8	± 3.1
$\tau_{Av\,Amp}$[µs]	764.6	± 1.9

Figure S71. Left: Time-resolved photoluminescence decay of **PdL_{OHex}** (10^{-5} M) in a frozen glassy matrix of DCM/MeOH (1:1) at 77 K, including the residuals (λ_{exc} = 376.7 nm, λ_{em} = 490 nm). Right: Fitting parameters including pre-exponential factors and confidence limits.

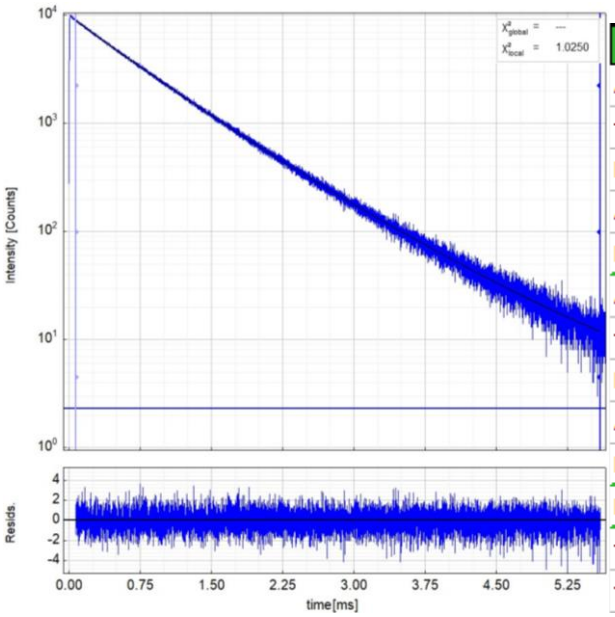

Parameter	Value	Error
A_1[kCnts/Chnl]	6.33	± 0.47
τ_1[µs]	604	± 14
I_1[kCnts]	7470	± 704
$A_{Rel\,1}$[%]	72.4	± 5.4
$I_{Rel\,1}$[%]	61.7	± 5.8
A_2[kCnts/Chnl]	2.41	± 0.48
τ_2[µs]	986	± 44
I_2[kCnts]	4645	± 691
$A_{Rel\,2}$[%]	27.6	± 5.4
$I_{Rel\,2}$[%]	38.3	± 5.8
$Bkgr_{Dec}$[kCnts]	0.0020	± 0.0010
$\tau_{Av\,Int}$[µs]	750.4	± 3.1
$\tau_{Av\,Amp}$[µs]	709.3	± 1.7

Figure S72. Left: Time-resolved photoluminescence decay of **PdL_{OHex}** (10^{-5} M) in a frozen glassy matrix of DCM/MeOH (1:1) at 77 K, including the residuals (λ_{exc} = 376.7 nm, λ_{em} = 525 nm). Right: Fitting parameters including pre-exponential factors and confidence limits.

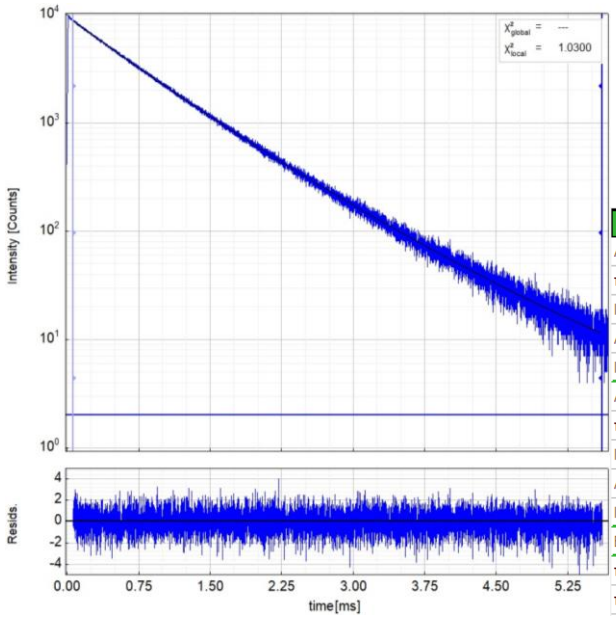

Parameter	Value	Error
A_1[kCnts/Chnl]	2.50	± 0.64
τ_1[µs]	978	± 60
I_1[kCnts]	4781	± 938
$A_{Rel\,1}$[%]	28.2	± 7.2
$I_{Rel\,1}$[%]	38.9	± 7.7
A_2[kCnts/Chnl]	6.38	± 0.64
τ_2[µs]	603	± 19
I_2[kCnts]	7512	± 950
$A_{Rel\,2}$[%]	71.8	± 7.2
$I_{Rel\,2}$[%]	61.1	± 7.7
$Bkgr_{Dec}$[kCnts]	0.0023	± 0.0010
$\tau_{Av\,Int}$[µs]	749.2	± 3.1
$\tau_{Av\,Amp}$[µs]	709.0	± 1.9

Figure S73. Left: Time-resolved photoluminescence decay of **PdL_{OHex}** (10^{-5} M) in a frozen glassy matrix of DCM/MeOH (1:1) at 77 K, including the residuals (λ_{exc} = 376.7 nm, λ_{em} = 560 nm). Right: Fitting parameters including pre-exponential factors and confidence limits.

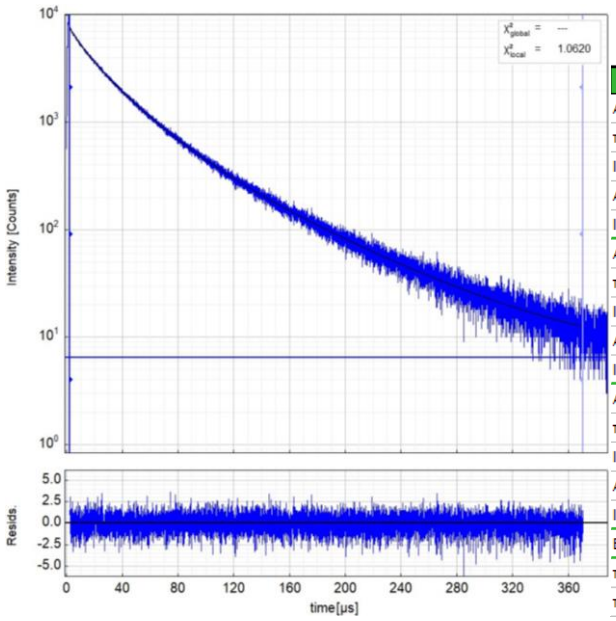

Parameter	Value	Error
A_1[kCnts/Chnl]	1.276	± 0.073
τ_1[ns]	68858	± 1170
I_1[kCnts]	2746	± 112
$A_{Rel\,1}$[%]	16.92	± 0.92
$I_{Rel\,1}$[%]	38.3	± 1.6
A_2[kCnts/Chnl]	4.72	± 0.11
τ_2[ns]	27220	± 827
I_2[kCnts]	4017	± 53
$A_{Rel\,2}$[%]	62.6	± 1.2
$I_{Rel\,2}$[%]	56.04	± 0.73
A_3[kCnts/Chnl]	1.54	± 0.16
τ_3[ns]	8374	± 844
I_3[kCnts]	404	± 85
$A_{Rel\,3}$[%]	20.5	± 2.1
$I_{Rel\,3}$[%]	5.6	± 1.2
$Bkgr_{Dec}$[kCnts]	0.0065	± 0.0004
$\tau_{Av\,Int}$[ns]	42113	± 120
$\tau_{Av\,Amp}$[ns]	30408	± 112

Figure S74. Left: Time-resolved photoluminescence decay of **PdL_{OHex}** in a PMMA film at r.t., including the residuals (λ_{exc} = 376.7 nm, λ_{em} = 495 nm). Right: Fitting parameters including pre-exponential factors and confidence limits.

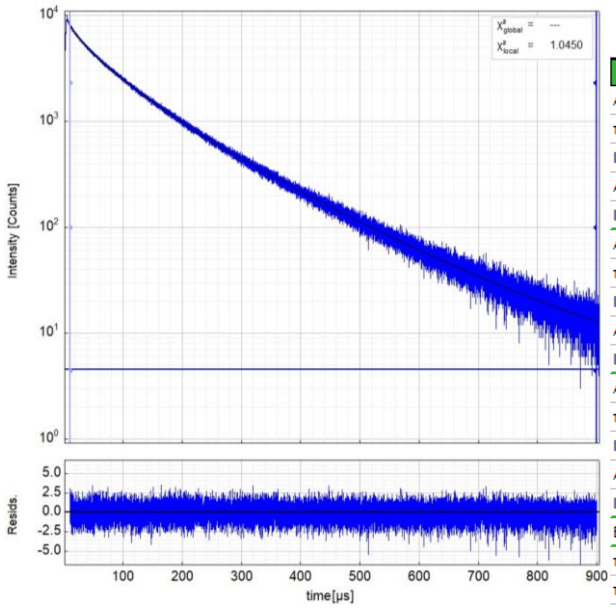

Parameter	Value	Error
A_1[kCnts/Chnl]	2.23	± 0.13
τ_1[ns]	159693	± 2602
I_1[kCnts]	11131	± 457
$A_{Rel\,1}$[%]	27.8	± 1.6
$I_{Rel\,1}$[%]	51.7	± 2.2
A_2[kCnts/Chnl]	4.223	± 0.056
τ_2[ns]	71708	± 2281
I_2[kCnts]	9463	± 399
$A_{Rel\,2}$[%]	52.70	± 0.72
$I_{Rel\,2}$[%]	44.0	± 1.9
A_3[kCnts/Chnl]	1.560	± 0.096
τ_3[ns]	18784	± 984
I_3[kCnts]	916	± 105
$A_{Rel\,3}$[%]	19.5	± 1.2
$I_{Rel\,3}$[%]	4.26	± 0.49
$Bkgr_{Dec}$[kCnts]	0.0045	± 0.0004
$\tau_{Av\,Int}$[ns]	114984	± 242
$\tau_{Av\,Amp}$[ns]	85891	± 155

Figure S74. Left: Time-resolved photoluminescence decay of **PdL_{OHex}** in a PMMA film at r.t., including the residuals (λ_{exc} = 376.7 nm, λ_{em} = 525 nm). Right: Fitting parameters including pre-exponential factors and confidence limits.

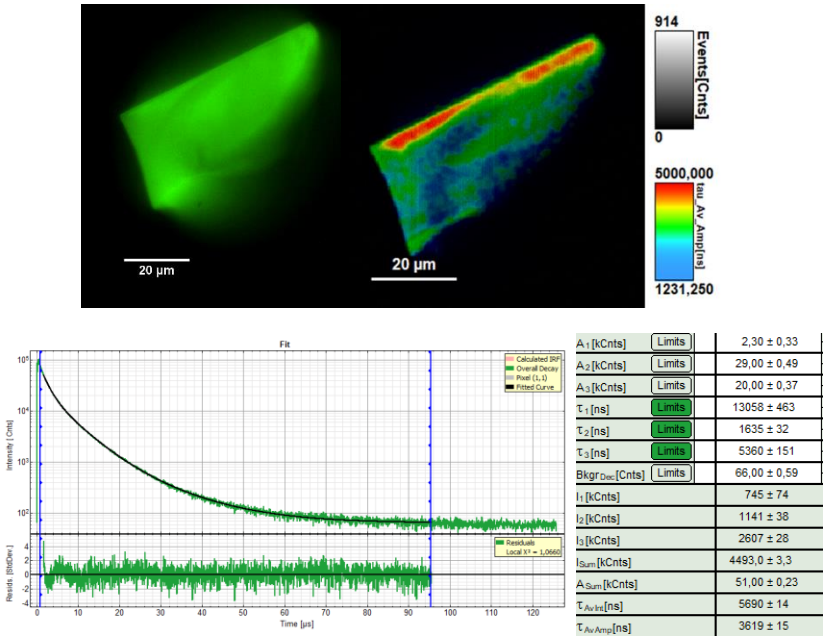

Figure S75. Photoluminescence of crystalline **PtL_{OMe}** before grinding. Top left: Photoluminescence micrograph. Top right: PLIM lifetime map. Bottom left: Time-resolved photoluminescence decay (λ_{exc} = 376.7 nm, low-pass cut-off filter 460LP). Bottom right: Fitting parameters including pre-exponential factors and confidence limits.

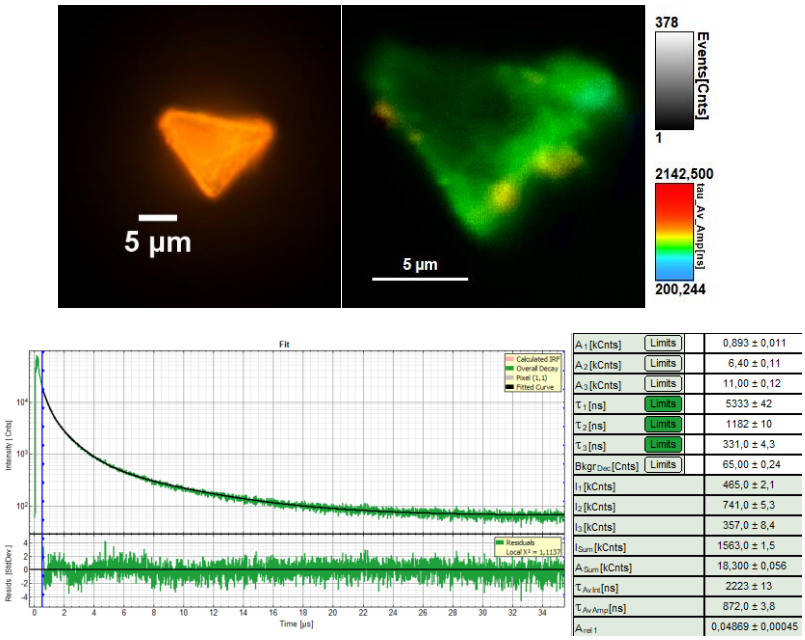

Figure S76. Photoluminescence of crystalline **PtL_{OMe}** after grinding. Top left: Photoluminescence micrograph. Top right: PLIM lifetime map. Bottom left: Time-resolved photoluminescence decay (λ_{exc} = 376.7 nm, low-pass cut-off filter 460LP). Bottom right: Fitting parameters including pre-exponential factors and confidence limits.

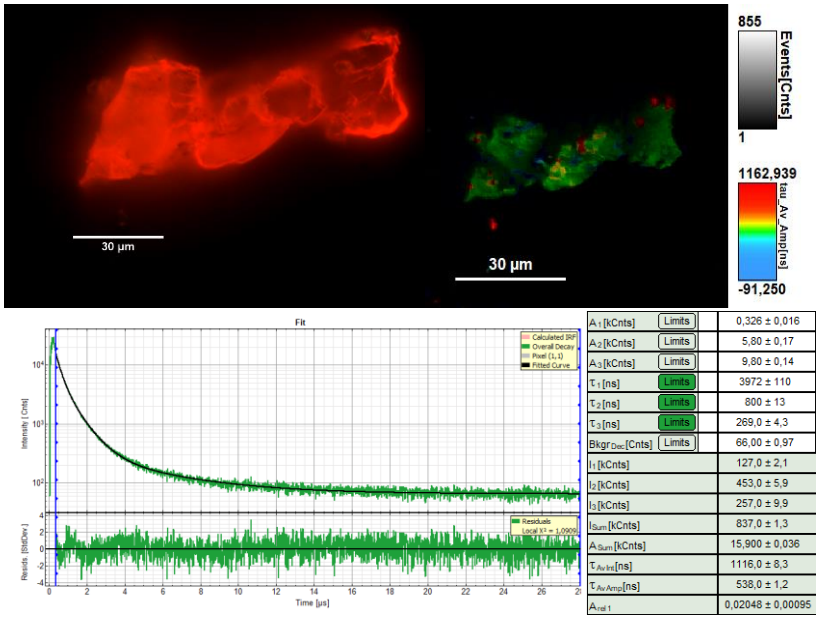

A_1 [kCnts]	Limits	0,326 ± 0,016
A_2 [kCnts]	Limits	5,80 ± 0,17
A_3 [kCnts]	Limits	9,80 ± 0,14
τ_1 [ns]	Limits	3972 ± 110
τ_2 [ns]	Limits	800 ± 13
τ_3 [ns]	Limits	269,0 ± 4,3
$Bkgr_{Dec}$ [Cnts]	Limits	66,00 ± 0,97
I_1 [kCnts]		127,0 ± 2,1
I_2 [kCnts]		453,0 ± 5,9
I_3 [kCnts]		257,0 ± 9,9
I_{Sum} [kCnts]		837,0 ± 1,3
A_{Sum} [kCnts]		15,900 ± 0,036
$\tau_{Av\,Int}$ [ns]		1116,0 ± 8,3
$\tau_{Av\,Amp}$ [ns]		538,0 ± 1,2
$A_{rel\,1}$		0,02048 ± 0,00095

Figure S77. Photoluminescence of crystalline **PtL_{OMe}** after grinding. Top left: Photoluminescence micrograph. Top right: PLIM lifetime map. Bottom left: Time-resolved photoluminescence decay (λ_{exc} = 376.7 nm, low-pass cut-off filter 460LP). Bottom right: Fitting parameters including pre-exponential factors and confidence limits.

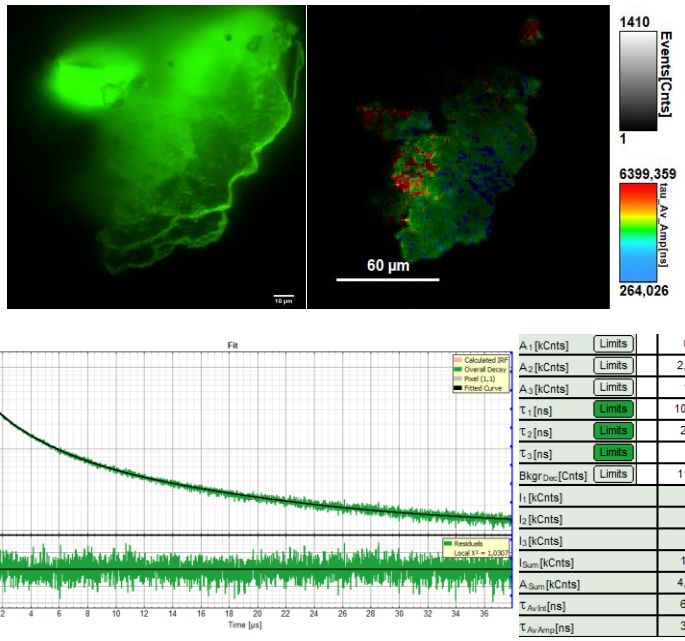

A_1 [kCnts]	Limits	0,92 ± 0,11
A_2 [kCnts]	Limits	2,500 ± 0,061
A_3 [kCnts]	Limits	1,50 ± 0,18
τ_1 [ns]	Limits	10265 ± 817
τ_2 [ns]	Limits	2558 ± 222
τ_3 [ns]	Limits	588 ± 56
$Bkgr_{Dec}$ [Cnts]	Limits	111,0 ± 6,4
I_1 [kCnts]		921 ± 31
I_2 [kCnts]		625 ± 31
I_3 [kCnts]		87 ± 19
I_{Sum} [kCnts]		1633 ± 29
A_{Sum} [kCnts]		4,940 ± 0,038
$\tau_{Av\,Int}$ [ns]		6799 ± 320
$\tau_{Av\,Amp}$ [ns]		3386 ± 93

Figure S78. Photoluminescence of crystalline **PdL_{OMe}** before grinding. Top left: Photoluminescence micrograph. Top right: PLIM lifetime map. Bottom left: Time-resolved photoluminescence decay (λ_{exc} = 376.7 nm, low-pass cut-off filter 460LP). Bottom right: Fitting parameters including pre-exponential factors and confidence limits.

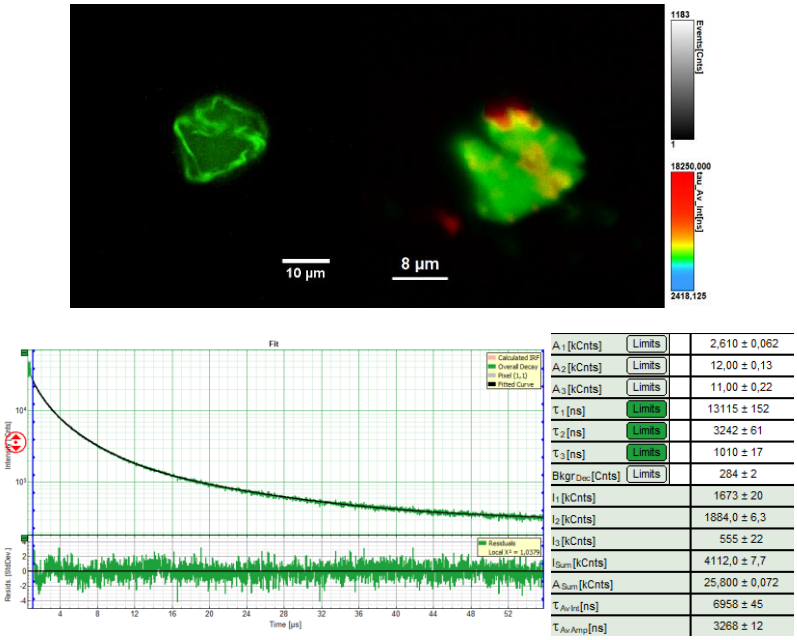

Figure S79. Photoluminescence of crystalline **PdL$_{OMe}$** after grinding. Top left: Photoluminescence micrograph. Top right: PLIM lifetime map. Bottom left: Time-resolved photoluminescence decay (λ_{exc} = 376.7 nm, low-pass cut-off filter 460LP). Bottom right: Fitting parameters including pre-exponential factors and confidence limits.

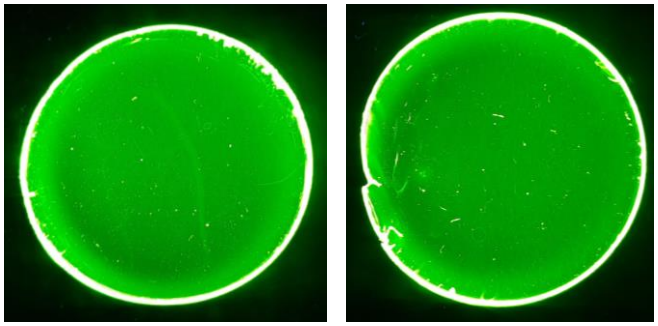

Figure S80. Photographic pictures showing the phosphorescence of PMMA films loaded with **PtL$_{OMe}$** (left) and **PtL$_{OHex}$** (right) under UV irradiation (λ_{exc} = 366 nm).

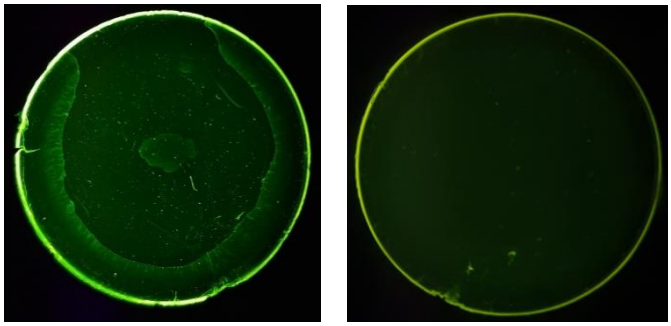

Figure S81. Photographic pictures showing the phosphorescence of PMMA films loaded with **PdL$_{OMe}$** (left) and **PdL$_{OHex}$** (right) under UV irradiation (λ_{exc} = 366 nm).